

Solvent inclusion properties of Triamterene crystal forms and solubility differences between Roxithromycin polymorphic forms

Yasmin Bawa
B.Pharm

Dissertation submitted in partial fulfilment of the
requirements for the degree Magister Scientiae in
the Department of Pharmaceutics at the
North-West University: Potchefstroom Campus.

Supervisor: Prof. W. Liebenberg
Co-Supervisor: Dr. E. van Tonder

April 2007
POTCHEFSTROOM

TABLE OF CONTENTS

Table of content	i
Abstract	ix
Uittreksel	xi

Chapter 1: Morphologic characteristics: Polymorphism

1.1	Introduction	1
1.2	Polymorphism	3
1.2.1	Types of polymorphs	4
1.2.2	Fundamentals	4
1.3	Pseudopolymorphs	13
1.3.1	Solvates	13
1.3.1.1	Types of solvates	14
1.3.1.1.1	Stoichiometric solvates	15
1.3.1.1.2	Non.stoichiometric solvates	15
1.3.2	Desolvates	16
1.3.3	Hydrates	16
1.4	Amorphous state	17
1.5	Forms vs. Habits	20
1.6	Importance of controlling the crystals	22
1.7	Pharmaceutical importance of polymorphic forms	23

1.8	Objectives and aims of this study	24
-----	-----------------------------------	----

Chapter 2: Methods of characterisation of triamterene and roxithromycin

2.1	Introduction	25
2.2	Method of analysis	26
2.2.1	Thermo-microscope	26
2.2.2	X-ray crystallography	26
2.2.2.1	X-ray powder diffractometry (XRPD)	28
2.2.3	Thermal method of analysis	28
2.2.3.1	Differential scanning calorimetry (DSC)	29
2.2.3.2	Thermogravimetric analysis (TGA)	30
2.2.4	Molecular motion : vibrational spectroscopy	31
2.2.4.1	Infrared absorption spectroscopy	32
2.2.5	Solubility	32
2.2.5.1	Validation of UV method	33
2.2.6	Karl Fischer titrations	34
2.3	Conclusion	35

Chapter 3: Triamterene

3.1	Introduction	36
3.2	Description	36
3.2.1	Nomenclature	36
3.2.2	Formulae	37

3.2.3	Molecular weight	37
3.2.4	Appearance and colour	37
3.3	Physical properties	37
3.3.1	Solubility	37
3.3.2	Crystal properties	38
3.4	Pharmceutics of triamterene	38
3.4.1	Pharmaceutics	38
3.4.2	Dosage and administration	39
3.5	Pharmacology of triamterene	40
3.5.1	Pharmacokinetic properties	40
3.5.1.1	Absorption	40
3.5.1.2	Metabolism	40
3.5.1.3	Distribution	40
3.5.1.4	Excretion	40
3.5.2	Working mechanism of triamterene	41
3.5.3	Indications and therapeutic uses of triamterene	41
3.5.4	Drug interaction	41
3.5.5	Side effects	43
3.6	Literature study	43
3.6.1	Recrystallisation results	43
3.6.2	Discussion of the data generated	46
3.7	Study of the physico-chemical properties of triamterene raw material	47
3.7.1	Results obtained during this study	47

3.7.1.1	Thermo-microscope (TM)	47
3.7.1.2	X-ray powder diffractometry (XRPD)	48
3.7.1.3	Differential scanning calorimetry (DSC)	51
3.7.1.4	Thermogravimetric analysis (TGA)	52
3.7.1.5	Infrared spectroscopy (IR)	53
3.8	Preparation of triamterene crystals	55
3.8.1	Method for preparation of triamterene crystals	56
3.8.2	Recrystallisation test results and outcomes	57
3.8.2.1	Acids	57
3.8.2.1.1	Thermo-microscope (TM)	57
3.8.2.1.2	X-ray powder diffractometry (XRPD)	58
3.8.2.1.3	Differential scanning calorimetry (DSC)	61
3.8.2.1.4	Thermogravimetric analysis (TGA)	61
3.8.2.1.5	Infrared spectroscopy (IR)	64
3.8.2.1.6	Discussion of data generated from acid solvents	66
3.8.2.2	Alcohols	67
3.8.2.2.1	Thermo-microscope (TM)	67
3.8.2.2.2	X-ray powder diffractometry (XRPD)	68
3.8.2.2.3	Differential scanning calorimetry (DSC)	71
3.8.2.2.4	Thermogravimetric analysis (TGA)	71
3.8.2.2.5	Infrared spectroscopy (IR)	72
3.8.2.2.6	Discussion of data generated from alcohol solvents	74
3.8.2.3	DMF (dimethylformamide) mixtures	75

3.8.2.3.1	Thermo-microscope (TM)	75
3.8.2.3.2	X-ray powder diffractometry (XRPD)	76
3.8.2.3.3	Differential scanning calorimetry (DSC)	78
3.8.2.3.4	Thermogravimetric analysis (TGA)	78
3.8.2.3.5	Infrared spectroscopy (IR)	80
3.8.2.3.6	Discussion of data generated from DMF mixtures as solvents	82
3.8.3	Conclusion	83

Chapter 4: Roxithromycin

4.1	Introduction	84
4.2	Description	85
4.2.1	Nomenclature	85
4.2.2	Formulae	85
4.3	Molecular weight	86
4.4	Pharmaceutics of roxithromycin	86
4.4.1	Pharmaceutics	86
4.4.2	Dosage and administration	86
4.5	Pharmacology of triamterene	87
4.5.1	Pharmacokinetic properties	87
4.5.1.1	Absorption	87
4.5.1.2	Metabolism and elimination	88
4.5.1.3	Distribution	89

4.5.2	Working mechanism of roxithromycin	89
4.5.3	Drug interactions	90
4.5.4	Side effects	90
4.6	Physico-chemical properties of roxithromycin raw material	91
4.6.1	Results generated during this study	91
4.6.1.1	Thermo-microscope (TM)	91
4.6.1.2	X-ray powder diffractometry (XRPD)	91
4.6.1.3	Differential scanning calorimetry (DSC)	95
4.6.1.4	Infrared spectra (IR)	96
4.6.1.5	Solubility	98
4.7	Characterisation of roxithromycin crystal forms	99
4.7.1	Preparation of roxithromycin crystals	99
4.7.2	Method for preparation of roxithromycin crystals	99
4.7.3	Ethyl acetate	100
4.7.3.1	Thermo-microscope (TM)	100
4.7.3.2	X-ray powder diffractometry (XRPD)	100
4.7.3.3	Differential scanning calorimetry (DSC)	103
4.7.3.4	Thermogravimetric analysis (TGA)	103
4.7.3.5	Infrared spectra (IR)	104
4.7.3.6	Solubility	106
4.7.3.7	Discussion of the data generated from ethyl acetate as solvent	107
4.7.4	Acetonitrile (ACN)	107
4.7.4.1	Thermo-microscope (TM)	107

4.7.4.2	X-ray powder diffractometry (XRPD)	108
4.7.4.3	Differential scanning calorimetry (DSC)	111
4.7.4.4	Thermogravimetric analysis (TGA)	111
4.7.4.5	Infrared spectra (IR)	112
4.7.4.6	Solubility	114
4.7.4.7	Discussion of the data generated from ACN as solvent	115
4.7.5	Dichloromethane	115
4.7.5.1	Thermo-microscope (TM)	115
4.7.5.2	X-ray powder diffractometry (XRPD)	116
4.7.5.3	Differential scanning calorimetry (DSC)	119
4.7.5.4	Thermogravimetric analysis (TGA)	119
4.7.5.5	Infrared spectra (IR)	120
4.7.5.6	Solubility	122
4.7.5.7	Discussion of the data generated from dichloromethane as solvent	123
4.7.6	Chloroform	124
4.7.6.1	Thermo-microscope (TM)	124
4.7.6.2	X-ray powder diffractometry (XRPD)	124
4.7.6.3	Differential scanning calorimetry (DSC)	126
4.7.6.4	Thermogravimetric analysis (TGA)	126
4.7.6.5	Infrared spectra (IR)	127
4.7.6.6	Solubility	129
4.7.6.7	Discussion of the data generated from chloroform as solvent	130

4.7.7 Conclusion	130
------------------	-----

Chapter 5: Conclusion	135
------------------------------	------------

Bibliography	140
---------------------	------------

Acknowledgements	141
-------------------------	------------

Annexure 1: Poster presented at 4th International Conference on Pharmaceutical and Pharmacological Sciences 21-23 September 2006	142
---	------------

ABSTRACT

Solvent inclusion properties of triamterene crystal forms and solubility differences between roxithromycin polymorphic forms

Polymorphism is very common among drug substances. Differences in the physical properties of a solid form may impact largely on the processing of a drug substance, while differences in solubility may impact on the absorption of the active drug from its dosage form, by affecting the dissolution rate and possibly the mass transport of the molecules. Changes in the crystal form at any stage of the production process can alter the bioavailability of the drug.

With this theory in mind, the following objectives were identified with respect to triamterene and roxithromycin, two active pharmaceutical ingredients that are known for their poor water solubility: a) The preparation of different polymorphic and / or pseudopolymorphic forms of triamterene and roxithromycin, in an attempt to isolate a more water-soluble form; b) The investigation of the physical properties (i.e. solubility, stability, crystal morphology and thermal properties) of the different forms being prepared; c) To identify those polymorphic forms of roxithromycin that are the most amorphous; and d) To investigate the respective solubility profiles of the various polymorphs of triamterene and roxithromycin, and to determine the influence of their crystal morphology on solubility.

Characterisations of these different crystal forms are important when considering the development of solid dosage forms. Various methods of analysis include microscopy, crystallography, thermal analysis, molecular motion, solubility, and Karl Fischer titrations. These methods were combined in this study for the identification and characterisation of triamterene and roxithromycin crystals.

Triamterene is insoluble in water, most of the organic solutions, but is more soluble in acids, such as formic acid. In this study triamterene was recrystallised from various organic solvents, i.e. acids, DMF and DMF:water mixtures, and alcohols. From the data being generated during this study it was concluded that: a) The recrystallisation products from the three acid solvents produced disolvates, i.e. novel pseudopolymorphic forms of triamterene; b) The 2-butanol recrystallisation products were either hydrates, solvates, or hydrated solvates; c) DMF and DMF:water mixtures only yielded solvates.

Recrystallisation of triamterene was unfortunately hampered by low solubility and hence crystal yield, which made it impossible to obtain enough crystals on which to perform

solubility studies. This was unfortunate, since it was reported in the literature that active pharmaceutical ingredients (API's) with low solubilities, such as mebendazole, showed significant differences in solubilities between the different polymorphic forms.

Roxithromycin is very slightly soluble in water, slightly soluble in diluted hydrochloric acid, and freely soluble in acetone, alcohol and dichloromethane. It was reported that some of the roxithromycin polymorphic forms gave problems during a powder dissolution study, due to poor wettability in the dissolution medium. Furthermore, prior to the dissolution, during vortexing of the powder, a gel formed, which complicated the quantitative transfer of the samples into the dissolution vessels, hence resulting in poor dissolution results.

The aim of this investigation thus was to prepare different crystal forms of roxithromycin, and, instead of performing powder dissolution studies, to determine the solubility thereof, which would arguably be a better method of discriminating between the solubilities of the different forms.

The different recrystallisation products that were obtained from the different solvents during this study were classified as: a) A ethyl acetate hemi-solvate (would require confirmation with single X-ray crystallography); b) A meta-stable lower melting point form recrystallised from acetonitrile; c) A dichloromethane hemi-solvate (would require confirmation with single X-ray crystallography); and d) An amorphous chloroform solvate.

The ethyl acetate hemi-solvate proved to be the only form with a significantly better solubility profile in all three media tested, than that of the raw material. These results have created new questions regarding the morphology and differences in crystal forms of roxithromycin. It should be challenging to prepare quality crystals, suitable for single X-ray crystallography, in order to clarify the actual crystal forms of this complex antibiotic, since all the recrystallisation products tended to be more amorphous, having low peak intensity counts (XRPD).

Furthermore, the fact that roxithromycin has no free hydroxyl groups, explains the poor wettability and the hydrophobicity, hence its poor solubility in water. The outcomes of this study, however, raised the question as to why the solubility of the prepared ethyl acetate crystal form differed so much from the other prepared forms, especially with regards to its higher solubility in water. This finding, especially, has therefore created the need for further investigation and it is anticipated that such further studies would solve the solubility problems of roxithromycin in aqueous media.

UITTREKSEL

Oplosmiddel-insluitingseienskappe van triamtereen-kristalvorme en oplosbaarheidsverskille tussen polimorfiese vorme van roksitromisien

Polimorfisme kom baie algemeen onder geneesmiddels voor. Verskille in die fisiese eienskappe van 'n soliede vorm mag 'n groot impak op die vervaardiging van 'n geneesmiddel hê, terwyl verskille in oplosbaarheid die absorpsie van die aktiewe bestanddeel vanuit sy doseervorm mag beïnvloed, deur die dissolusie-tempo, en moontlik die massa-oordrag van die molekules, te affekteer. Veranderinge in die kristalvorm, op enige stadium in die vervaardigingsproses, kan die bio-beskikbaarheid van die geneesmiddel verander. Dit is teen hierdie agtergrond wat die volgende doelwitte ten opsigte van triamtereen en roksitromisien, twee aktiewe farmaseutiese bestanddele, wat vir hulle swak wateroplosbaarheid bekend is, geïdentifiseer is: a) Die bereiding van verskillende polimorfiese - en / of pseudopolimorfiese vorme van triamtereen en roksitromisien, in 'n poging om 'n meer wateroplosbare vorm te isoleer; b) Die ondersoek van die fisiese eienskappe (nl. oplosbaarheid, stabiliteit, kristalmorfologie en termiese eienskappe) van die verskillende vorme berei; c) Om die mees amorfie polimorfiese vorme van roksitromisien te identifiseer; en d) Om die individuele oplosbaarheidsprofile van die verskillende polimorfe van triamtereen en roksitromisien te ondersoek, en om die invloed van kristalmorfologie op die oplosbaarheid daarvan te bepaal.

Wanneer die ontwikkeling van vaste doseervorme beplan word, is die karakterisering van die verskillende kristalvorme van uiterste belang. Verskeie metodes van analise sluit mikroskopie, kristallografie, termiese analise, molekulêre beweging, oplosbaarheid en Karl Fischer-titrasies, in. Hierdie metodes is tydens hierdie studie gekombineer vir die identifisering en die karakterisering van triamtereen - en roksitromisien – kristalle.

Triamtereen is onoplosbaar in water en in die meeste organiese oplosmiddels, maar dit is meer oplosbaar in sure, soos bv miersuur. Triamtereen is tydens hierdie studie uit verskeie organiese oplosmiddels gerekrystalliseer (sure, DMF en DMF:water-mengsels, en alkohole). Na aanleiding van die data wat tydens hierdie studie versamel is, is die volgende afleidings gemaak: a) Rekrystallasie uit asynsuur, miersuur en propioonsuur het disolvate gelewer, nl. nuwe pseudopolimorfiese vorms van triamtereen; b) Die 2-butanol rekrystallasie-produkte was enige van hydrate, of solvate, of gehidreerde solvate; en c) DMF and DMF:water-mengsels het slegs solvate opgelewer. Die rekrystallasie van triamtereen is ongelukkig deur lae oplosbaarheid, met gevolglike lae kristalopbrengs benadeel, wat dit onmoontlik gemaak het om genoegsame kristalle vir oplosbaarheidstudies te berei. Dit was jammer, aangesien daar in die literatuur rapporteer is dat aktiewe farmaseutiese bestanddele, met lae oplosbaarheid, soos mebendasool, beduidende verskille in oplosbaarheid tussen die verskillende polimorfiese vorme getoon het.

Roksitromisien is baie min oplosbaar in water, is redelik oplosbaar in verdunde soutsuur, en is baie oplosbaar in asetoon, alkohol en dichlorometaan. Na aanleiding van 'n vorige studie is rapporteer dat sommige van die polimorfe van roksitromisien probleme tydens dissolusie-studies gelewer het, weens swak benatting daarvan deur die dissolusie-medium. Voorts is rapporteer dat, tydens die voorafgaande vermenging van die poeier, het 'n gel gevorm wat die kwantitatiewe oordrag van die toetsmonsters na die dissolusie-houers bemoeilik het, aldus die swak dissolusie-resultate.

Die doel van hierdie ondersoek was dus om verskillende kristalvorme van roksitromisien te berei, en om, in plaas van dissolusie-studies daarop uit te voer, eerder die oplosbaarheid daarvan te bepaal, aangesien daar gereken is dat dit 'n beter metode van onderskeiding tussen die oplosbaarheid van die verskillende vorme sou wees. Die verskillende rekristallasie-produkte wat tydens hierdie studie vanuit die verskillende oplosmiddels berei is, is as volg geklassifiseer: a) 'n Hemi-solvaat vanuit etielasetaat (enkelkristal X-straal-kristallografie sou nodig wees om dit te bevestig); b) 'n Meta-stabiele laer smeltpunt vorm vanuit asetonitriël; c) 'n Hemi-solvaat vanuit dichloormetaan (enkelkristal X-straal-kristallografie sou nodig wees om dit te bevestig) en d) 'n Amorfe -solvaat vanuit chloroform.

Die etielasetaat hemi-solvaat was die enigste vorm wat 'n beduidende beter oplosbaarheidsprofiel, in al drie media getoets, as die grondstof gelewer het. Hierdie resultate het nuwe vrae rondom die morfologie en verskillende kristalvorme van roxithromycyn laat ontstaan. In toekomstige studies behoort een van die uitdagings te wees om kwaliteit kristalle, geskik vir enkelkristal X-straal-kristallografie, te berei, ten einde die ware kristalvorme van hierdie komplekse antibiotikum uit te klaar, aangesien al die rekristallasie-produkte in hierdie studie berei, daarna geneig het om meer amorf te wees, met lae piek intensiteit-tellings (XRPD). Voorts, die feit dat roksitromisien geen vrye hidroksielgroepe bevat nie, verklaar die swak benatbaarheid en hidrofobisiteit daarvan, en gevolglik sy swak oplosbaarheid in water. Die uitkomstes van hierdie studie het die vraag laat ontstaan, waarom die oplosbaarheid van die bereide etielasetaat-kristalvorm soveel van die ander vorms verskil het, veral met betrekking tot die hoë oplosbaarheid daarvan in water. Dit is veral hierdie bevinding wat die noodigheid en entoesiasme vir verdere studie laat posvat het, aangesien daar verwag word dat verdere studies die welbekende oplosbaarheidsprobleme van roksitromisien in water-media behoort op te los.

CHAPTER 1

Polymorphism

1.1 Introduction

According to Vippagunta *et al.* (2000), organic and inorganic compounds of pharmaceutical relevance can exist in one, or more, crystalline forms. The term crystalline implies an ideal crystal, hence a solid, in which the structural unit is repeated regularly and indefinitely in three dimensions in space.

McCrone (1965, as quoted by Bernstein, 2002) defined a polymorph as a solid crystalline phase of a given compound, resulting from the possibility of at least two different arrangements of the molecules of that compound in the solid state (Bernstein, 2002).

According to McCrone also, flexible molecules include conformational polymorphs, wherein the molecule can adopt different conformations in the different crystal structures (McCrone 1965, as quoted by Bernstein, 2002)

The structures of crystals may be different, due to different inter- and intramolecular interactions, such as van der Waal interactions and hydrogen bonds. This may lead to different polymorphs, each having different free energies and therefore different physical properties, such as solubility, chemical stability, melting point, density, etc. (Hilfiker *et al.*, 2006).

Differences in the physical properties of a solid form may impact largely on the processing of a drug substance, while differences in solubility may impact on the absorption of the active drug from its dosage form, by affecting the dissolution rate and possibly the mass transport of the molecules (Vippagunta *et al.*, 2000).

The common crystalline forms of a given drug substance include polymorphs and solvates. Crystal polymorphs have the same chemical composition, but different internal crystal structures, and therefore possess different physico-chemical properties. When the drug substance crystallises into different crystal packing arrangements and / or different conformations, the different crystal structures / polymorphs arise (Vippagunta *et al.*, 2000).

Crystalline polymorphs and solvates differ in crystal packing and molecular conformation, as well as in lattice energy and entropy. These usually cause significant differences in their physical properties, such as density, hardness, tabletability, refractive index, melting point,

enthalpy of fusion, vapour pressure, solubility, dissolution rate, other thermodynamic and kinetic properties, and even colour (Vippagunta *et al.*, 2000).

Condensed matter can exist in various mesophases, in addition to their crystalline, amorphous and liquid states. These mesophases are characterised by exhibiting partial order between that of a crystalline and an amorphous state. Several drug substances form liquid crystalline phases, which can be either thermotropic, when liquid crystal formation is induced by temperature, or lyotropic, when the transition is solvent induced (Hilfiker *et al.*, 2006).

Polymorphism is very common among drug substances and are mostly small, organic molecules, with molecular weights below 600 g.mol^{-1} (Hilfiker *et al.*, 2006).

When a compound is acidic, or basic, it is often possible to create a salt with a suitable base or acid, and hence various polymorphs or solvates of that compound. Such crystalline salts may also exist as various polymorphs, or solvates (Hilfiker *et al.*, 2006).

Figure 1.1 is a schematic representation of various types of solid forms, according to Hilfiker *et al.* (2006).

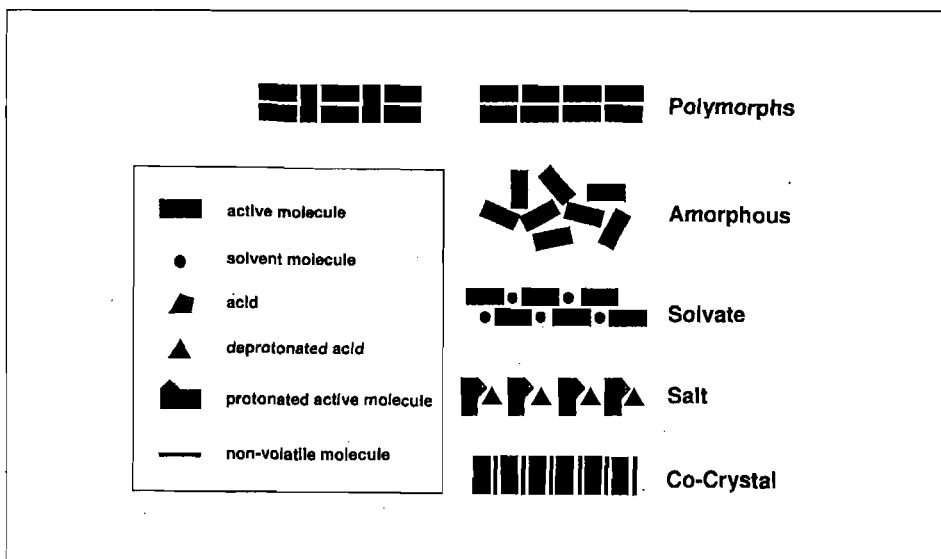


Figure 1.1 Schematic representation of various types of solid forms (Hilfiker *et al.*, 2006).

The free energy of a polymorph determines its stability, hence a more stable polymorph has less free energy. Under a defined set of experimental conditions, with the exception of transition points, only one polymorph has the lower free energy. This polymorph then is the

thermodynamically stable form, whilst the other polymorph is called the metastable form (Hilfiker *et al.*, 2006).

A metastable form is one that is thermodynamically unstable, but that has a finite existence as a result of its relatively slow rate of transformation. The metastable form is sometimes desirable in the pharmaceutical industry, because of its special properties, such as higher bioavailability, better behaviour during grinding and compression, or lower hygroscopicity. However, it has a thermodynamic tendency to reduce its free energy, by transforming into the stable form (Hilfiker *et al.*, 2006).

There are two mechanisms from which structural differences between the crystalline lattices of polymorphs originate, namely, packing polymorphism and conformational polymorphism. Packing polymorphism is a mechanism by which molecules that are conformationally relatively rigid, can be packed into different three-dimensional structures. Conformational polymorphism is a mechanism by which conformationally flexible molecules can fold into different shapes that can pack into different three-dimensional structures (Hilfiker *et al.*, 2006).

1.2 Polymorphs

Polymorphism is believed to be characteristic of all substances. The actual non-occurrence arises from the fact that a polymorphic transition is above the melting point of the substance, or in the area of yet unattainable values of external equilibrium factors, or other conditions providing for the transition (Bernstein, 2002).

According to Frankenheim's (Frankenheim, 1939) detailed study of the mercuric iodide system, he established many of the principles still being recognised today, regarding the nature of polymorphism. Some of these are:

- Different melting and boiling points are observed in polymorphs and their vapours have different densities.
- The specific temperature of transition distinguishes the transition from a low-temperature form (A) to a high-temperature form (B).
- The low-temperature form (A) cannot exist at a temperature above that at which the transition into form B occurs, but B can exist below this transition point; in which case B is then a metastable form.

- At temperatures below the transition point, form B will transform into form A, upon contact with A, the transition proceeding in all directions, but with differing velocities.
- Mechanical shock, or scratching may, in some cases, convert form B into form A, without contact with A.
- Heat is absorbed upon the inter-transition of form A, or form B, into each other (Bernstein, 2002).

1.2.1 Types of polymorphs

Polymorphs can be classified as either enantiotropes or monotropes, depending on whether one form can transform reversibly into the other, or not (Vippagunta *et al.*, 2000).

According to Vippagunta *et al.* (2000), an enantiotropic system is where a reversible transition between polymorphs is possible at a definite transition temperature that is below the melting point. With the monotropic system, there is no reversible transition between the polymorphs below the melting point.

Crystal lattices can be formed through two different mechanisms, namely packing polymorphism and conformational polymorphism (Vippagunta *et al.*, 2000).

Packing polymorphism occurs when conformationally, relatively rigid molecules, are assembled into different three-dimensional structures through the invocation of different intermolecular mechanisms. Conformational polymorphism arises when a non-conformationally rigid molecule is folded into different arrangements, which can subsequently be packed into alternative crystal structures (Vippagunta *et al.*, 2000).

1.2.2 Fundamentals

Polymorphic structures of molecular crystals are different phases of a particular molecular entity. The classic tools of the Phase Rule, and the thermodynamics and kinetics of polymorphs are used, to understand the formation of those phases and relationships between them (Bernstein, 2002).

The Phase Rule

Gibbs formulated the Phase Rule, based on the thermodynamic principles, and it was then applied to physical chemistry by Roozeboom. The Phase Rule is simply stated as (Bernstein, 2002).

$$F = C - P + 2$$

Where: F = the number of degrees of freedom of the system,

C = the number of components, and

P = the number of phases.

A phase is defined as any homogeneous and physically distinct part of a system, which is separated from other parts of the system by definite bounding surfaces. The number of components is the minimum number of independent species required to define the composition of all of the phases in the system.

The number of degrees of freedom is the number of variable factors, such as temperature, pressure, and concentration that must be fixed in order to define the condition of a system at equilibrium (Bernstein, 2002).

Thermodynamic relations in polymorphs

The key questions regarding polymorphic systems include the relative stability of the various crystal modifications, and the changes in thermodynamic relationships, accompanying phase changes and different domains of temperature, pressure, and other conditions (Bernstein, 2002).

These considerations will be demonstrated by a discussion of two theoretical polymorphic solids, whilst the extension to more complex systems is based on precisely the same principles, as described by Bernstein (2002).

As was mentioned, the relative stability of two polymorphs depends on their free energies, with the more stable one having the lower free energy. The less stable form is energetically driven to transform into the more stable form, because of this energy relationship, although kinetic factors may prevent this transformation.

Since the differences in volume between polymorphs are small fractions of the volumes of the solids themselves, for solids, volume and pressure changes with energy are negligible

(Bernstein, 2002). Under these conditions of constant temperature and pressure, the free energy of a solid phase may be represented by the Helmholtz relationship

$$A = E - TS$$

Where: E is the internal energy,
T the absolute temperature, and
S the entropy.

According to Bernstein (2002), at absolute zero, TS vanishes and the Helmholtz free energy equals the internal energy. At absolute zero the more stable polymorphic modification should have the lower internal energy. Above absolute zero, the entropy term will play a role, which may differ for the two polymorphs. Therefore the behaviour of the free energy as a function of temperature, can differ for the two polymorphs, as presented by the curves A1 and A11 in Figure 1.2 (Bernstein, 2002).

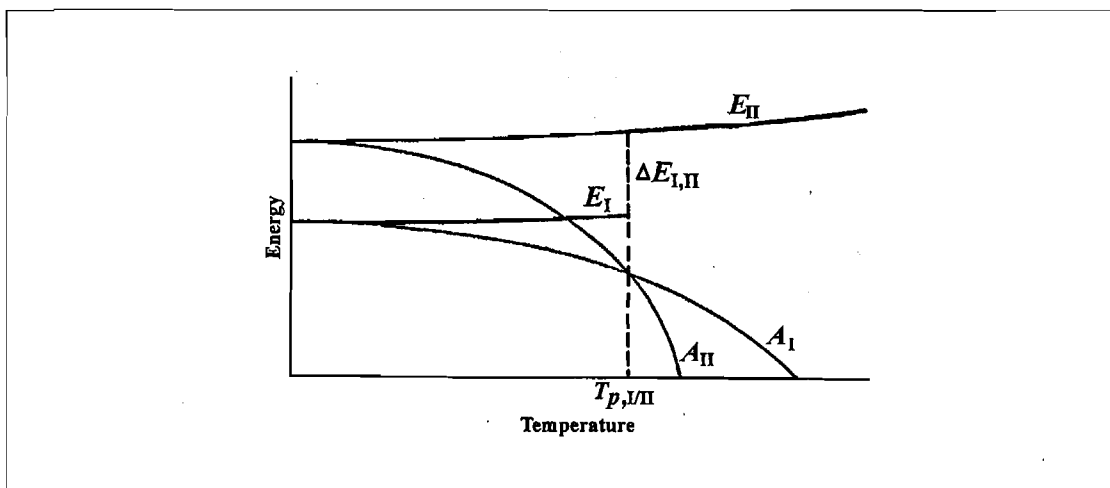


Figure 1.2 Energy relative to temperature curves for two polymorphs (Bernstein, 2002).

At absolute zero, Form I is more stable and the two curves behave differently, crossing at the transition temperature point, $T_{p,III}$. Form II is more stable above this transition temperature. At the transition temperatures the free energy of the two forms are identical, but since the internal energy of Form I is less than that of Form II, a quantity of energy, ΔE , is required to commence the phase transition (Bernstein, 2002).

The thermodynamic relationships between the polymorphs, i.e. enantiotropy and monotropy, are usually described by means of two types of graphs, namely energy-temperature graphs and pressure-temperature graphs (Lohani *et al.*, 2006).

Energy-temperature graphs

Phase transformations in crystalline solids are represented by internal energy (U) and Helmholtz free energy (A), relative to temperature. It was argued that the enthalpy of crystalline solids under normal pressure conditions has a negligible contribution from pressure-volume energy (PV). Therefore, for crystalline solids at ambient pressure according to Lohani *et al.* (2006):

$$H = U + PV \approx U$$

$$G = H - TS \approx U - TS = A$$

Figure 1.3 shows a typical energy-temperature curve of a crystalline solid.

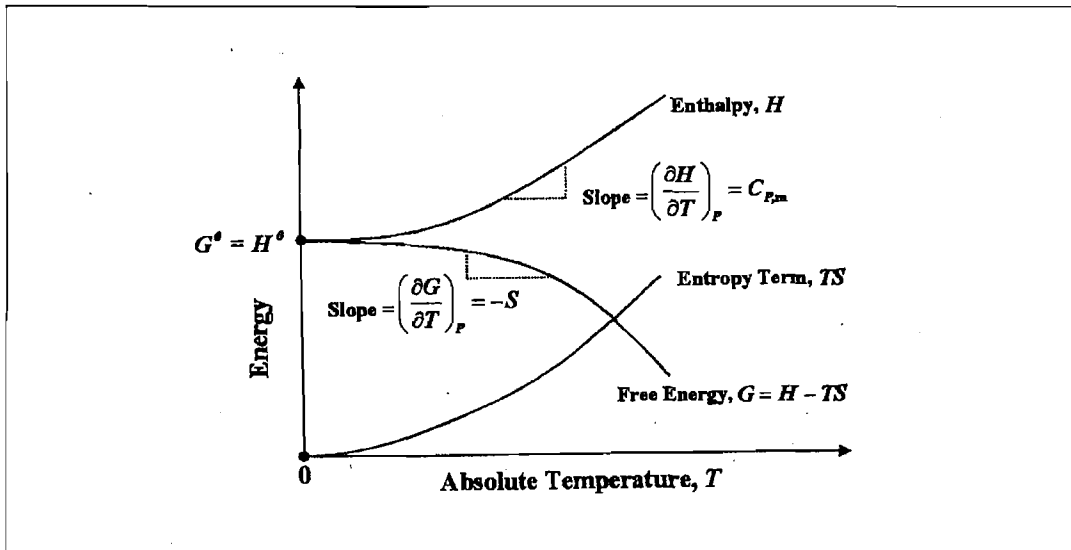


Figure 1.3 Energy-temperature graph of a crystalline solid under constant pressure (Lohani *et al.*, 2006).

As the temperature increases, the molar heat capacity of a crystalline substance increases as well. Thus in Figure 1.3, the enthalpy (H) isobar is shown as increasing with increasing temperature. The entropy term (TS) is also shown as increasing with temperature, because entropy is always positive as result of the third law of thermodynamics. However, the free

energy isobar (G) decreases with increasing temperature, because the slope of the curve is equal to the negative value of the entropy (Lohani *et al.*, 2006).

As illustration, two polymorphs are used, where A is more stable at absolute zero, than B.

Figure 1.4 illustrates an enantiotropic system.

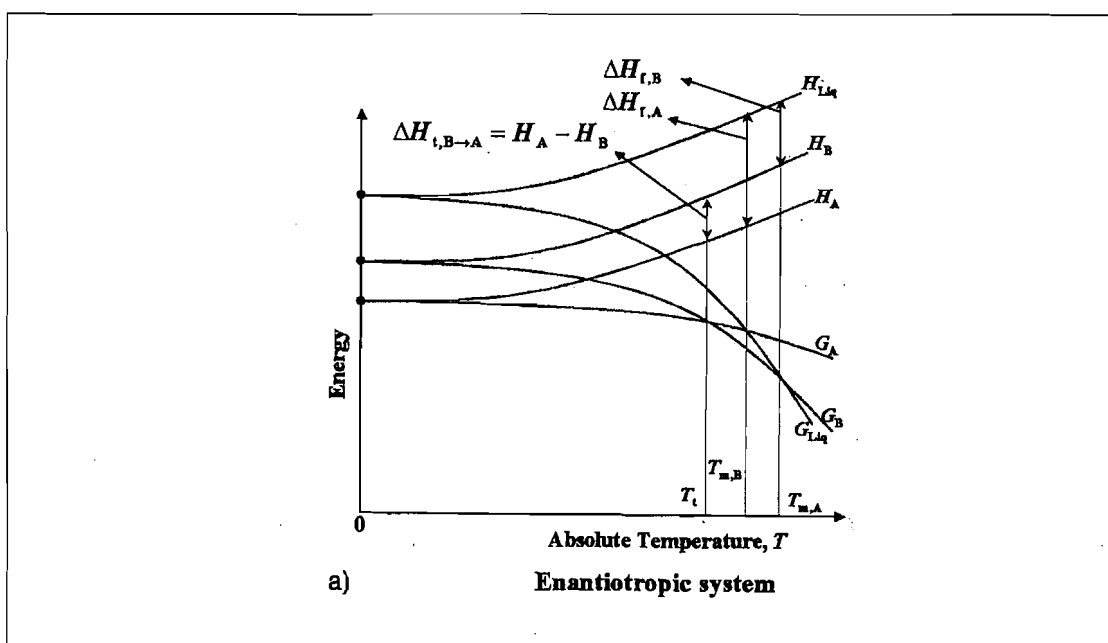


Figure 1.4 Energy–temperature graph of an enantiotropic system (Lohani *et al.*, 2006).

An enantiotropic relationship exists between two polymorphs if, at the transition point, the two polymorphs can undergo reversible solid-solid transformation. The existence of a transition point (T_t) below the melting point of both polymorphs, is the defining feature of such a system.

The melting point of a polymorph can be defined as the temperature at which the free energy isobar of the polymorph intersects the free energy isobar of the liquid. However, the transition temperature is defined as the temperature at which the free energy isobar of polymorph B intersects the free energy isobar of polymorph A. This indicates that at T_t , both polymorphs have equal free energy, i.e. $G_A = G_B$, and consequently are in equilibrium with each other. Below T_t , the free energy of A is lower than that of B, which means polymorph A is the stable solid phase i.e., $G_A < G_B$.

Consequently, below T_t , polymorph B can undergo spontaneous exothermic transformation into polymorph A. Above T_t , however, polymorph B is the stable solid phase, because its free energy is lower than that of polymorph A, i.e. $G_B < G_A$. Therefore, above T_t , polymorph A can undergo spontaneous endothermic transformation into polymorph B (Lohani *et al.*, 2006).

Figure 1.5 represents a monotropic system.

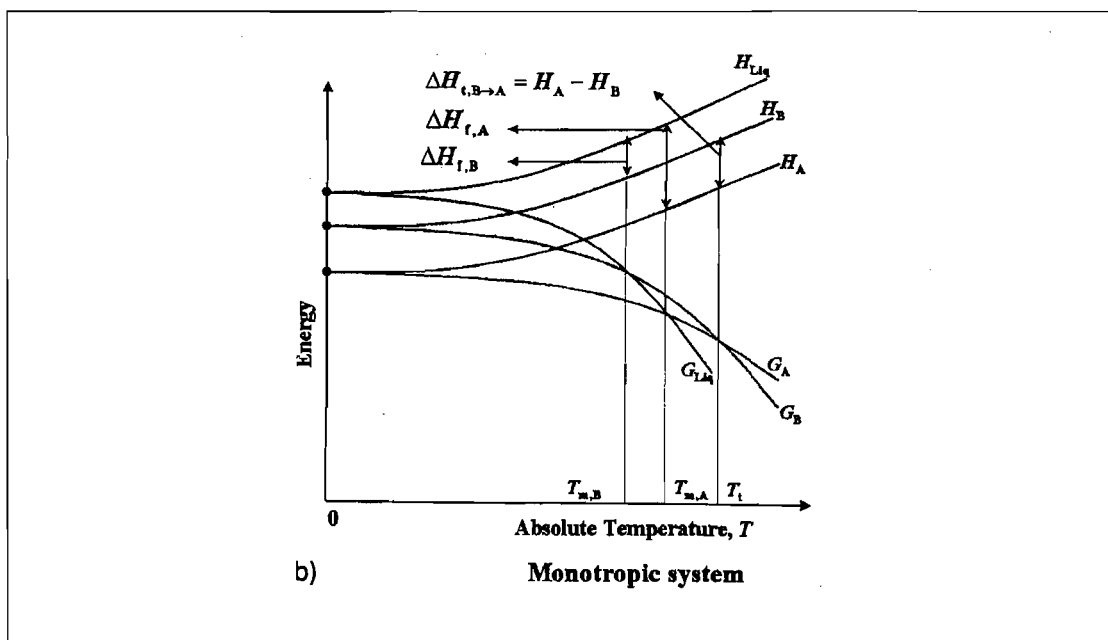


Figure 1.5 Energy–temperature graphs for a monotropic system (Lohani *et al.*, 2006).

A monotropic relationship exists between two polymorphs, when one of the polymorphs is always stable below melting point. As shown in the graph above, the free energy of polymorph A is always less than that of polymorph B, i.e. $G_A < G_B$, at all temperatures below $T_{m,A}$. Hence, in this case, polymorph B can undergo a spontaneous exothermic transformation into polymorph A. For a monotropic system, such transformation is thermodynamically feasible at any temperature, because $G_A < G_B$ at all temperatures.

Solid-solid transformations are kinetically hindered, because of the activation energy associated with them; in general, solid-solid transformation occurs at a temperature that provides the system with sufficient thermal energy to cross the activation energy barrier. The transition point (T_t) in a monotropic system is a virtual transition point, because it lies above the melting points of both polymorphs. This notion assumes that the free energy curves of the two polymorphs converge beyond their melting points.

Another possible situation relating to monotropic behaviour is the divergence of free energy curves of the polymorphs. In this case the virtual transition point lies below absolute zero. The heat of transition - and the heat of fusion rules are used to determine whether the relationship between a pair of polymorphs is enantiotropic, or monotropic (Lohani *et al.*, 2006).

Heat of transition rule: This rule states that if an endothermic phase transition is observed at a particular temperature, the thermodynamic transition point lies below this temperature. This allows one to conclude that the two polymorphs are enantiotropically related, or not. If an exothermic phase transition is observed at a particular temperature, there is no thermodynamic transition point below this temperature. This can occur, when the two polymorphs are enantiotropically related, and in addition, when their thermodynamic transition temperature is higher than the experimentally observed transition temperature (Lohani *et al.*, 2006).

Heat of fusion rule: This rule states that if the higher melting polymorph has the lower heat of fusion, the two polymorphs are enantiotropic, otherwise they are monotropic. The rate of polymorphic transition is too slow to allow for an accurate measurement of the heat of transition, in which case the heat of fusion rule may be applied (Lohani *et al.*, 2006).

Pressure-Temperature graphs

Figure 1.6 represents a typical pressure-temperature graph of a one-component system for which only one solid phase exists, corresponding to the absence of polymorphism.

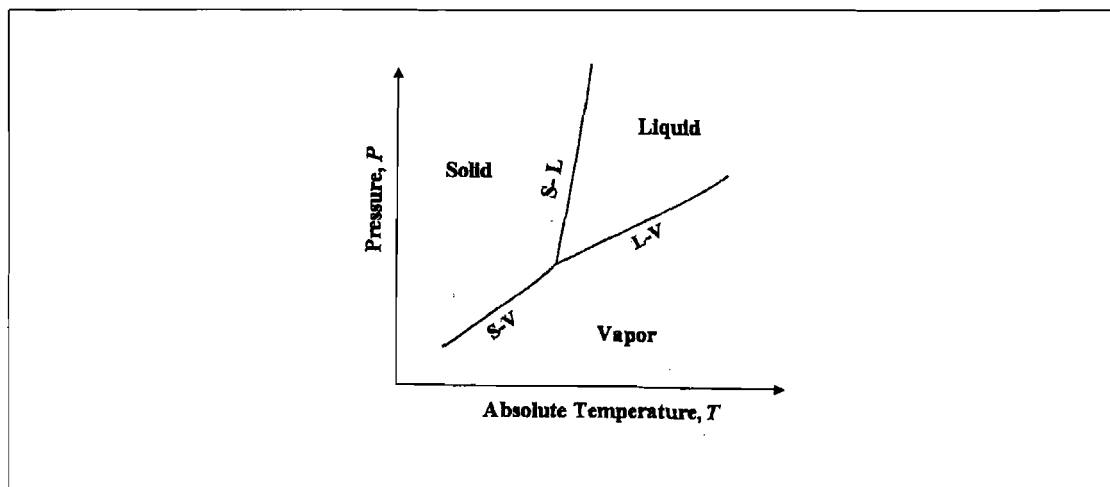


Figure 1.6 Pressure-temperature graph of a crystalline solid (Lohani *et al.*, 2006).

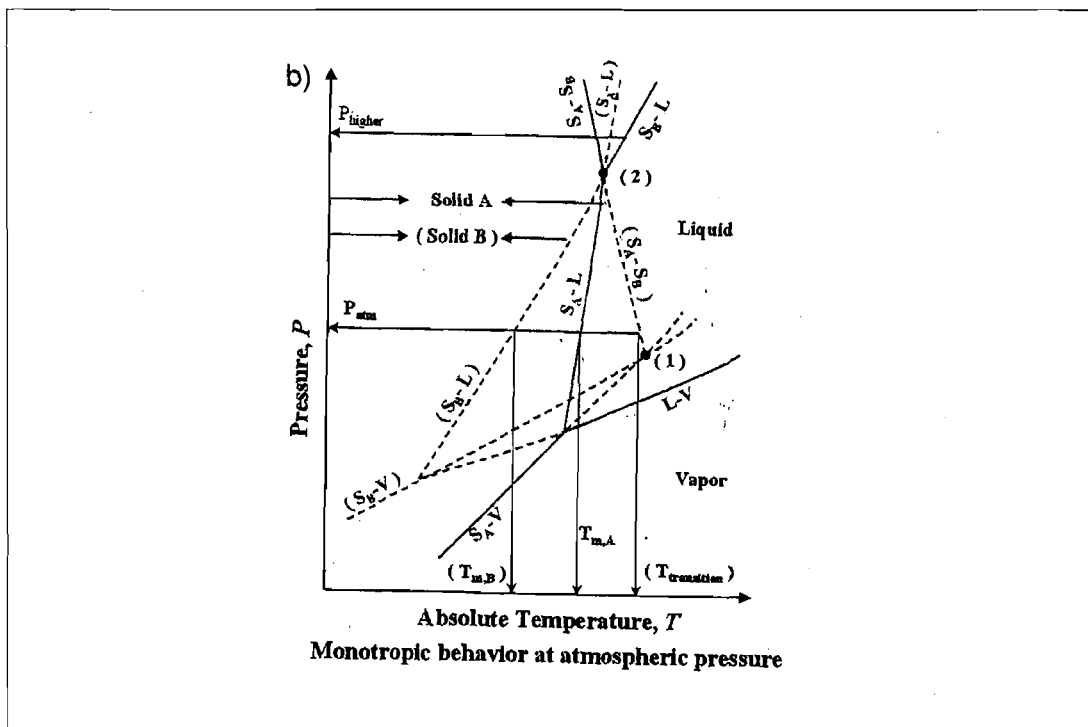


Figure 1.7(b) Pressure–temperature graphs of a monotropic system (Lohani *et al.*, 2006).

Inversion of polymorphic behaviour

A change from monotropic to enantiotropic, and *visa versa*, may result from the application of high pressure.

In Figure 1.7(a), the line corresponding to P_{higher} (a higher pressure beyond point 2) intersects the melting point curves for polymorphs A and B, before it intersects the S_A - S_B equilibrium curve. This shows that the polymorphic system that is enantiotropic at atmospheric pressure appears to show monotropic behaviour at higher pressure.

Similarly, in Figure 1.7(b), the line corresponding to P_{higher} (a higher pressure beyond point 2) intersects the S_A - S_A equilibrium curve before it intersects the melting point curves for polymorphs A and B. In this case, the polymorphic system appears to change from monotropic, at atmospheric pressure, to enantiotropic, at a higher pressure.

Thus, the terms enantiotropy and monotropy appear to be somewhat restricted in their application and is it therefore necessary to specify the pressure and temperature under which the polymorphs are enantiotropic, or monotropic (Lohani *et al.*, 2006).

1.3 Pseudopolymorphs

Pseudopolymorphism has been used to describe a number of phenomena that are related to polymorphism. Among them are desolvation, second-order transitions, dynamic isomerism, mesomorphism, grain growth, boundary migration, recrystallisation in the solid state, and lattice strain effects (Bernstein, 2002).

1.3.1 Solvates

Solvates are crystalline solid adducts that contain a solvent molecule within the crystal structure. It has either stoichiometric, or non-stoichiometric proportions, which gives rise to a unique difference in the physical and pharmaceutical properties of the drug (Vippagunta *et al.*, 2000).

If non-volatile molecules play the same role, the solids are called co-crystals. Solvates and co-crystals can also exist as different polymorphs (Griesser, 2006).

Pseudopolymorphic solvates can be defined as solvates for which the solvent can be removed from the crystal and added back to the crystal, reversibly, without greatly changing the X-ray powder diffraction pattern. Those which undergo a change in structure, as evidenced by different powder diffraction patterns, would be described as polymorphic solvates (Bernstein, 2002).

According to Vippagunta *et al.* (2000) adducts frequently crystallise more easily, since two molecules can often pack together with less difficulty, than single molecules can, due to their ability to form hydrogen bonds through the solvent molecules.

Figure 1.8 indicates how a solvent may be associated with a crystalline solid in different ways. The binding of solvent molecules to the surface occurs by weak interactions, i.e. hydrogen bonding, van der Waal, and dipole-dipole.

The affinity to individual crystal faces is different and therefore, the amount of surface absorbed solvent, or water, in crystalline materials, depends on their morphology, besides many other parameters. The solvent may also simply become physically entrapped in a growing crystal, which is called liquid inclusion. Since these pockets are filled with a saturated solution of the mother liquid, other kinds of impurities also remain associated with the crystal in this way (Griesser, 2006).

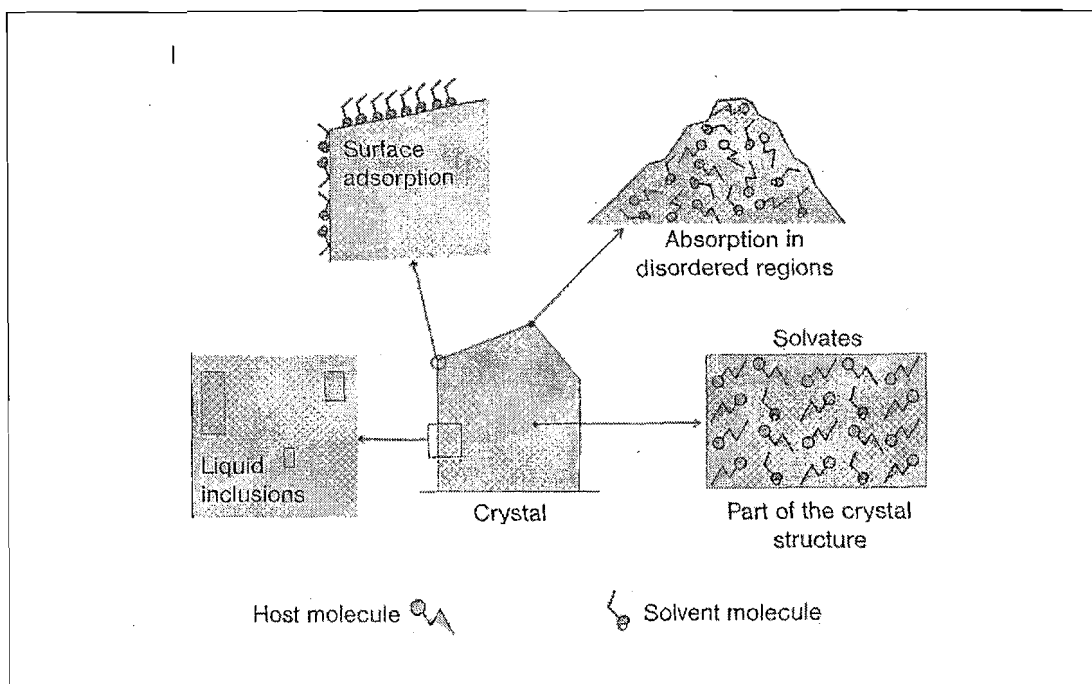


Figure 1.8 Illustration of different principles of solvent associations with crystalline solids (Griesser, 2006).

1.3.1.1 Types of solvates

Solvates, in the context of pharmaceutical solids, are subdivided into two main classes, i.e. stoichiometric and non-stoichiometric solvates, or hydrates.

Figure 1.9 shows the relationship of these two groups of solvates to the main classes of binary (multinary) systems. The circles of the two classes overlap to emphasise the existence of possible cases that do not allow for a clear classification (Griesser, 2006).

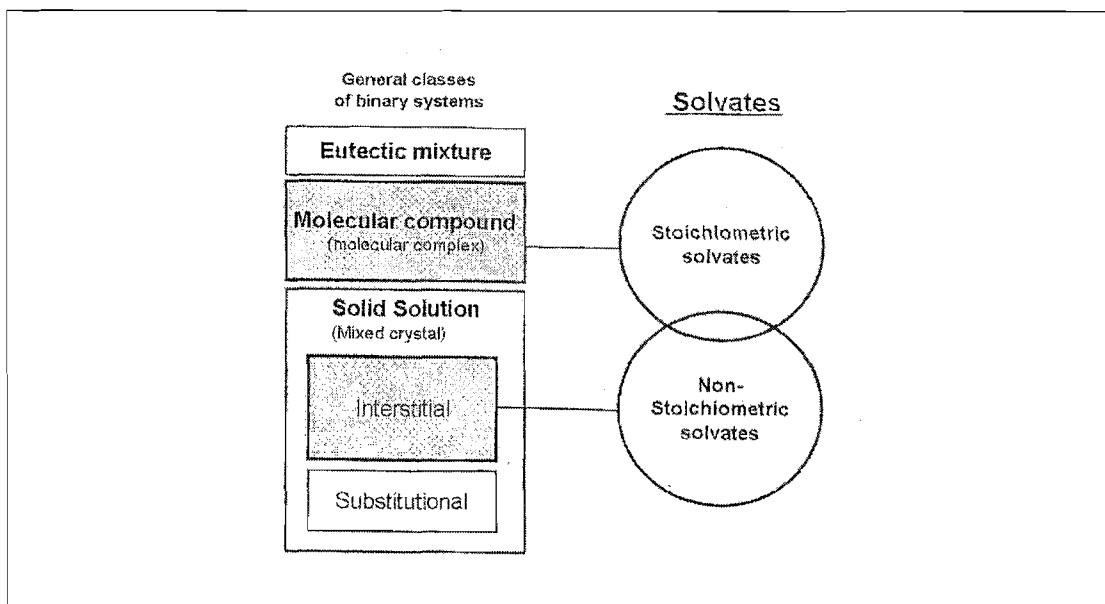


Figure 1.9 Classification of solvates in relation to the classical types of binary systems (Griesser, 2006).

1.3.1.1.1 Stoichiometric solvates

These solvates are regarded as molecular compounds. A solvate is an individual phase and the binary phase graph shows an eutectic and / or a peri-tectic, with the parent components (compound and solvent). The term implies a fixed, although not necessarily integral, ratio of solvent to compound. The solvent in stoichiometric hydrates is usually an integral part of the crystal structure and is essential for the maintenance of the molecular network. Desolvation of stoichiometric solvates always leads to a different crystal structure, or results in a disordered, or amorphous state (Griesser, 2006).

1.3.1.1.2 Non-stoichiometric solvates

Non-stoichiometric solvates comprise a type of inclusion compound. These solvates often cause problems and puzzles. They may also be regarded as interstitial solid solutions, or interstitial co-crystals. These crystal structures only form in the presence of the solvent, which is usually located in structural voids, or channels, and acts more or less as a space filler of these voids. These structures cannot pack closely, because of their particularly large and awkwardly shaped molecules. The structure of this class of solvates is retained, while the solvent content can take on all values between zero and a multiple of the molar compound ratio, with the latter being the most important feature of a these solvates. The

amount of solvent in the structure depends on the partial pressure of the solvent in the environment of the solid, as well as on the temperature (Griesser, 2006).

1.3.2 Desolvates

Desolvates are formed when a solvate is desolvated and the crystal retains the structure of the solvate. They are less ordered than their crystalline counterparts (Vippagunta *et al.*, 2000).

1.3.3 Hydrates

Hydrates are crystalline solid adducts that contain a water molecule within the crystal structure. On the basis of water uptake behaviour at different water activities, hydrates can be classified as either stoichiometric, or non-stoichiometric. Stoichiometric hydrates for which the mole ratio of water:host is constant, as indicated in Figure 1.10, have a defined stoichiometry over a range of water activities.

For non-stoichiometric hydrates, as shown in Figure 1.11, the mole ratio, water:host, may vary continuously as a function of water activity (Lohani *et al.*, 2006).

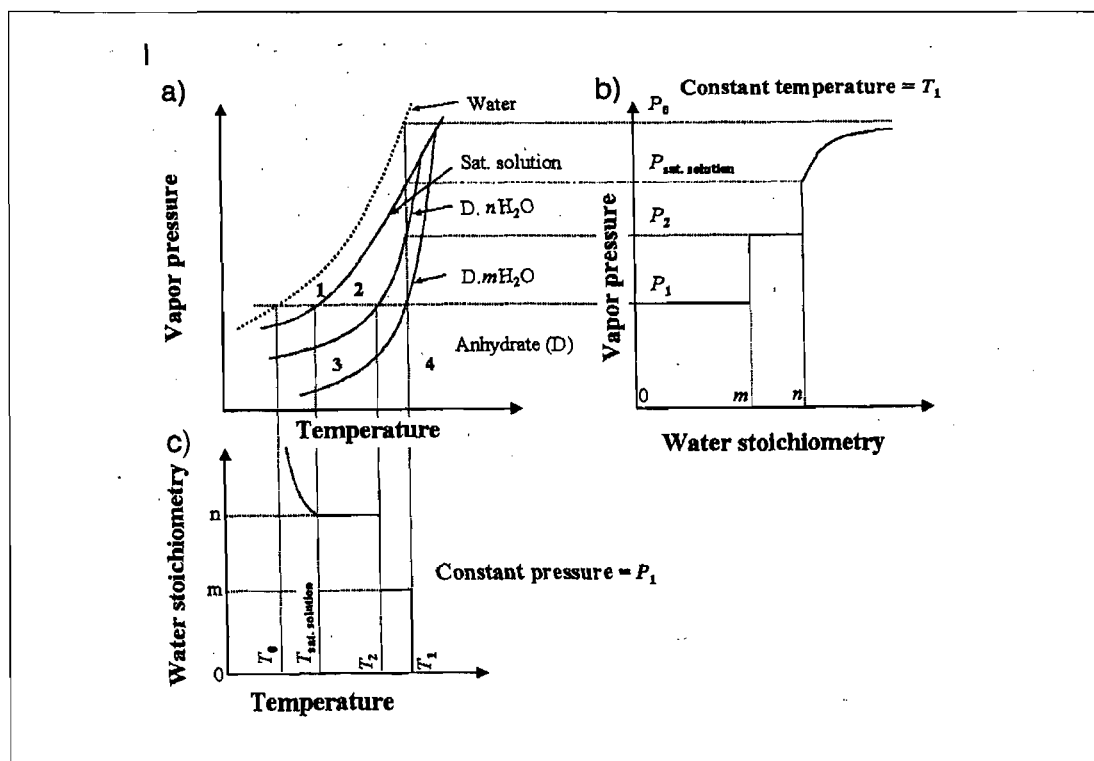


Figure 1.10 (a) Graph of vapour pressure of water against temperature.

(b) Graph illustrating dependence of water stoichiometry on vapour pressure at constant temperature, T_1 .

(c) Dependence of water stoichiometry on temperature at constant pressure, P_1 (Lohani *et al.*, 2006).

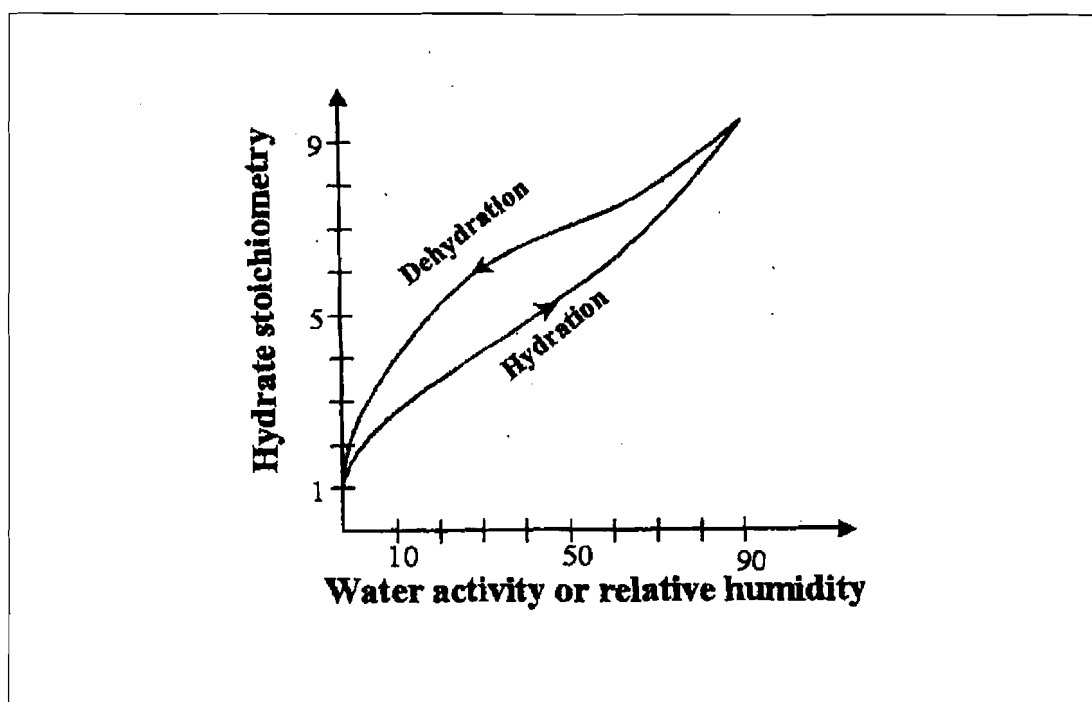


Figure 1.11 Graph illustrating water uptake behaviour for a non-stoichiometric hydrate (Lohani *et al.*, 2006).

1.4 Amorphous state

An amorphous state is defined as a non-crystalline solid. Since molecular units in a crystal lattice are assumed to be repeated according to a three-dimensional pattern along crystallographic directions, the relative location and orientation, as well as the interactions between neighbouring components, can be accurately described at the molecular level. The crystal packing usually corresponds to a high density arrangement, and therefore to minimal molar volume (Petit *et al.*, 2006).

In an amorphous solid, the absence of translational and rotational order can be ascribed, at first sight, to a random distribution in the relative orientation of neighbouring molecular units,

implying that only the molar volume could give an estimate of the probability of finding a molecule at a given distance from another.

A local, or short-range order exists in amorphous solids in reality, and has been experimentally established for inorganic glasses, for instance, by means of X-ray spectroscopy. It can therefore be concluded that the immediate environment of a molecule may be similar, or even identical, in crystalline and amorphous phases. When considering that non-covalent interactions could have the same self-organising role in both types of solids, a recent suggestion is that the amorphous state may be considered as a precursor to the crystalline state (Petit *et al.*, 2006).

No clear-cut definition was found to differentiate between crystalline and amorphous solids. This was supported by the existence of several types of solid phases, where no intermediate states, having different types of disorders, occur. These partially crystalline solids are called mesophases (Petit *et al.*, 2006).

Depending on the type of disorder, mesophases can be classified into three categories of condensed matter. (1) In liquid crystals, the molecular shape induces an orientational order, but the packing lacks three-dimensional translational and conformational order. (2) The second category corresponds to plastic crystals, also called glassy crystals. In these crystals, only a translational order exists, and the absence of orientation and / or conformational order is often caused by the rounded shape of the molecules. (3) Finally, conformationally disordered crystals are well-known among organic and pharmaceutical compounds (Petit *et al.*, 2006).

Energetic aspects: thermodynamics and kinetics

Amorphous solids are commonly defined as thermodynamically, out of equilibrium states, since they necessarily contain an excess of Gibbs energy in the crystalline phases.

Theoretically, the various excess properties, i.e. enthalpy, entropy and free energy, can be quantified from heat capacities, as determined over the same temperature range for both the crystalline and the amorphous phases. The stored internal energy means that an amorphous solid is by definition an unstable state, which can release its energy excess, either completely through crystallisation associated with $\Delta G < 0$, or partially by means of irreversible relaxation processes (Petit *et al.*, 2006).

Figure 1.12 illustrates some energetic features of the amorphous state of enthalpy, or volume variations, as a function of temperature.

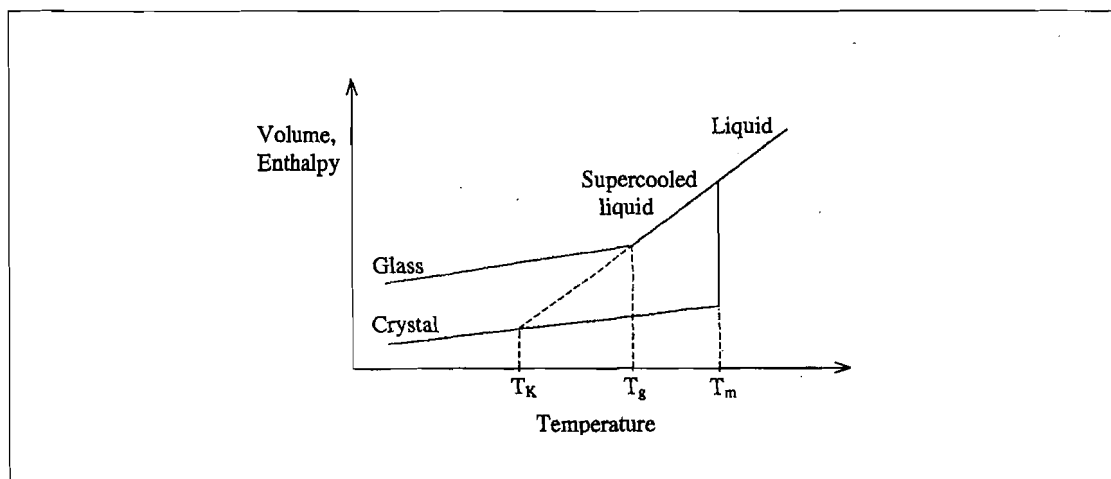


Figure 1.12 Graphic representation of enthalpy, or volume variations, as a function of temperature, for condensed materials (Petit *et al.*, 2006).

The slope of each segment in this graph represents the heat capacity of the corresponding state. When cooling a liquid to the melting point (T_m) of its crystal phase, a first-order phase transition should occur, which is associated with a decrease of free volume, because of thermal contraction effects. Water, however, is the exception to this phenomenon. Since the heat exchange that is associated with crystallisation, or melting of a compound, and because the T_m is purely of thermodynamic origin, its determination can be accurately achieved. Such value can thus, for example, be used to calibrate thermal analysis equipments (Petit *et al.*, 2006).

A huge challenge lies in establishing the nature and origin of different thermal, physical, and / or kinetic behaviours of two amorphous samples that are prepared by different routes. Such information may generate new ideas for the optimisation of stabilisation and manufacturing procedures.

Crystallisation of amorphous solids:

- “difficult-to-crystallise” compounds,
- inadvertent crystallisation, and
- crystallisation as a tool for insight into the amorphous state.

1.5 Forms versus habits

A form refers to the internal crystal structure, coming from the Greek word, morph. Hence, polymorph refers to a number of different crystal modifications, or different crystal structures, directly resulting in the classification of different structures as 'Form I', or '∞ Form'.

Only the structures which are thermodynamically accessible can ever exist, but there often is a question of thermodynamic *versus* kinetic control, regarding which particular structure may be obtained under any particular set of crystal growth conditions (Bernstein, 2002).

Habit comes from the Latin and Old French word for, mode of growth, and describes the shape of a particular crystal. That shape is greatly influenced by the environment. It is essentially a manifestation of kinetic factors, which determine the relative rate of growth along various directions of the crystal, and hence the preferential growth, or inhibition of the development of the different crystal faces that ultimately define the shape of the crystals. Figure 1.13 illustrates different habits and the variation in habits, resulting from changes in crystal growth conditions (Bernstein, 2002).

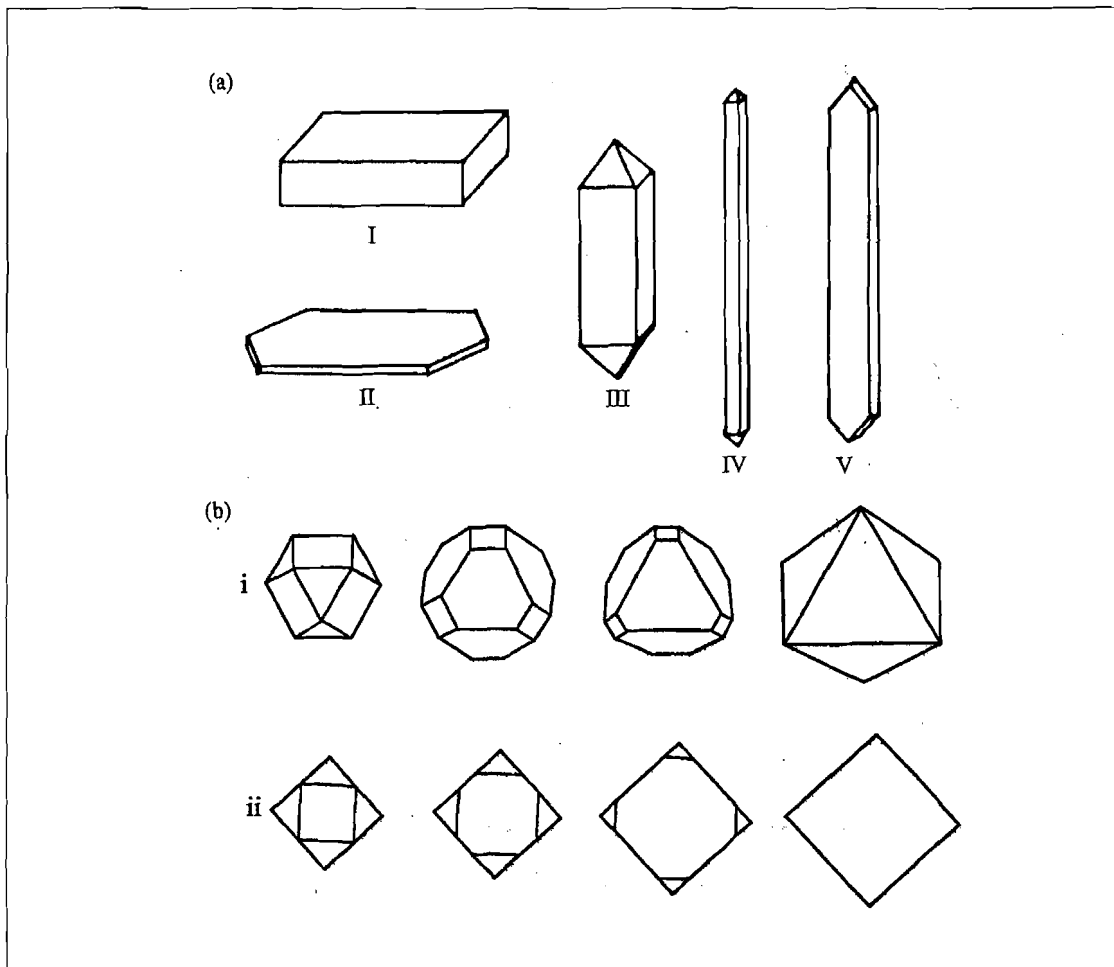


Figure 1.13 (a) Schematic representation of different crystal habits: (I) tubular; (II) platy; (III) prismatic; (IV) acicular; (V) bladed.

(b) Illustration of the differences in growth rates of cubic, or octahedral faces of a crystal, as governed by the rate of deposition on different crystal faces (Bernstein, 2002).

The term, form, is thus used to describe a set of crystal faces, which are alike, or symmetrically related, whereas habit describes the collection of the forms that are exhibited.

The study of the external shape and symmetry of crystals is called *crystal morphology*. It is important to note that the differences in external crystal shape, habit, or crystal morphology, may not necessarily indicate a change in the polymorphic form, or polymorphic crystal structure. An example of this distinction is given in Figure 1.14 (Bernstein, 2002).

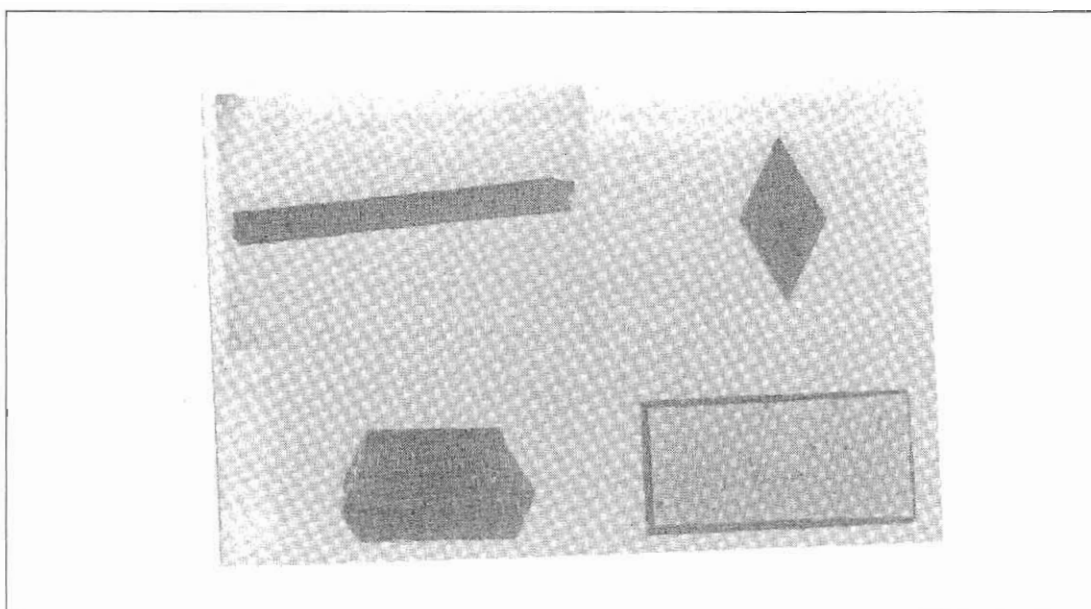


Figure 1.14 Illustration of the differences between crystal habit and polymorphic form for three polymorphs: Upper left = polymorph A; upper right = polymorph B; bottom two = polymorph C in two different habits (Bernstein, 2002).

1.6 Importance of controlling crystal forms

Knowledge of the polymorphic behaviour of a drug is important in the pharmaceutical industry, to ensure that the final product contains the desired polymorph. Sudden appearances, or disappearances of polymorphs, can present a problem in the development of the manufacturing process (Hilfiker *et al.*, 2006).

If the metastable form of a monotropic system is desired, precautions must be taken to maintain appropriate conditions that will avoid transformation from a metastable form into its stable polymorph. No such precautions are necessary if the stable form of a monotropic system is preferred (Hilfiker *et al.*, 2006).

According to Vippagunta *et al.* (2000), it is very important to control the crystal forms during the various stages of drug development, since any phase change, due to polymorphic interconversions, desolvation of solvates, formation of hydrates, or a change in the degree of crystallinity, can alter the bioavailability of the drug.

When a crystal goes through a phase transition, it may undergo a change in its thermodynamic properties, with consequent changes in its dissolution and transport characteristics.

Crystallisation thus plays a critical role in controlling the crystalline form and the distribution in size and shape of the drug.

1.7 Pharmaceutical importance of polymorphic forms

As was mentioned, polymorphism occurs frequently in pharmaceutical compounds. The investigation of polymorphism has become essential in the pharmaceutical industry, because the physico-chemical properties, such as solubility and particle morphologies of each polymorphic form, may differ.

The dissolution rate and solubility in a solvent medium are two of the most important characteristics of an active pharmaceutical ingredient, because these quantities determine the bioavailability of the drug for its intended therapeutic use (Brittain & Grant, 1999).

Crystal structures may have a direct effect on the solubility of a solid. Different lattice energies of polymorphs, or solvates, give rise to different solubilities and dissolution rates. If the solubilities of two forms are sufficiently different, it is important to consider such implications on the absorption of the active from the dosage form during the processing of drug substances into products (Haleblian & McCrone, 1969; Higuchi *et al.*, 1963).

The effect of polymorphism becomes especially critical, because the rate of compound dissolution must also be dictated by the balance of attractive and disruptive forces existing at the crystal-solvent interface. A solid having a higher lattice free energy, i.e. the less stable polymorph, will tend to dissolve faster, because the release of a higher amount of stored lattice free energy will increase the solubility (Brittain & Grant, 1999).

For a drug to be absorbed into the body from the gastro-intestinal tract, it must normally be in solution. For a drug to dissolve, it should be moistened by the liquid phase first (Forster *et al.*, 1991). Drugs with low water solubility, especially, require careful investigation in order to improve such formulations (Brittain & Grant, 1999).

It still remains one of the largest challenges to predict the number of polymorphic forms that a drug may have (Vippagunta *et al.*, 2001). Although computer technology aids in predicting possible polymorphic forms, based on the molecular structure of a substance, there are still many limitations to computational methods for such theoretical predictions (Vippagunta *et al.*, 2001).

1.8 Aims and objectives of this study

With the above theory in mind, the following objectives were identified with respect to triamterene and roxithromycin, two active pharmaceutical ingredients that are known for their poor water solubility:

- The preparation of different polymorphic and / or pseudopolymorphic forms of triamterene and roxithromycin, in an attempt to isolate a more water-soluble form.
- The investigation of the physical properties (i.e. solubility, stability, crystal morphology and thermal properties) of the different forms being prepared.
- To identify those polymorphic forms of roxithromycin that are most amorphous. In a study (Du Plessis, 2004) it was found that amorphous forms of roxithromycin became gel-like in dissolution media, causing major difficulties during dissolution studies.
- To investigate the respective solubility profiles of the various polymorphs of triamterene and roxithromycin, and to determine the influence of their crystal morphology on solubility.

CHAPTER 2

Methods for characterisation of triamterene and roxithromycin

2.1 Introduction

Every physical and / or chemical property of the polymorphic structures of a material may vary, since polymorphs represent different crystal structures. Any technique that measures the properties of a solid material may, in principle, be used to detect polymorphic structures. Some techniques are more sensitive to the differences in crystal structure, or molecular environment, as opposed to molecular structure, and in many cases these are preferred for detecting and characterising polymorphs (Bernstein, 2002).

The purpose of this chapter was to describe the analytical methods that were used during this study, for identifying and characterising the different polymorphic, pseudopolymorphic and amorphous forms being obtained from the recrystallisation of triamterene and roxithromycin. The analytical methods were:

- Microscopy:
 - thermo microscopy,
- Crystallography:
 - X-ray powder diffractometry (XRPD).
- Thermal methods of analysis:
 - differential scanning calorimetry (DSC),
 - thermogravimetry (TGA).
- Molecular motion:
 - infrared absorption spectroscopy.
- Solubility.
- Karl Fischer titrations.

2.2 Methods of analysis

2.2.1 Thermo microscopy

This method involves the microscopic observation of the behaviour of a crystal over a temperature range. The crystals are usually placed on a microscope slide (object plate), covered by a layer of silicone and a cover slide /plate.

The following types of behaviour are generally noticed during this analysis:

- The loss of solvent ;
- Sublimation of the crystal, where the crystal slowly disappears and condenses on the inside of the cover plate;
- Melting and re-solidification, indicating a phase change (polymorphic transformation), or solid-state reaction;
- Chemical reaction, which is characterised by a visible change in the appearance of the crystals (Byrn, 1982).

The most obvious application is the determination of the melting point of small samples. With experience, the true melting point, i.e. the temperature at which the solid and its melt are maintained at equilibrium, can be readily determined. This is hence used to characterise solids, although different polymorphs can have similar melting points (Bernstein, 2002).

A Nikon Eclipse E400 (Nikon, Japan) thermo microscope, equipped with a Metrathern 1200d heating unit and a Nikon Coolpix 5400 digital camera, was used to observe and record small samples of each triamterene and roxithromycin, after immersion in a drop of silicone oil on an object plate, and covered with a cover plate.

2.2.2 X-ray crystallography

This analytical method can lead to a complete determination of the structure of the solid and the determination of the packing relationships between individual molecules in the solid. X-ray crystallography generates an image of objects of atomic dimensions, not visible by light microscopy. This method makes use of Fourier synthesis (normally calculated on a computer) of the diffracted radiation, to achieve a focus on an image (Byrn, 1982).

In most cases, X-ray crystallographic methods, which reflect differences in crystals, can be definitive in the identification and characterisation of polymorphs. Single crystal structure

solution techniques are used for the determination of detailed molecular and crystal structures, whilst X-ray powder diffractometry (XRPD) is used for the qualitative identification of individual polymorphic phases, such as pseudopolymorphic and amorphous phases, or mixtures thereof (Bernstein 2002).

Figure 2.1 illustrates the diffracted X-ray beams from a crystal lattice, representing a distribution, or scattered radiation.



Figure 2.1 X-rays diffracted from a crystal lattice with spacing (d) between the planes and a diffraction angle of θ (Byrn, 1982).

All XRPD techniques are based on Bragg's law, with Bragg's condition being:

$$n\lambda = 2d \sin \theta$$

Where: d = particular spacing between individual parallel planes,

λ = wavelength of the x-ray radiation, and

θ = angle of incidence (Bernstein, 2002).

This equation states that an integer (n) times the wavelength (λ) must equal twice the distance (d) between planes, multiplied by the sine of the angle of incidence (θ) (Byrn, 1983).

The condition can be satisfied when the angle, θ , between the incident radiation and that set of planes, results in constructive interference (Bernstein, 2002).

2.2.2.1 X-ray powder diffractometry (XRPD)

The X-ray powder diffraction (XRPD) pattern of a solid is thus a graph of the diffraction intensity, as a function of 2θ values (or equivalently, (d) spacing) and may be considered to be a fingerprint of that solid (Bernstein, 2002).

XRPD is therefore the most specific method for identifying and distinguishing among polymorphs. Single crystal X-ray crystallographic techniques are used to determine details of the molecular and crystal structures of the solid-bond lengths, bond angles, intermolecular interactions, etc. Three-dimensional results are obtained and these results may be used to computationally simulate the two-dimensional diffraction patterns to be expected from powders of the same material. Such a calculated powder pattern may serve as a standard for the powder diffraction pattern, unencumbered by impurities, the presence of other polymorphs (Bernstein, 2002).

The preparation of the powder for powder diffraction, can lead to variations and inconsistencies among measurements on the same sample. Variations, such as those that may result from grinding, can lead to amorphism strain in individual particles, decomposition, solid state reaction, or contamination (Bernstein, 2002).

A Bruker D8 Advanced diffractometer (Bruker, Germany) was used to collect data on triamterene and roxithromycin. The procedure comprised the packing of approximately 200 mg of powdered samples into aluminium sample holders. The measurement conditions were: target, Cu; voltage, 40 kV; current, 30 mA; divergence slit, 2 mm; antiscatter slit, 0.6 mm; detector slit, 0.2 mm; monochromator; scanning speed, $2^\circ/\text{min}$ with step size, 0.025° and step time, 1.0 sec.

2.2.3 Thermal methods of analysis

Thermal methods have been a mainstay method for the study of polymorphs, providing a means of both identification and characterisation (Craig *et al.*, 2006).

Thermal analysis provides quantitative information about the relative stability of polymorphic modifications, the energies involved in phase changes between them, and the monotropic, or enantiotropic nature of those transitions.

Thermal methods are based on the principle that a change in the physical state of a material is accompanied by the liberation, or absorption of heat. These various techniques of thermal analysis are designed for the determination of the enthalpy accompanying the changes, by

measuring the differences in heat flows between the sample under study and an inert reference (Bernstein, 2002).

2.2.3.1 Differential scanning calorimetry (DSC)

In this method, the sample and reference are heated individually, and a null balance principle is employed, whereby any change in the heat flow in the sample is compensated for by the reference. This results in the temperature of the sample being maintained at the reference of heat flow. The signal which is recorded (dH/dt), is actually proportional to the differences between the heat inputs into the two channels, as a function of time (temperature), so that the integration under the area of the peak directly yields the enthalpy of the transition (Bernstein, 2002).

This method is also known as power compensation DSC, whereby the sample and reference are maintained at the same temperature and the heat flow, required to keep the two at thermal equilibrium, is measured, thereby allowing both the temperature and the energy, associated with a thermal event, to be easily assessed (Craig *et al.*, 2006).

Another closely related approach is heat flux DSC, whereby the heat differential between the two samples is measured as a function of temperature. The energy associated with the transition is calculated with the following equation (Craig *et al.*, 2006).

$$dQ / dt = \Delta T / R$$

Where: dQ / dt = heat flow,

ΔT = temperature difference between the furnace and the crucible, and

R = thermal resistance of the heat part between the furnace and the crucible.

DSC raw data shows the heat flow against temperature, where the heat flow refers to the heat flux difference between the sample and reference.

As a sample undergoes a thermal event, it is effectively altering the total heat capacity of the system, due to the latent heat associated with the melting, crystallisation, etc. This can be seen as a peak, or in the case of a glass transition, as a shift in the baseline. It should be noted, from a practical point of view, that unfortunately, some instruments show endotherms

as upward peaks and crystallisation exotherms as downward curves, while other use the opposite convention (Craig *et al.*, 2006).

A mass of approximately 2 – 4 mg each was weighed and heated in closed aluminium crimp cells with pierced lids, at a heating rate of 10°C/min. The Mettler Toledo DSC 823^e (Mettler, Switzerland) was used. The samples were heated under a nitrogen purge with a flow rate of 50 ml/min, to a maximum temperature of 330°C (triamterene) and 120°C (roxithromycin). The thermogram being recorded is a graph of the difference in heat flow (heat flow of the sample and heat flow of the reference) against T (temperature).

The endothermic peaks represent the absorbed heat, solvent loss, phase transitions, or melting (Byrn *et al.*, 1999).

2.2.3.2 Thermogravimetric analysis (TGA)

This instrument consists of a microbalance that is connected to a sample compartment, situated in a small oven, with computer-controlled temperature programming. A dry nitrogen atmosphere is mostly used. This method of analysis measures the change in mass with temperature and is often used to study the loss of solvent or crystallisation of other solid → solid and gas reactions (Byrn *et al.*, 1999).

TGA provides information on the presence of volatile components, which, in the context of this study include solvents and water, which form the basis of solvates or hydrates, respectively. TGA also gives information relating to processes, such as decomposition and sublimation (Bernstein, 2002).

The major use of TGA is the quantitative determination of total volatile content of a solid, such as when a solid decomposes by means of several discrete, sequential reactions, the magnitude of each step can be separately evaluated. Analysis of compound decomposition can also be used to compare the stability of similar compounds (Brittain, 1995).

The TGA is usually performed in one of three modes:

1. Isothermal mode – the temperature is kept constant.
2. Quasi-isothermal mode – the sample is heated to a constant mass through a series of increasing temperatures.
3. Dynamic mode – the temperature is raised at a known rate, typically linear (Byrn *et al.*, 1999).

The TGA curves are affected by a number of factors and conditions, such as: heating rate, atmosphere, geometry of the sample holder (pan), particle size of the sample, nature of the reaction, treatment of the sample, thermal conductivity of the sample, and sample weight (Byrn *et al.*, 1999).

A quantity of 5 – 8 mg of the sample each was weighed into 100 µl aluminium pans with pierced lids that were not crimped. The changes in mass at elevated temperatures were recorded on the Mettler, TGA / SDTA851° (Mettler, Switzerland) and the Shimadzu TGA-50 instruments (Shimadzu, Kyoto, Japan). The samples in the Mettler were heated at a rate of 10°C/min under a nitrogen purge of 50 ml/min, to a maximum temperature of 260°C (triamterene) and 120°C (roxithromycin). Samples heated in the Shimadzu were heated at a heating rate of 10°C/min under a nitrogen purge of 35 ml/min, to a maximum temperature of 330°C (triamterene).

The theoretical weight loss was calculated using the equation below, and then compared to the weight loss as determined with the two thermal analysis instruments, as mentioned above, for solvated samples.

$$\% \text{ weight loss} = \frac{\text{Molecular weight (solvent)}}{\text{Molecular weight (solvent) + molecular weight (API)}}$$

2.2.4 Molecular motion: vibrational spectroscopy

Infrared (IR) spectroscopy is one form of vibrational analysis of a molecular entity and it is used as an identification assay for various intermediates and final bulk drug products, and also as a quantitative technique for solution-phase studies (Brittain, 1995).

Most solid-state investigations of bulk drug materials involve the identification and quantification of polymorphic and pseudopolymorphic systems. Different polymorphic forms exhibit different three-dimensional structures, meaning that the vibrational motion for each polymorphic form is potentially different, hence the ability to investigate polymorphism by vibrational spectroscopy techniques. Other areas include: drug delivery systems, drug-excipient interactions, crystallisation studies, mixing studies, particulate / contaminant characterisation, and solid state transformations (Brittain, 1995).

2.2.4.1 Infrared absorption spectroscopy (IR)

IR spectroscopy is very useful for the analysis of solids, because it can be performed without dissolution of the sample. The generation of IR spectra of solids comprises grinding of the sample and measuring its IR spectrum, after mixing the powdered sample with KBr (Byrn *et al.*, 1999).

The IR spectrum is extremely sensitive to the structure, conformation, and environment of an organic compound, and is thus a powerful method for the characterisation and identification of different solid forms (Byrn *et al.*, 1999).

IR spectra were recorded on a Nicolet Nexus 470-FT-IR spectrometer (Nicolet instrument corporation, Maddison, USA) over a range of 400 – 4000 cm^{-1} . Potassium bromide (KBr) was used as a background. The sample was dispersed in a matrix of powdered KBr. The IR-spectra were measured in a reflectance cell, using diffuse reflectance infrared Fourier transform spectroscopy (DRIFTS).

The IR spectral results being generated were then compared to determine possible differences that could indicate different polymorphic, pseudopolymorphic, or amorphous forms.

2.2.5 Solubility

A 24-hour solubility test was performed, using three media, i.e. 0.1 N HCl, phosphate buffer, and milli-Q water. Approximately 0.2 g of each sample was weighed into 10 ml test tubes with screw caps; 5 labeled test tubes for each solvent. 5 ml of solvent was added to the samples. These samples were rotated at 54 rpm (Heidolph RZR-2000 rotator, Germany), in a thermostatically (Julabo EM/4 thermostat, Germany) controlled water bath at $39 \pm 2^\circ\text{C}$.

After 24 hours the samples were removed from the bath and withdrawn, using a 10 ml syringes per sample, to which a 0.45 μm , low protein binding, durapore (PVDF) membrane was attached. 2 ml of each sample was diluted to 50 ml, using the 3 mediums. The concentrations of the diluted samples were determined spectrophotometrically at 206 nm. A Beckman DU-650i spectrophotometer (USA) was used.

2.2.5.1 Validation of UV method

A calibration curve was obtained by measuring the absorbances of various concentrations of roxithromycin solutions. A Beckman DU-650i spectrophotometer (USA) was used.

A 0.22 g/ml standard solution was made, by dissolving 0.11 g of roxithromycin raw material in approximately 10 ml of methanol, which was then further diluted to 50 ml with milli-Q water. From this standard solution 1, 3, 5, 7, 8, and 10 ml samples were taken, and each further diluted to 100 ml with milli-Q water.

Table 2.1 shows the results that were generated.

Table 2.1 The absorbance of roxithromycin solutions at different concentrations

Concentration (mg/ml)	Absorption
0	0.000
2.2	0.116
6.6	0.312
11	0.510
15.4	0.711
17.6	0.847
22	1.069

The calibration curve of the above results is illustrated in Figure 2.2.

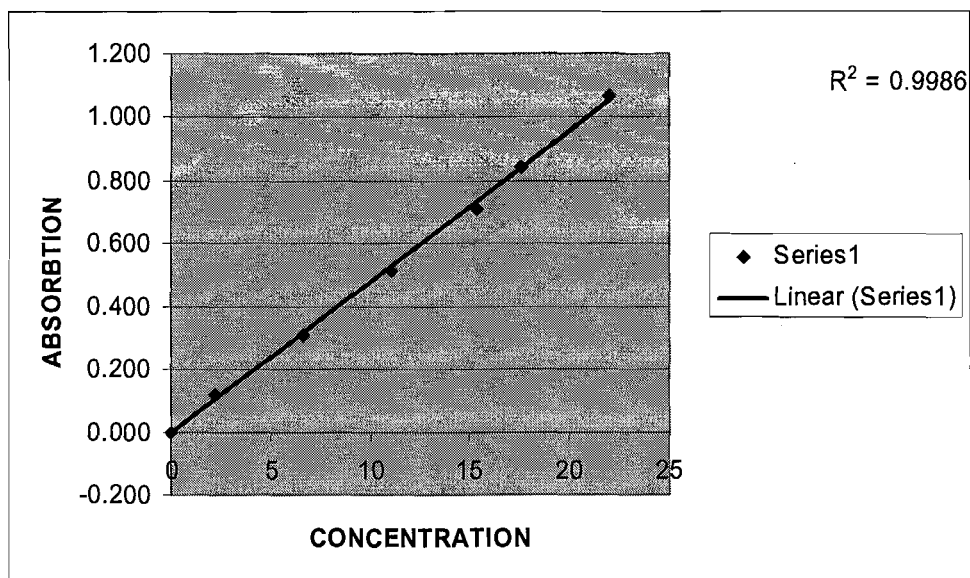


Figure 2.2 Calibration curve of the absorbances of roxithromycin solutions at different concentrations.

The following equation was used to calculate the percentages being dissolved:

$$\% \text{ Dissolved} = \frac{\text{absorbance (sample)} \times \text{concentration (standard)} \times \text{volume (solvent)} \times 100 \times 50}{\text{Average (standard absorbance)} \times \text{mass (sample)} \times 2}$$

2.2.6 Karl Fischer titrations

The moisture content in a crystalline solid is determined by Karl Fischer titration. This assists in the identification and characterisation of pseudopolymorphs. Karl Fischer is often used in conjunction with TGA, to determine the total volatile content of a sample, as discussed in section 2.2.3.2.

The moisture contents of the samples were determined, using a Metrohm 701 KF Titrino autotitrator (Metrohm, Switzerland). Calibration of the instrument was performed using a predetermined mass of water and approximately 250 mg of sodium tartrate dihydrate dibasic powder. Approximately 0.05 mg to 0.150 mg of each sample was used for the moisture determination. The test was performed in duplicate for each crystal form. The percentages of water (m/m) within the samples were then calculated.

2.3 Conclusion

Drug substances can exist in various solid forms. Characterisations of these physico-chemical properties are important when considering the development of solid dosage forms.

Various methods of analysis include microscopy, crystallography, thermal analysis, molecular motion, solubility, and Karl Fischer titrations. These methods are combined in this study for the identification and characterisation of triamterene and roxithromycin crystals. The results obtained for the different crystal forms will be discussed in the following chapters.

CHAPTER 3

Triamterene

3.1 Introduction

Triamterene, a 6-phenyl-2,4,7-pteridinetriamine, is widely used as a potassium sparing diuretic, when on its own, and also in combination with diuretics, such as furosemide and hydrochlorothiazide (Dahl *et al.*, 1987).

According to Dahl *et al.* (1987), it had been shown through several physico-chemical techniques, that the existence of different crystal forms of triamterene, as well as the crystalline products, recrystallised from different solvents, with distinct differences in melting points, did not necessarily imply polymorphic crystal forms.

Polymorphism means many forms of a molecule in the crystalline state, but not necessarily having the same conformation in the crystal lattice. The differences in the melting points of 316°C and 327°C for triamterene, which have been reported, can either be due to polymorphism, or pseudopolymorphism (Dahl *et al.*, 1987).

3.2 Description

3.2.1 Nomenclature

Chemical name

2, 4, 7-triamino-6-phenylpteridine or 6-phenyl-2, 4, 7-pteridinetriamine.

(Dahl *et al.*, 1987).

Non-proprietary name

Triamterene.

Proprietary names

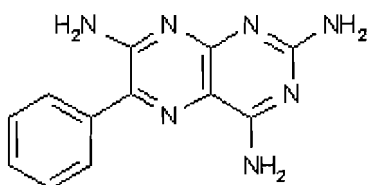
Maxzide®, Byazide®, Dyrenium®.

3.2.2 Formulae

Empirical formula

C₁₂H₁₁N₇ (Kapoor, 1994).

Structural formula



(Axxora platform, 2007).

3.2.3 Molecular weight

253.27 g/mol (Kapoor, 1994).

3.2.4 Appearance and colour

Triamterene is a yellow, crystalline and odourless powder (Kapoor, 1994).

3.3 Physical properties

3.3.1 Solubility

Triamterene is insoluble in benzene, toluene, absolute butanol, dimethylformamide, ethyl acetate, and absolute ethanol and methanol.

It is slightly soluble in water (1 in 1000), in ethanol (1 in 3000) and in chloroform (1 in 4000) and it is practically insoluble in ether (Kapoor, 1994).

Triamterene is soluble in formic acid, and also in a number of solvents at various temperatures, such as: dimethylformamide:water (1:1 v/v), butanol:water (1:1 v/v), methanol:water (1:0.5 v/v), dry methanol, and ethyl acetate:water (Kapoor, 1994).

Mixtures of glycols and lactic acid, or lactate, have also been used to solubilise triamterene, or in combination with hydrochlorothiazide (Kapoor, 1994).

3.3.2 Crystal properties

In a previous study (Kapoor, 1994), various crystal forms with different morphologies were obtained from different recrystallisation solvents, as summarised in Table 3.1.

Table 3.1 Various crystal forms recrystallised from different recrystallisation solvents (Kapoor, 1994)

Solvents	Crystals
DMF:water	Colourless parallelepiped
Butanol Methanol Ethanol Ethyl acetate	Needle growth
Ethanol:water Butanol:water DMF:water	Columnar shaped and condensed
Butanol:water	Spiny plates
Ethyl acetate:water	Needle growth
Benzene:ethanol (butanol) Ethyl acetate	Needle growth

3.4 Pharmaceutics of triamterene

3.4.1 Pharmaceutics

Triamterene is a potassium sparing diuretic and is only available in combination preparations in South Africa Formulary (SAMF), (Gibbon, 2003).

The combination of a thiazide diuretic with a potassium sparing component is usually not essential, but it reduces concern about the potential adverse arrhythmogenic effects of low plasma potassium or magnesium, or other side-effects, which may be related to electrolyte imbalances (Gibbon, 2003).

Triamterene and hydrochlorothiazide preparations that are available on the market are, according to the Monthly Index of Medical Speciality (Johnnic communications, Feb. 2004):

- Dyazide® (PharmaAfrica)
 - This combination contains 25 mg hydrochlorothiazide and 50 mg triamterene;
 - Schedule 3 medication;
 - Available as capsules and therefore only for oral administration;
 - Available in packaging of 28;
 - Store at room temperature and away from light.

- Renezide® (Pharmacare)
 - This combination contains 25 mg hydrochlorothiazide and 50 mg triamterene;
 - Schedule 3 medication;
 - Available as tablets and therefore only for oral administration;
 - Available in blister packaging of 28 and securitainers of 250 tablets;
 - Store below 25°C and in tightly closed containers. Protect from light.

- Rolab-Triamterene/ Hydrochlorothiazide® (Rolab)
 - This combination contains 25 mg hydrochlorothiazide and 50 mg triamterene;
 - Schedule 3 medication;
 - Available as tablets and therefore only for oral administration;
 - Available in packaging of 30 and 1000.

- Loretic® (Merck generics)
 - This combination contains 25 mg hydrochlorothiazide and 50 mg triamterene;
 - Schedule 3 medication.

3.4.2 Dosage and administration

An oral dose of 25 – 50 mg daily, as a single dose, is recommended for adults. The dose regimens vary from 1 tablet twice daily, or every second day, to 1 tablet daily or alternative day. Maximum number of tablets allowed per day is 4. It is advised to take the tablet after meals (Johnnic communications, Feb. 2004).

The safety and efficacy have not been established in paediatric dosages. If triamterene medication upsets the stomach, it should be taken with food or milk (Johnnic communications, Feb. 2004).

3.5 Pharmacology of triamterene

3.5.1 Pharmacokinetic properties

Studies have been carried out on guinea pigs, baboons, rats, rabbits and on human subjects (Kapoor, 1994).

3.5.1.1 Absorption

Triamterene is variably, but fairly rapidly absorbed from the gastrointestinal tract (Kapoor, 1994).

3.5.1.2 Metabolism

Triamterene is metabolised extensively and is mainly excreted in the urine as metabolites, with some unchanged triamterene (Kapoor, 1994).

According to the SAMF (Gibbon, 2003), hepatic metabolism is extensive, with some active metabolites having half lives up to 12 hours. Triamterene is mainly eliminated in the faeces *via* the bile, but also renally.

3.5.1.3 Distribution

The plasma and urinary levels of triamterene and its two metabolites have been measured, using a specific method of analysis. Urinary excretion was completed after 48 hours and a rough estimate of triamterene's half life was estimated as 6 - 12 hours (Kapoor, 1994). According to the SAMF, triamterene's half life is 1.5 - 2.5 hours. Peak plasma triamterene concentrations of 0.03 - 0.15 µg/ml were obtained in 1 - 2 hours, after single oral doses of 150 - 300 mg were administered (Gibbon, 2003).

3.5.1.4 Excretion

Peak plasma concentrations of p-hydroxytriamterene sulfate averaged at approximately 2 - 4 hours. Both the unchanged drug and the metabolite exhibited a second peak concentration several hours later, possibly due to entering the hepatic circulation. The concentrations of triamterene were 672.5 and 1311.3 µg/ml × hours after oral administration of 150 mg and 300 mg, respectively, and correspondingly 4.2 and 3.7% of the doses were excreted as

unchanged drug. The principal metabolite of triamterene was found to be p-hydroxytriamterene sulfate conjugate. The concentrations of this metabolite were 6.672 and 11.941 $\mu\text{g/ml} \times \text{hours}$ after administration of doses of triamterene of 150 and 300 mg, respectively (Kapoor, 1994).

3.5.2 Working mechanism of triamterene

According to Ives (2001), potassium sparing diuretics reduce sodium (Na) absorption in the collecting tubules and ducts. These sites of Na absorption and potassium (K) secretion are regulated by aldosterone. At any given rate of Na delivery, the rate of distal K secretion is positively correlated with the aldosterone level. Aldosterone is responsible for enhancing K secretion by increasing Na/K ATPase activity and Na and K channel activities in the collecting tubule, where Na absorption takes place and a lumen negative electrical potential is generated, which enhances K secretion (Ives, 2001).

Triamterene does not block the aldosterone receptor, instead it directly interferes with Na entry through the Na selective ion channels in the apical membrane of the collecting tubule. Since K secretion is coupled with Na entry in this segment, these agents are also effective K sparing diuretics (Ives, 2001).

3.5.3 Indications and therapeutic uses of triamterene

Triamterene is used for the treatment of oedematous states and hypertension, especially where a potassium sparing effect is required (Gibbon, 2003).

Diuretics increase the amount of urine that is passed, which causes the body to lose water and salt. Triamterene is used to treat water retention and swelling caused by conditions, such as heart -, kidney -, and liver diseases. Triamterene does not reduce the body's potassium the way that diuretics do (St. John Health, 2006).

3.5.4 Drug interactions

Triamterene has an interaction with a number of drugs and should therefore not be taken with the following drugs (St. John Health, 2006):

- Amantadine;
- Anti inflammatory drugs;

- Cyclosporins;
- Dofetilide;
- Heparin;
- Lithium;
- Medicines for diabetes that are taken by mouth;
- Medicines for high blood pressure;
- Potassium salts; and
- Water pills.

Abnormal elevations of the blood potassium are generally found in patients with kidney disorders, and in the elderly. This combination of drugs may, during medication, cause sunburns on direct exposure to the sun (Medicinenet, 2006).

There are also drug interactions with the following dietary supplements (Dilicious living, 2007):

- Calcium: triamterene causes an increase in calcium loss.
- Folic acid: triamterene acts as a folic acid antagonist and may cause folic acid anemia.
- Magnesium: triamterene is believed to inhibit the urinary excretion of magnesium.
- Potassium: urinary loss of potassium is reduced by triamterene and can lead to elevated levels of potassium.
- Sodium: triamterene causes an increased loss of sodium in the urine.

Interactions with herbs were also reported (Dilicious living, 2007). It is therefore advisable to avoid taking herbs that have a diuretic effect, because they enhance the effect of these drugs and may lead to cardiovascular side-effects. The following herbs should be avoided:

- Dandelion;
- Uva ursi;
- Juniper;
- Buchu;
- Cleavers;
- Horsetail; and
- Gravel root.

3.5.5 Side-effects

Triamterene has the following side-effects and their occurrence should be reported to a health care professional as soon as possible (St.John Health, 2006):

- Black, tarry stools;
- Blood in urine;
- Bright red tongue, burning feeling in tongue, dry mouth, cracked corners of mouth;
- Confusion, nervousness;
- Cough hoarseness;
- Fast, or irregular heartbeats, palpitations, chest pain;
- Fever, or chill;
- Lower back, or side pain;
- Muscle pain, or cramps; numbness, or tingling in hands, teeth, or lips;
- Pain, or difficulty passing urine; reduced amount of urine passed;
- Skin rash, itching;
- Unusual bleeding, or bruising; pinpoint red pots on the skin;
- Unusual tiredness, or weakness;
- Yellowing of the eyes, or skin.

The following sides effects may also be present and don't require medical attention (St.John Health, 2006):

- Diarrhoea;
- Dizziness;
- Headache;
- Increased sensitivity to the sun;
- Nausea, vomiting.

3.6 Literature study

In a study by Dahl *et al.* (1987), they prepared triamterene crystals with water free DMF (dimethylformamide) and DMF:water mixtures containing 10% (m/m) water.

3.6.1 Recrystallisation results

The results obtained by Dahl *et al.* (1987) showed that triamterene crystals, obtained from DMF:water solutions, were colourless, parallelepiped crystals.

The melting point of the crystals obtained from DMF solution ranged between 321 - 324°C, and those obtained from DMF:water solutions ranged between 310 - 318°C.

The thermogravimetric analysis determined a 26% weight loss in crystals obtained from a DMF:water solution. Figures 3.1(a) and (b) illustrate the DSC and TGA results that were obtained.

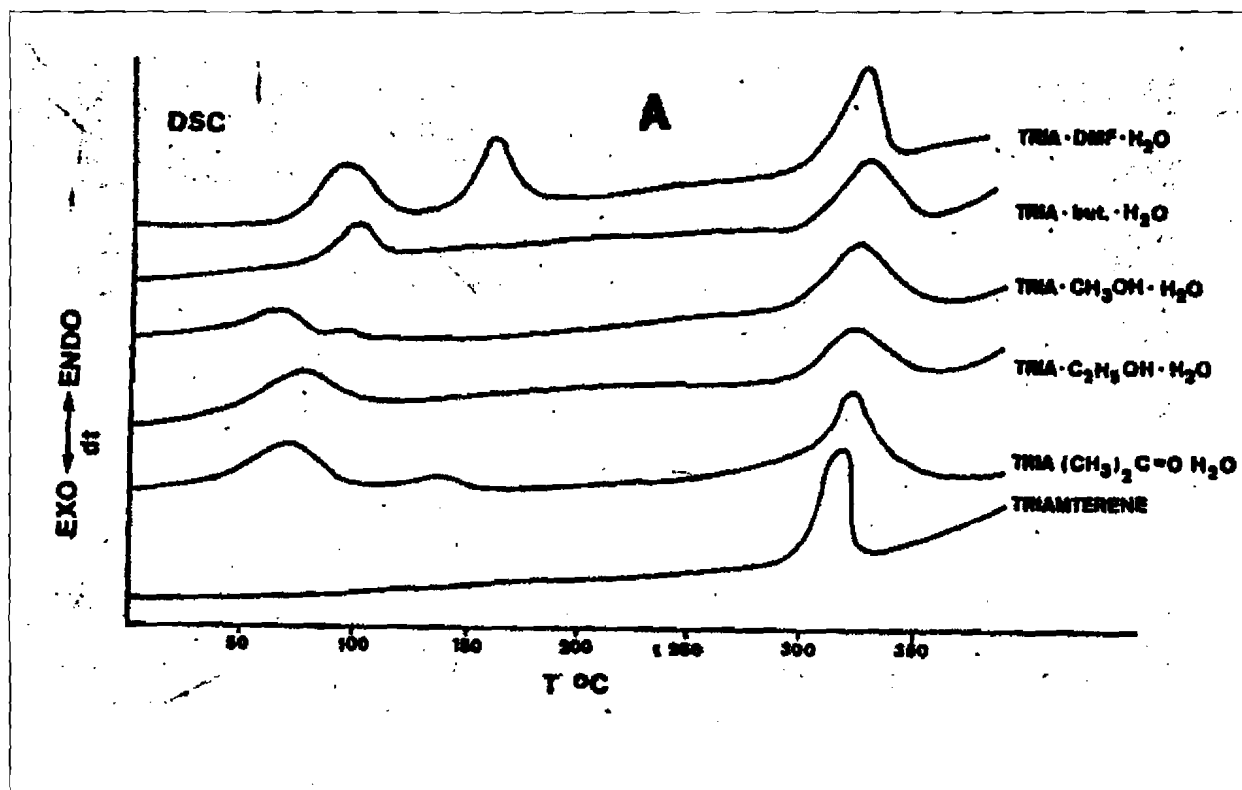


Figure 3.1(a) DSC thermogram of recrystallised DMF crystals (Dahl *et al.*, 1987).

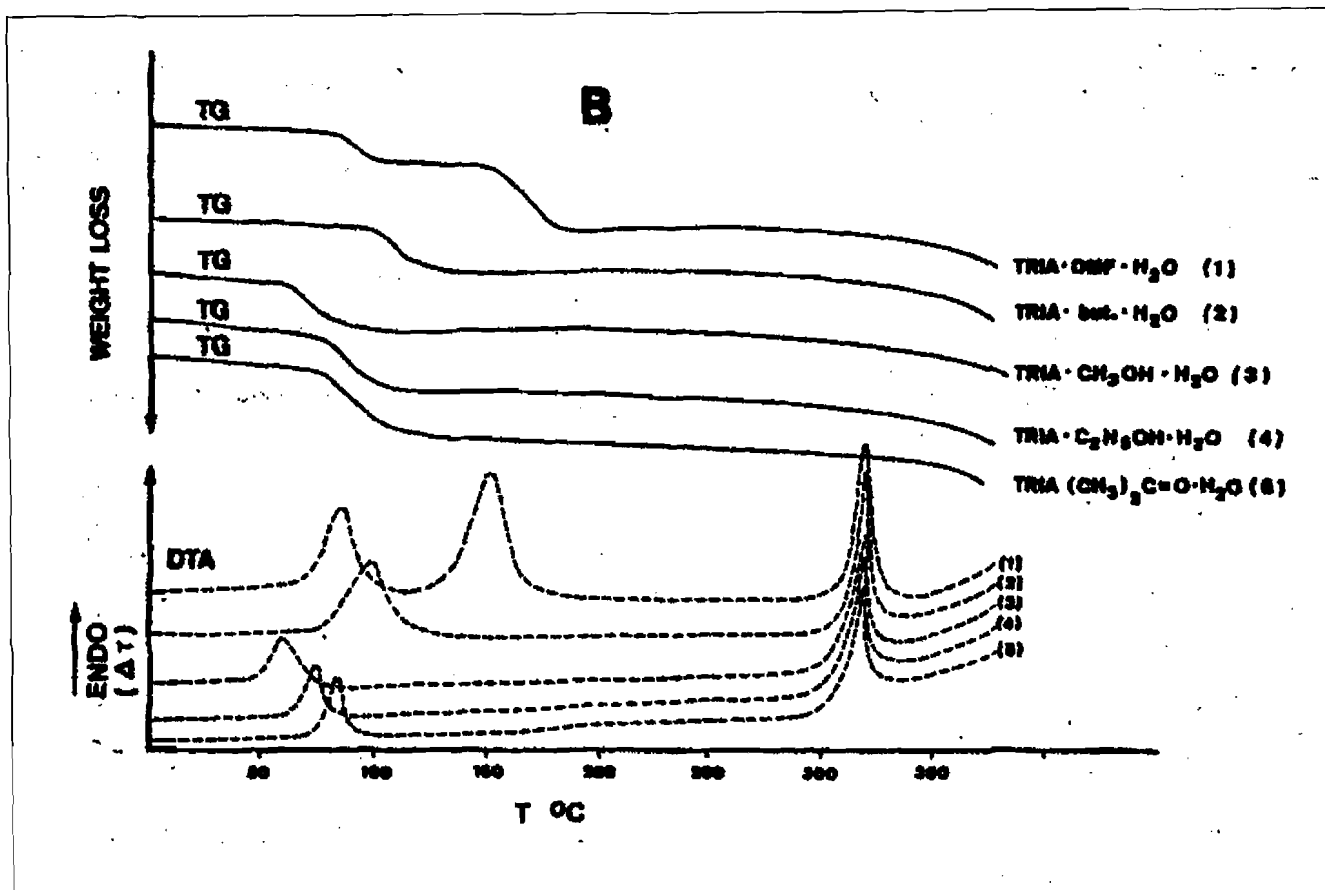


Figure 3.1(b) TGA and DTA thermogram of recrystallised DMF crystals (Dahl *et al.*, 1987).

IR spectroscopy showed that crystals, obtained from DMF, and DMF:water solutions, differed between 500 and 1800 cm^{-1} . This distinguished the triamterene crystals, obtained from DMF:water solutions, from the other triamterene crystals that formed in the absence of DMF and water, which were all similar.

Figure 3.2 shows the XRPD that were obtained with their study.

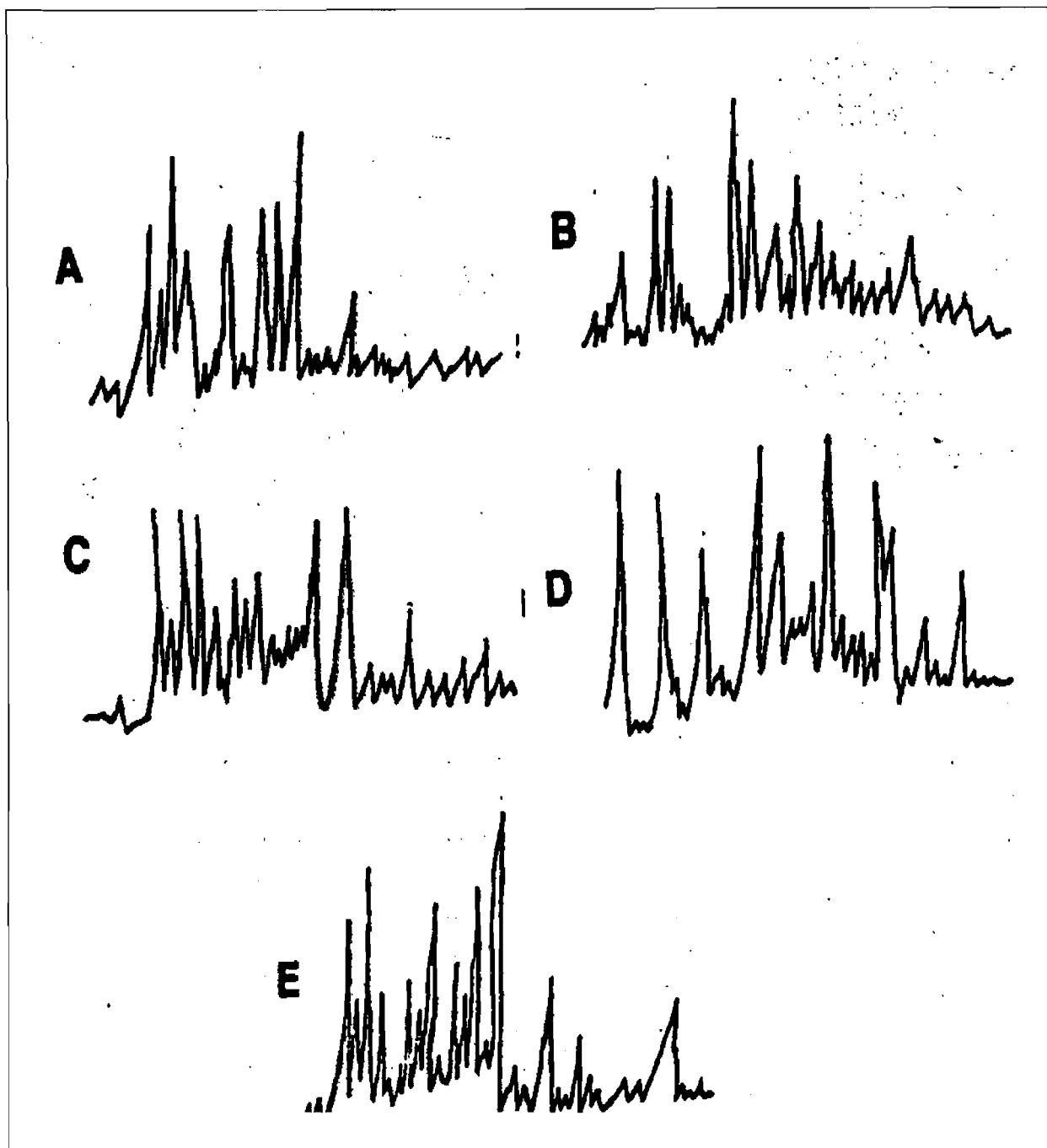


Figure 3.2 XRPD patterns of different crystalline forms of triamterene: (A) CH₃OH-triamterene-H₂O; (B) triamterene-H₂O; (C) triamterene-H₂O-C₄H₉OH; (D) triamterene-C₂H₅OH; and (E) triamterene-DMF (Dahl *et al.*, 1987).

3.6.2 Discussion of the data generated

From the test results obtained by Dahl *et al.* (1987), it can be deduced that hydrate solvate crystals were recrystallised from DMF, and DMF:water solutions. These crystals showed

different behaviour than those obtained from alcohol solutions in the absence of water and other solvents (Dahl *et al.*, 1987).

3.7 Study of the physico-chemical properties of triamterene raw material

3.7.1 Results obtained during this study

The physico-chemical properties of the triamterene polymorphic forms and that of the raw material were investigated using the analytical methods as was described in Chapter 2.

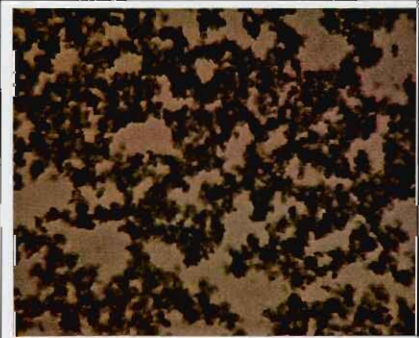
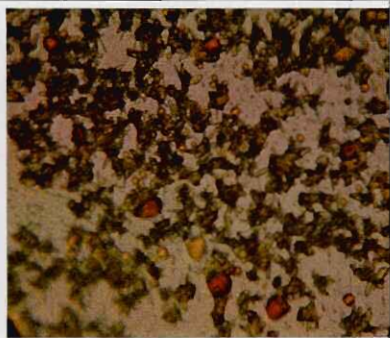
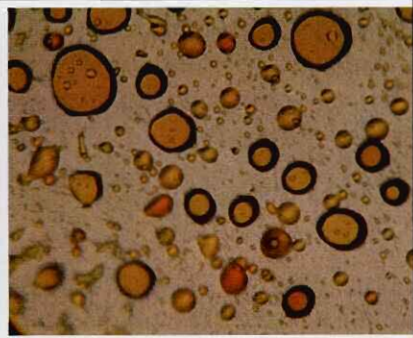
3.7.1.1 Thermo-microscopy (TM)

The triamterene raw material (B/N: 0503428, Dipharma Franscis) was observed on a thermo-microscope at elevated temperatures.

A small sample of triamterene raw material was immersed in a drop of silicone oil on an object plate, and covered with a cover plate.

Table 3.2 illustrates TM pictures of the triamterene raw material, at elevated temperatures.

Table 3.2 TM results of triamterene raw material

		
Triamterene raw material at 56°C	Triamterene raw material at 316°C	The melting process at 317°C

3.7.1.2 X-ray powder diffractometry (XRPD)

According to Bernstein (2002), an XRPD pattern serves as a fingerprint of a specific crystal form. This technique can therefore be used as a reliable method to characterise and identify the different crystals forms of triamterene. It is also the primary method of polymorphic characterisation, according to Brittain (1999).

Triamterene raw material was carefully ground and prepared for XRPD analysis.

The procedure comprised the packing of approximately 200 mg of powdered samples into aluminium sample holders. The measurement conditions were: target, Cu; voltage, 40 kV; current, 30 mA; divergence slit, 2 mm; antiscatter slit, 0.6 mm; detector slit, 0.2 mm; monochromator; scanning speed, 2°/min with step size, 0.025° and step time, 1.0 sec.

The peak angles ($^{\circ}2\theta$) and relative intensities (I/I_0) of the main peaks of the XRPD are listed in Table 3.3, whilst the XRPD pattern of triamterene raw material is illustrated in Figure 3.3.

Table 3.3 Main XRPD intensity ratios (I/I_0) and main peak angles ($^{\circ}2\theta$) of triamterene raw material

Peak angles ($^{\circ}2\theta$)	Relative intensities (I/I_0)
9.4	100
11.4	13.3
13.0	4.9
14.8	11.7
15.0	10.4
15.4	3.9
16.0	1.7
16.5	6.7
16.9	8.8
17.9	9.1
18.9	3.4
19.6	7.3
20.3	0.8
21.0	13
21.4	21.3
21.6	22.3

21.8	15.2
23.0	3.5
23.4	1.7
24.3	2.2
25.1	4.8
26.4	45.2
28.7	5.3
29.1	4.8
29.8	3.8
30.6	2.1
31.0	2.8
31.4	4.5
33.0	1.7
34.3	1.1
21.6	22.3
21.8	15.2
23.0	3.5

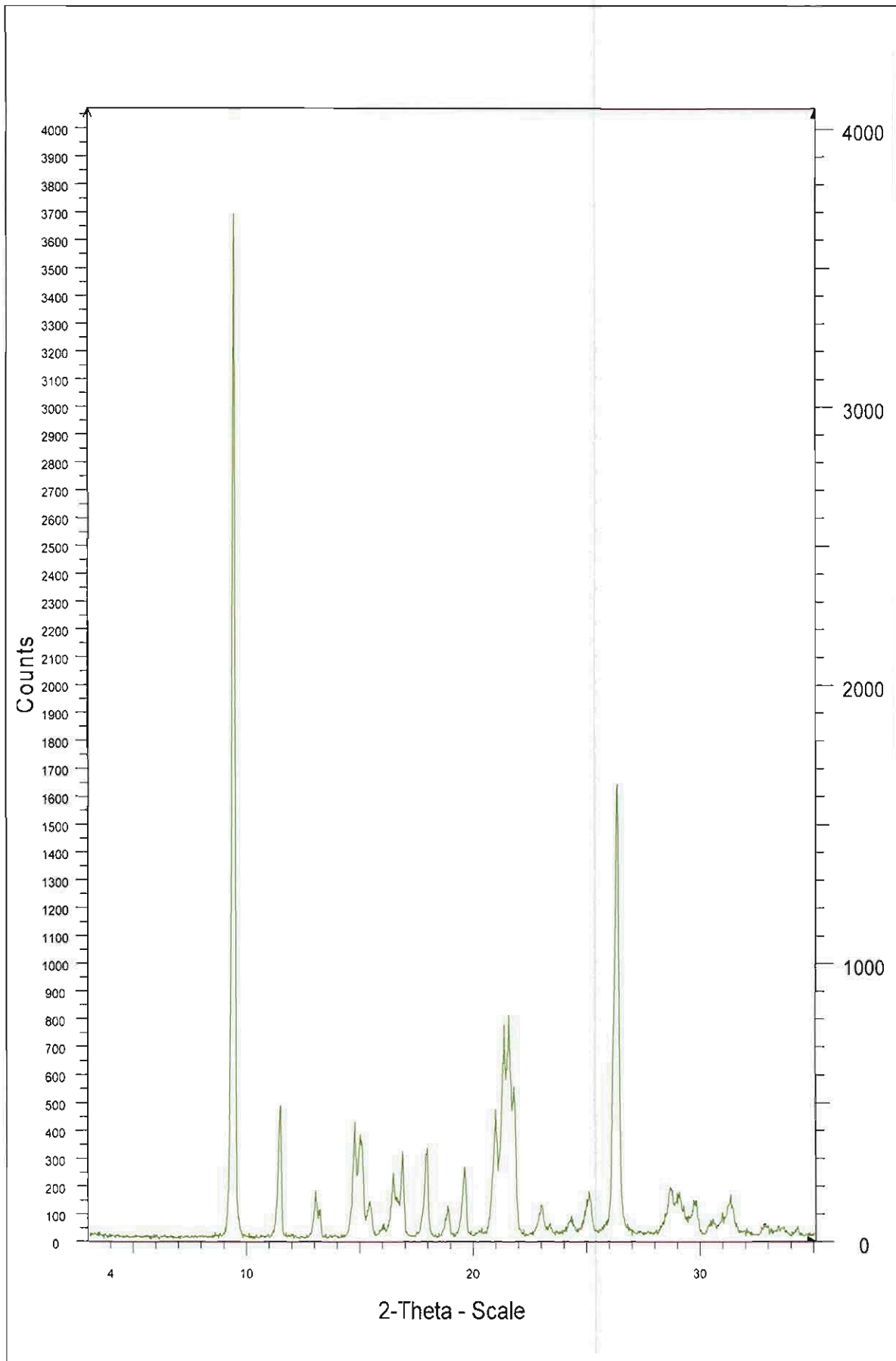


Figure 3.3 XRPD pattern obtained for triamterene raw material.

3.7.1.3 Differential scanning calorimetry (DSC)

According to Craig *et al.* (2006), thermal methods have been a mainstay method for the study of polymorphs, providing a means of both identification and characterisation. According to Bernstein (2002) also, thermal methods are based on the principle that a change in the physical state of a material is accompanied by the liberation, or absorption, of heat.

Thermal analysis includes differential scanning calorimetry (DSC), thermogravimetric analysis (TGA) and thermo-microscopy (TM).

According to Byrn *et al.* (1999), the sample and reference are maintained at the same temperature, and the heat flow, required to keep the two at thermal equilibrium, is measured, thereby allowing both the temperature and the energy, associated with a thermal event, to be easily assessed. Hence, it measures the difference in energy between the reference and sample.

A mass of approximately 2 – 4 mg each was weighed and heated in closed aluminium crimp cells with pierced lids, at a heating rate of 10°C/min. The samples were heated under a nitrogen purge with a flow rate of 50 ml/min, to a maximum temperature of 400°C.

Figure 3.4 illustrates the thermogram of triamterene raw material.

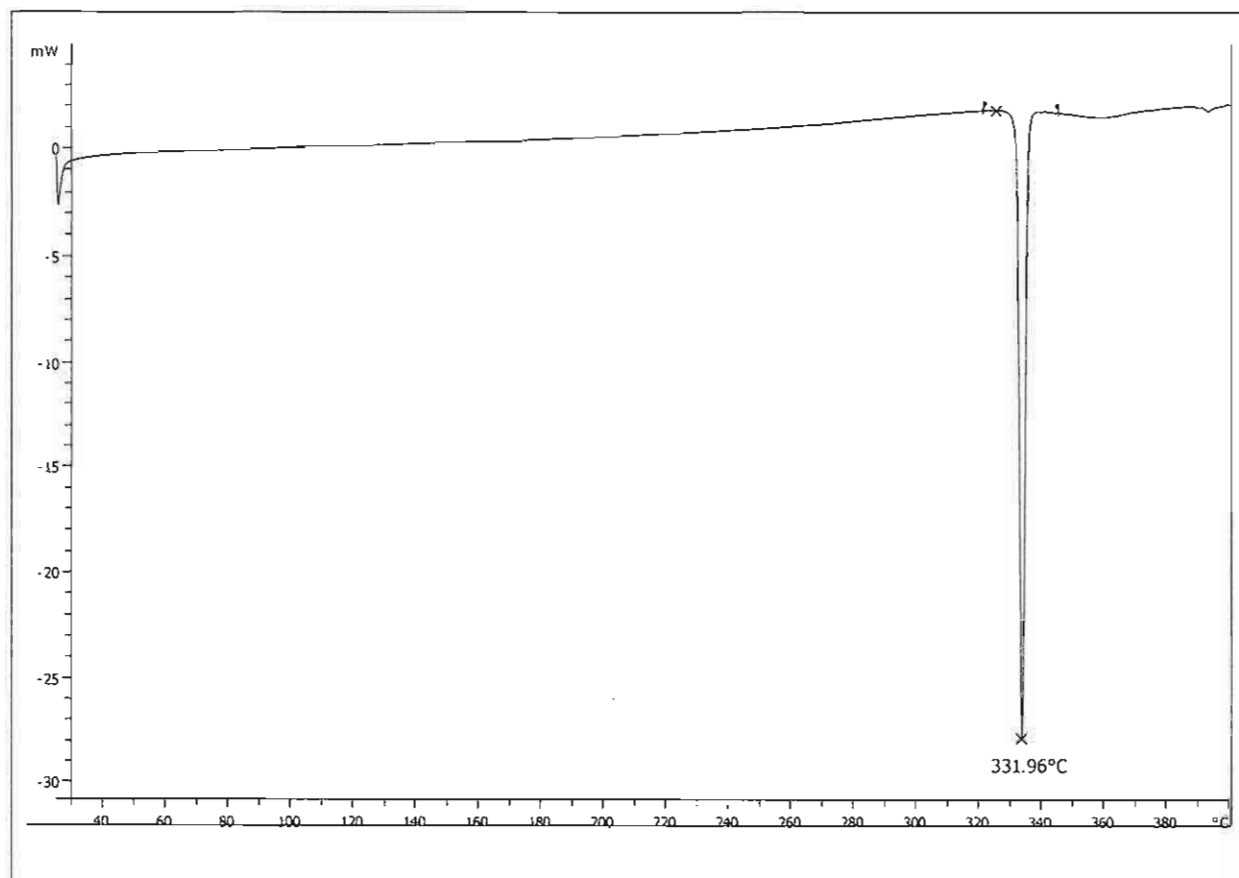


Figure 3.4 The DSC thermogram of triamterene raw material.

3.7.1.4 Thermogravimetric analysis (TGA)

According to Bernstein (2002), the TGA provides information on the presence of volatile components, which, in the context of this study include solvents and water, which form the basis of solvates or hydrates, respectively. TGA also gives information relating to processes, such as decomposition and sublimation (Bernstein, 2002).

A quantity of 5 – 8 mg of the sample each was weighed into 100 μ l aluminium pans with pierced lids that were not crimped. The samples in the Mettler were heated at a rate of 10°C/min under a nitrogen purge of 50 ml/min, to a maximum temperature of 240°C. Samples heated in the Shimadzu were heated at a heating rate of 10°C/min under a nitrogen purge of 35 ml/min, to a maximum temperature of 240°C.

Figure 3.5 illustrates the TGA thermogram of triamterene raw material. A weight loss of < 1% indicates that the raw material in the solid state is not a hydrate, or a solvate.

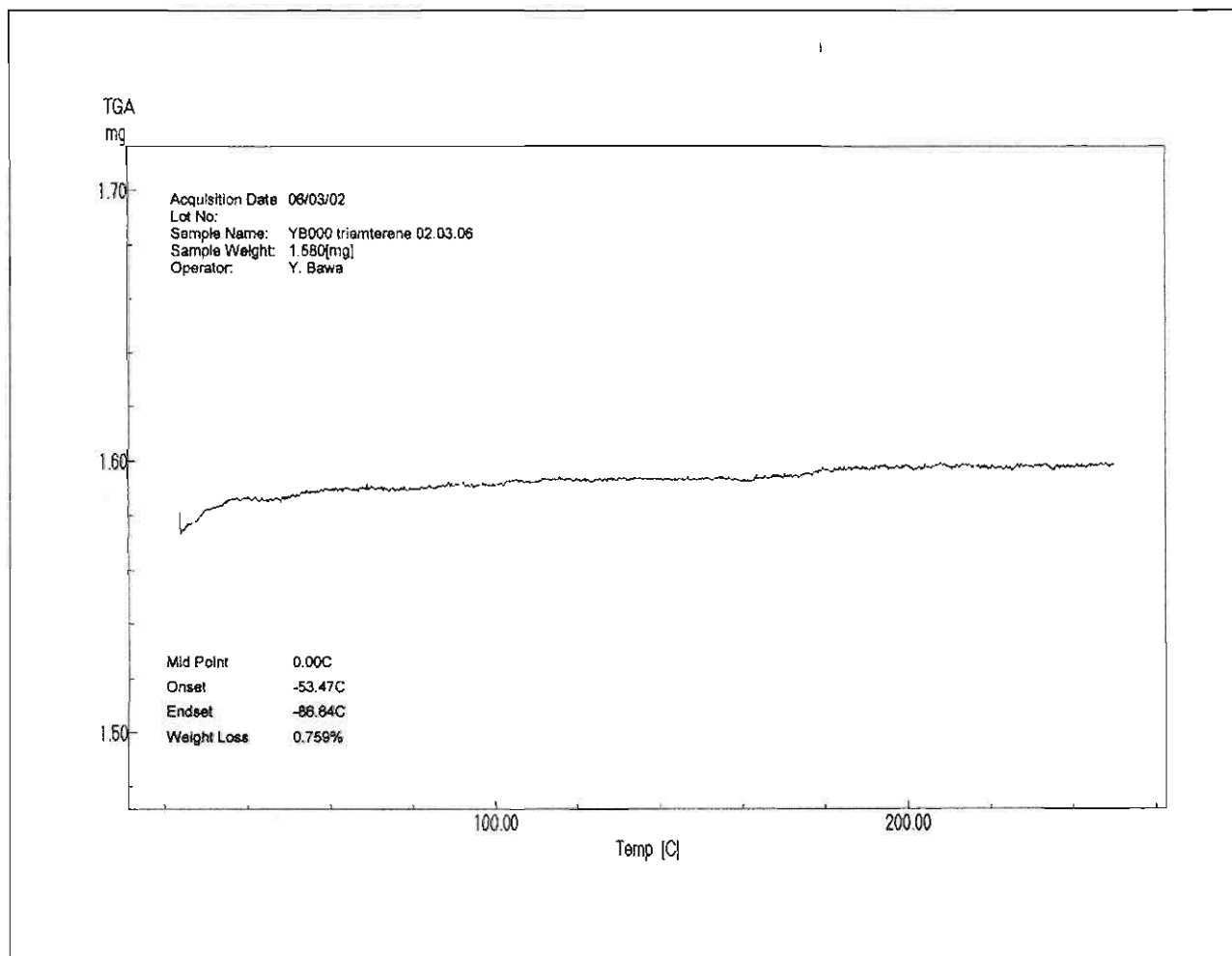


Figure 3.5 The TGA thermogram of triamterene raw material.

3.7.1.5 Infrared spectroscopy (IR)

According to Brittain (1995), IR spectroscopy is used as an identification tool for various intermediates and final, bulk, drug products, and it is also a quantitative technique for solution phase studies.

Triamterene raw material and KBr powder were ground and placed in the IR spectrophotometer and the IR measured by means of diffuse reflectance infrared Fourier transform spectroscopy (DRIFTS) over a range of 400 – 4000 cm^{-1} .

Table 3.4 lists the main absorption peaks with their corresponding wavenumbers (cm^{-1}), whilst Figure 3.6 illustrates the IR spectrum of triamterene raw material.

Table 3.4 Main absorption peaks of triamterene raw material

Main absorptions	Wavenumbers (cm ⁻¹)
1	3952.0
2	3908.1
3	3770.1
4	3720.5
5	3622.0
6	3472.4
7	3368.3
8	3136.6
9	2892.8
10	2838.8
11	2781.2
12	2630.6
17	1960.6
18	1911.8
19	1853.6
20	1775.6
21	1677.7
22	1535.0
23	1483.5
24	1428.0
25	1356.3
26	1254.1
27	1186.5
28	1110.4
29	1079.5
30	1042.1
31	1019.2
32	973.8
33	929.1
34	845.7
35	819.4
37	742.2
38	706.5

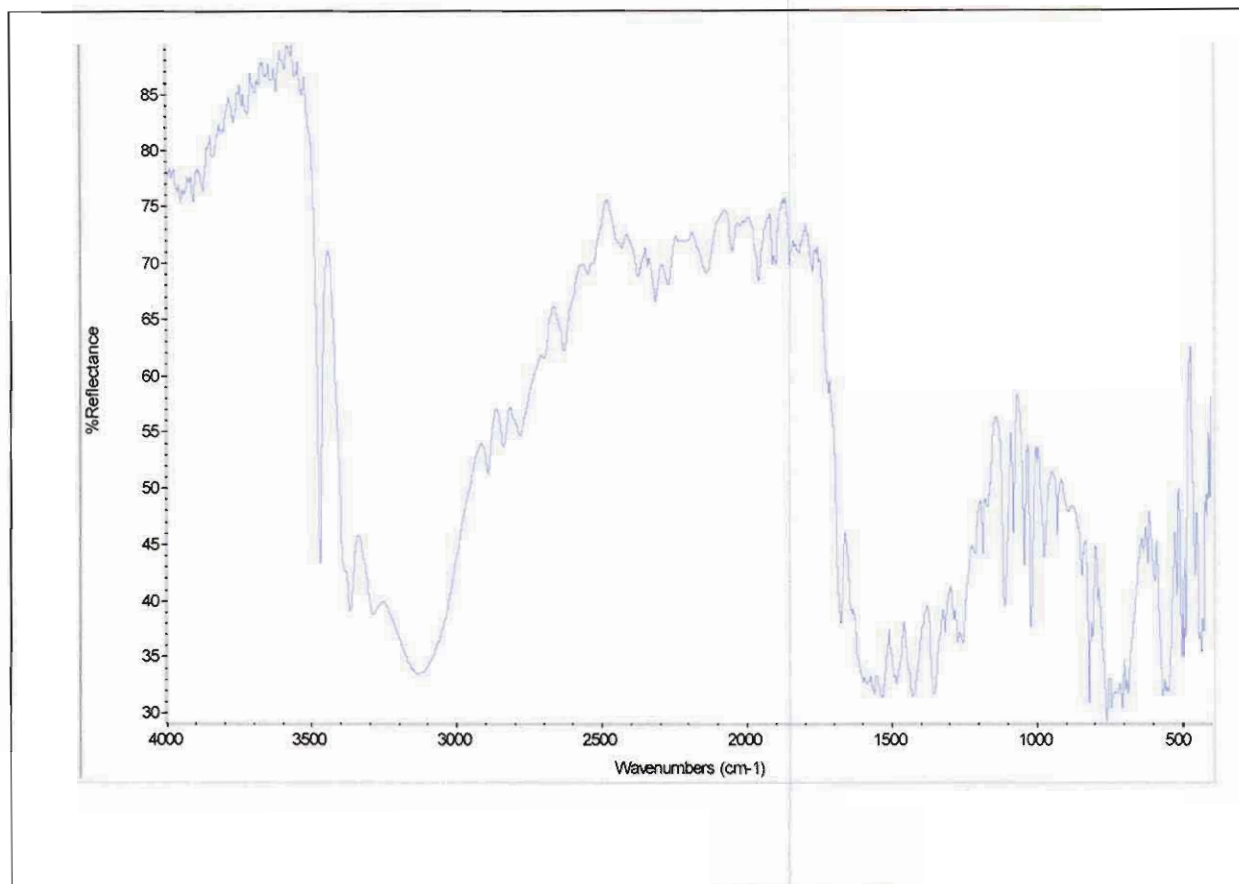


Figure 3.6 IR spectrum of triamterene raw material.

3.8 Preparation of triamterene crystals

In the pharmaceutical industry, an early identification and characterisation of different crystal forms of a drug substance are of utmost importance. It is important to understand the solid state chemistry of the drug because:

- Most drugs are used in a crystalline form;
- Crystals are held together by molecular forces;
- The arrangement of molecules in a crystal determines its physical properties;
- The physical properties of a drug can affect its performance (Byrn *et al.*, 1999).

As discussed in chapter 1, a drug substance can exist as different crystal forms, due to different intramolecular arrangements within the crystal, which may lead to different physico-chemical properties and thus different bioavailability.

As was mentioned, triamterene is a very weakly soluble drug, and it is partially soluble in DMF, alcohols, and acids (Kapoor, 1994). The physico-chemical properties of various polymorphic forms of triamterene, being recrystallised from different solvents, and the classification of these forms are discussed further in this chapter.

3.8.1 Method of preparation of triamterene crystals

For each of the various solvents, the following procedure was followed for the recrystallisation of triamterene. A small volume of each solvent was transferred into a clean beaker and placed on a hot plate (Heidolph MR 3001 K, Heidolph, Germany). A spatula point full of triamterene powder was added to the beaker. After adding a stirring magnet and whilst stirring, more of each solvent was gradually added, until the solution was clear. The beaker was then removed from the hot plate, the stirring magnet removed and the beaker opening covered with perforated parafilm. The samples were stored in a cupboard, and left undisturbed for a period of time, to allow for the slow evaporation of solvents at room temperature. The solvents used are listed in Table 3.5.

Table 3.5 Solvents used for the recrystallisation of triamterene

Solvents	Boiling point at NTP	Manufacturer
Dimethylformamide (DMF)	153	BDH Laboratory Suppliers, England
n-Butanol	117.5	Saarchem, South Africa
Methanol	64.7	Saarchem, South Africa
Ethanol	78.5	BDH Laboratory Suppliers, England
n-Propanol	97.2	Saarchem, South Africa
2-Butanol	74.12	Riedel-de Haen
Iso-propanol	82.5	Saarchem, South Africa
Formic acid	100.8	Saarchem, South Africa
Acetic acid	118	Saarchem, South Africa
Propionic acid	135.4	Merck, Schuchardt

The results of these recrystallisation studies are discussed under the categories, as summarised in Table 3.6.

Table 3.6 Framework for discussion of recrystallisation outcomes and results of this study

Solvent group	Solvent	Sample ID
Acid	Formic acid	YB008
	Acetic acid	YB009
	Propionic acid	YB010
Alcohol	n-Butanol	YB002
	2-Butanol	YB006
	Methanol	YB003
	Ethanol	YB004
	n-Propanol	YB005
	iso-Propanol	YB007
DMF and DMF:Water (90:10)	DMF	YB001
	DMF:water	YB011

3.8.2 Recrystallisation test results and outcomes

3.8.2.1 Acids

3.8.2.1.1 Thermo-microscopy (TM)

Tables 3.7(a), (b) and (c) illustrate the TM pictures taken over the temperature range for crystals obtained from formic acid, acetic acid and propionic acid, respectively.

Table 3.7(a) TM results of crystals recrystallised from formic acid (YB008)


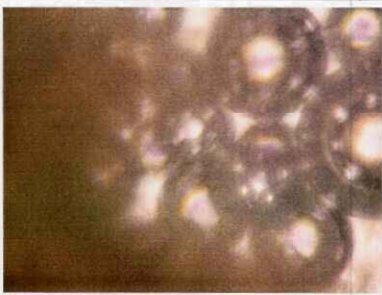

		
Crystals at 30°C	Gas evolution, i.e. desolvation at 211°C	The melting process at 318°C

Table 3.7(b) TM results of crystals recrystallised from acetic acid





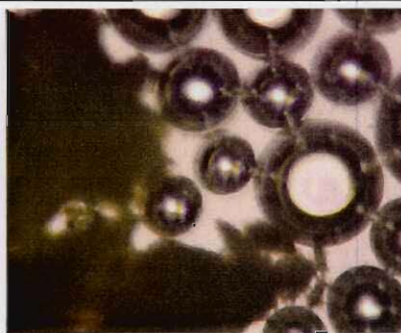

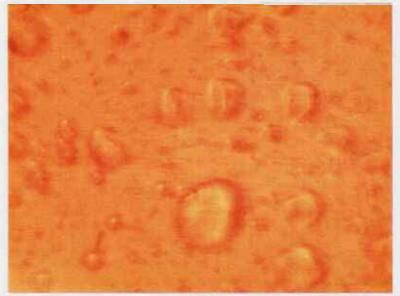
		
Crystals before desolvation at 184°C	Gas evolution, i.e. desolvation at 202°C	The melting process at 333°C

Table 3.7(c) TM results of crystals recrystallised from propionic acid

		
Crystals at 30°C	Gas evolution, i.e. desolvation at 185°C	Crystals form needle-like growths at 276°C
		
The melting process at 333°C		

3.8.2.1.2 X-ray powder diffractometry (XRPD)

The peak angles ($^{\circ}2\theta$) and relative intensities (I/I_0) of the main peaks of the XRPD are listed in Table 3.8 for formic acid (YB008), acetic acid (YB009), and propionic acid (YB010). The XRPD patterns of triamterene crystals obtained from the acid solutions are illustrated in Figure 3.7, formic acid (YB008), acetic acid (YB009), and propionic acid (YB010).

Table 3.8 Main XRPD intensity ratios (I/I₀) and main peak angles (°2θ) of triamterene crystals recrystallised from acidic solutions

Peak angles (°2θ)	Relative intensities (I/I ₀)	Peak angles (°2θ)	Relative intensities (I/I ₀)	Peak angles (°2θ)	Relative intensities (I/I ₀)
Crystals obtained from formic acid YB008		Crystals obtained from acetic acid YB009		Crystals obtained from propionic acid YB010	
5.2	5.7	5.4	100	6.8	12.6
5.8	100	9.5	2.7	7.6	100
6.6	1.1	10.8	1.6	11.1	65
9.1	0.9	11.5	1.4	15.9	25.3
12.9	0.8	12.3	1.3	16.6	24.6
13.2	7.3	13.1	2.3	17.5	16.2
13.9	2.5	13.9	1.7	18.2	14.2
14.9	8	15.7	6.9	18.3	15.7
15.8	0.6	16.3	11.2	18.4	17.9
17.0	0.8	16.9	10.5	22.2	87.2
17.6	7	18.3	5	24.6	22.2
18.4	1	19.3	1.7	24.7	25
19.3	3.5	19.9	7.2	28.4	35.9
19.9	2	20.3	8.4	34.3	9.1
20.3	0.9	20.9	2.9	-	-
21.3	3.1	21.7	2.3	-	-
22.4	2.3	22.9	4.1	-	-
22.9	2	23.5	2	-	-
23.6	2.2	24.5	7	-	-
24.3	3	24.9	17.3	-	-
24.9	1.9	25.5	6.3	-	-
25.6	2.6	26.2	22.6	-	-
26.0	4	26.6	3.9	-	-
26.8	11.9	27.4	4.9	-	-
27.7	3.2	28.0	5.3	-	-
28.4	2.9	28.5	4.4	-	-
28.8	2.2	29.2	2.1	-	-
29.5	0.9	30.6	3.5	-	-
30.7	0.9	31.5	2.1	-	-

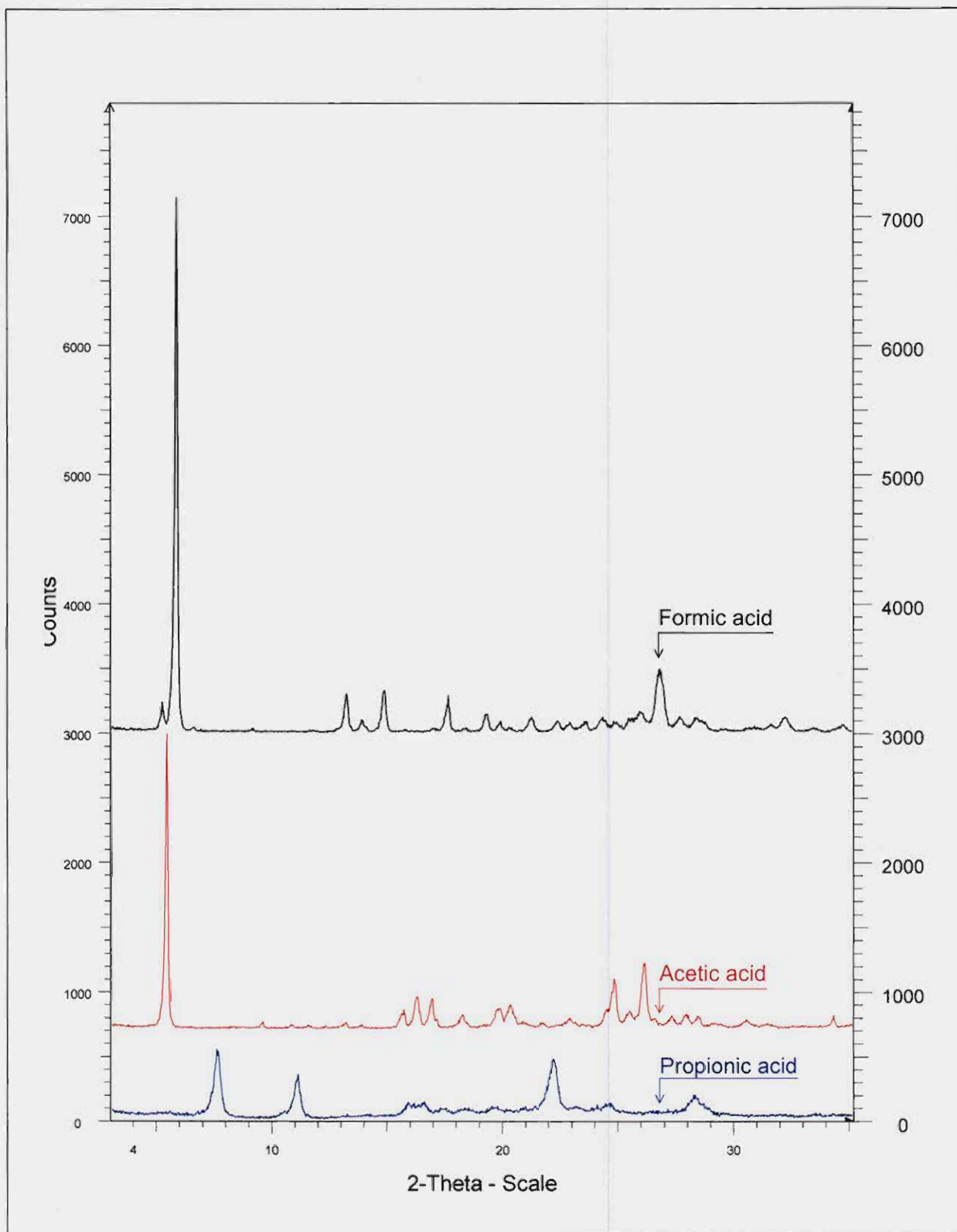


Figure 3.7 XRPD overlay of crystals recrystallised from formic acid (black = YB008), acetic acid (red = YB009) and propionic acid (blue = YB010).

3.8.2.1.3 Differential scanning calorimetry (DSC)

Figure 3.8 illustrates the overlay of the DSC results obtained from formic acid (YB008), acetic acid (YB009) and propionic acid (YB010).

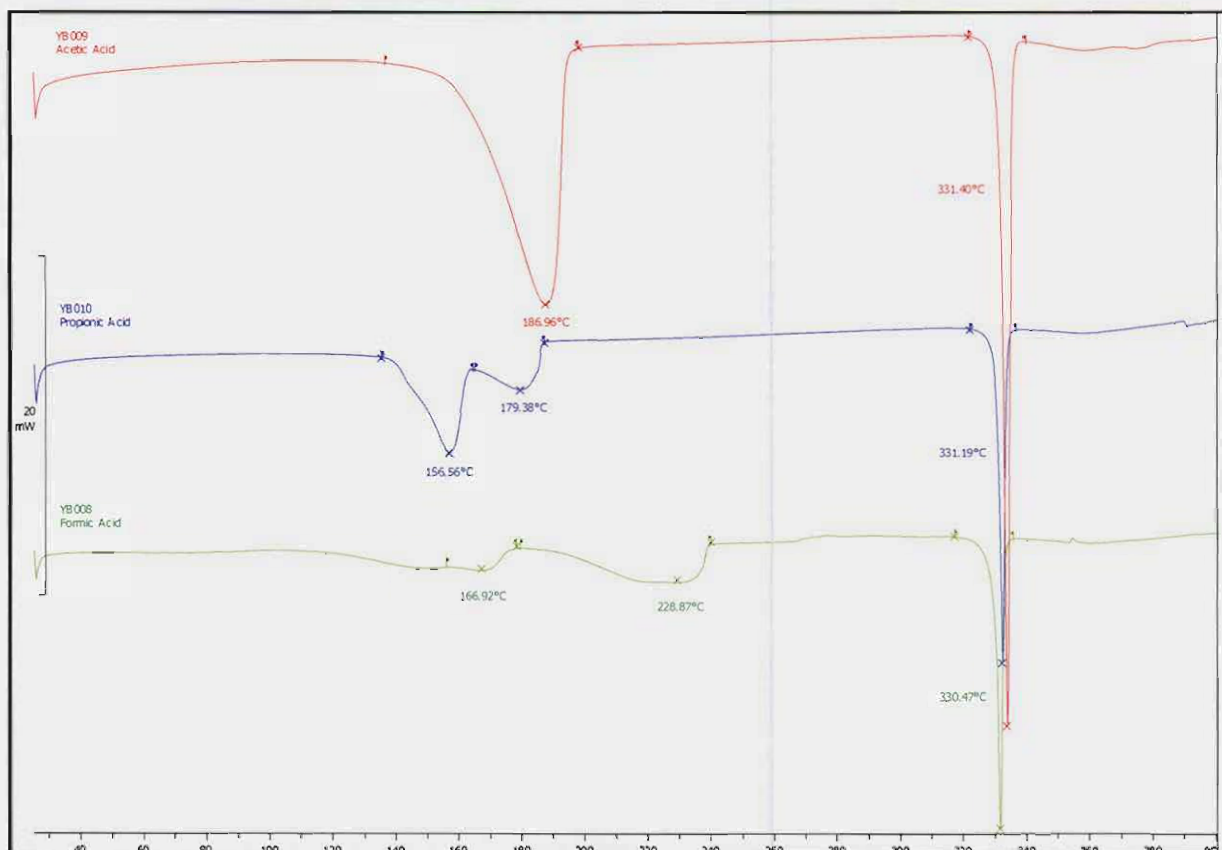


Figure 3.8 The DCS overlay of the crystals recrystallised from formic acid (YB008 = green), acetic acid (YB009 = red) and propionic acid (YB010 = blue).

3.8.2.1.4 Thermogravimetric analysis (TGA)

Figures 3.9(a), (b), and (c) illustrate the TGA thermograms of formic acid (YB008), acetic acid (YB009) and propionic acid (YB010), respectively. Karl Fischer determinations were done on the three crystals and the values for the crystals obtained from formic acid, acetic acid and propionic acid were 0.35%, 2.1% and 0.55%, respectively.

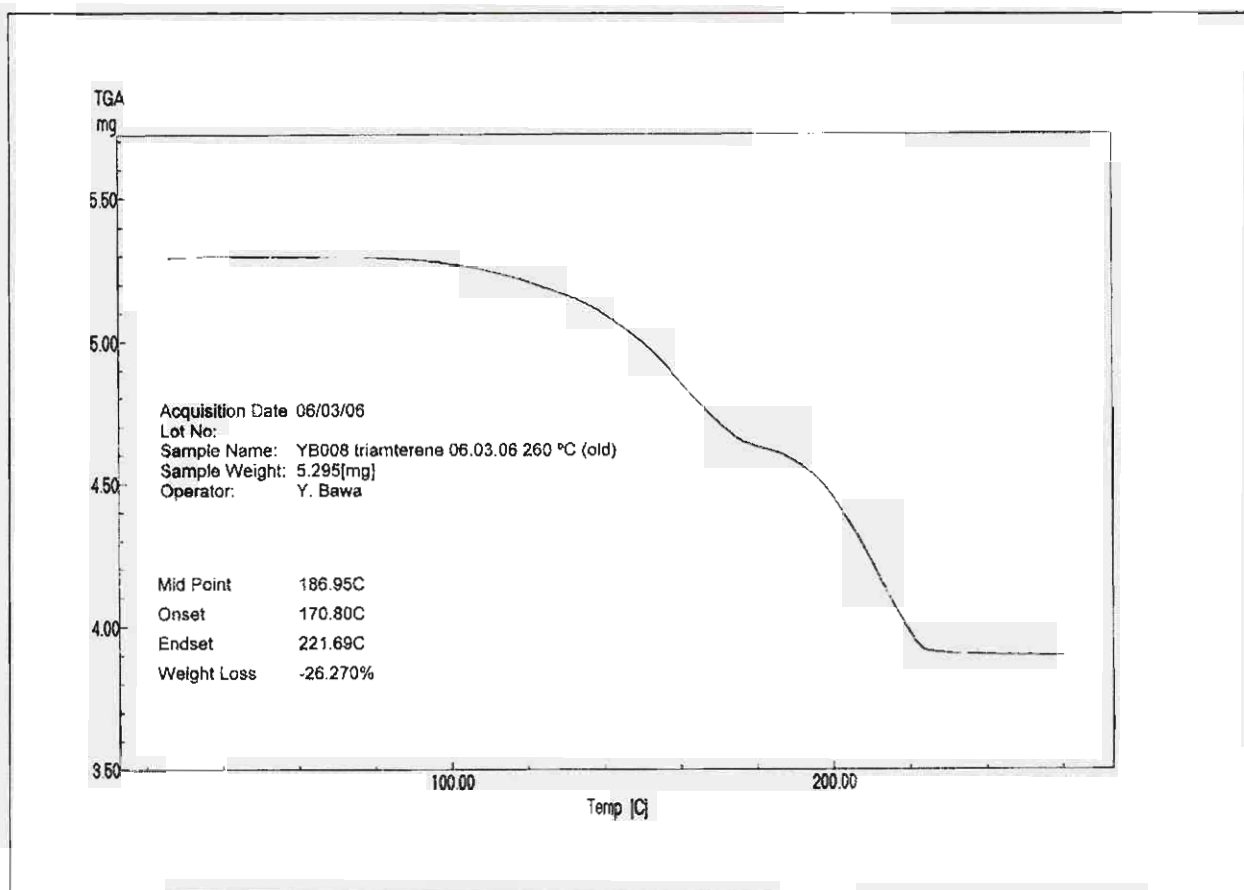


Figure 3.9(a) The TGA thermogram of crystals recrystallised from formic acid with a 26.27% weight loss (theoretical weight loss for a formic acid solvate = 15.5%).

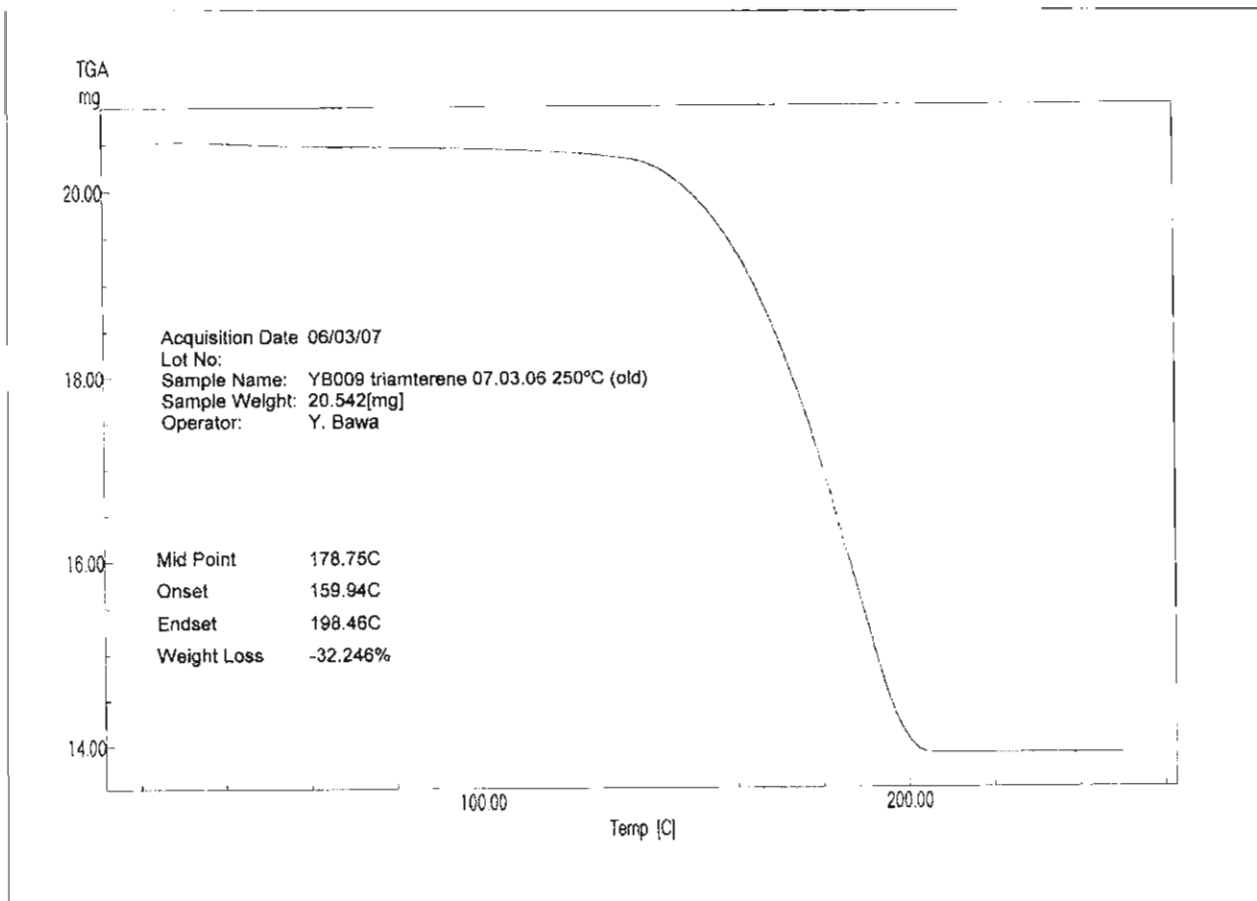


Figure 3.9(b) The TGA thermogram of crystals recrystallised from acetic acid with a 32.25% weight loss (theoretical weight loss for an acetic acid solvate = 19.2%).

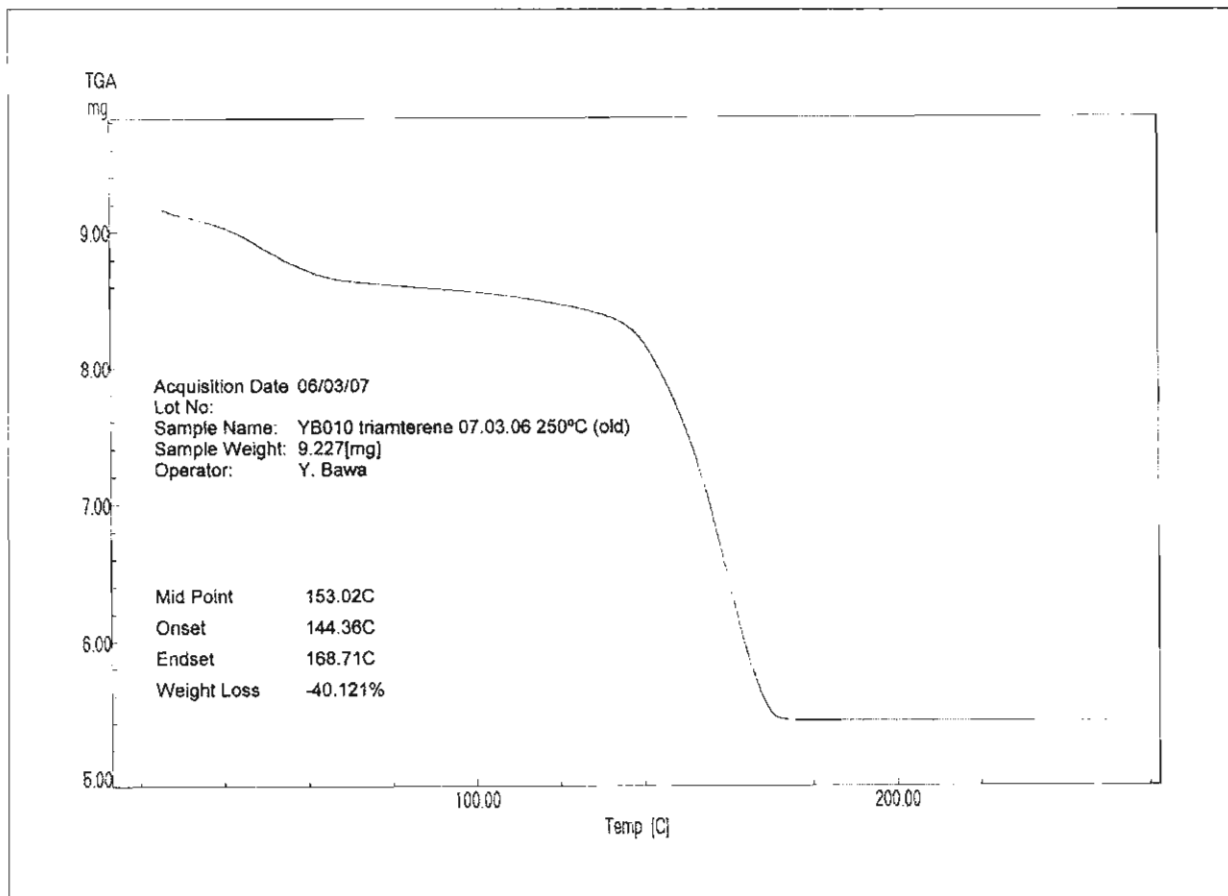


Figure 3.9(c) The TGA thermogram of crystals recrystallised from propionic acid with a 40.1% weight loss (theoretical weight loss for a propionic acid solvate = 22.6%).

3.8.2.1.5 Infrared spectroscopy (IR)

Table 3.9 lists the main absorption peaks with their corresponding wave numbers (cm^{-1}), of the crystals obtained from acidic solutions, whilst Figure 3.10 illustrates the IR spectra of formic acid (YB008), acetic acid (YB009), and propionic acid (YB010).

Table 3.9 Main absorption peaks of triamterene crystals recrystallised from formic acid (YB008), acetic acid (YB009) and propionic acid (YB010)

Main absorptions	Wave numbers (cm ⁻¹)		
	YB008	YB009	YB010
1	3413.3	3435.9	3579.4
2	3326.2	3161.7	2991.1
3	3099.3	2733.6	1789.5
4	2974.7	1959.0	1731.3
5	2822.2	1690.3	1470.2
6	1705.6	1591.1	1420.2
7	1685.3	1521.4	1244.9
8	1647.8	1447.0	1152.7
9	1595.2	1408.0	1078.2
10	1551.1	1344.9	936.0
11	1483.8	1282.3	811.3
12	1459.1	1153.6	754.9
13	1375.1	1015.1	704.8
14	1350.1	967.8	587.7
15	1290.2	885.3	508.5
16	1225.1	833.7	403.7
17	1162.7	809.2	
18	1139.0	799.1	
19	1050.5	781.1	
20	1015.4	755.3	
21	983.4	746.3	
22	924.1	728.4	
23	876.3	685.3	
24	837.1	654.7	
25	808.3	615.7	
26	769.3	579.1	
27	742.6	558.4	
28	726.9	510.8	
29	679.7	470.1	
30	621.7	448.9	
31	597.9	417.8	

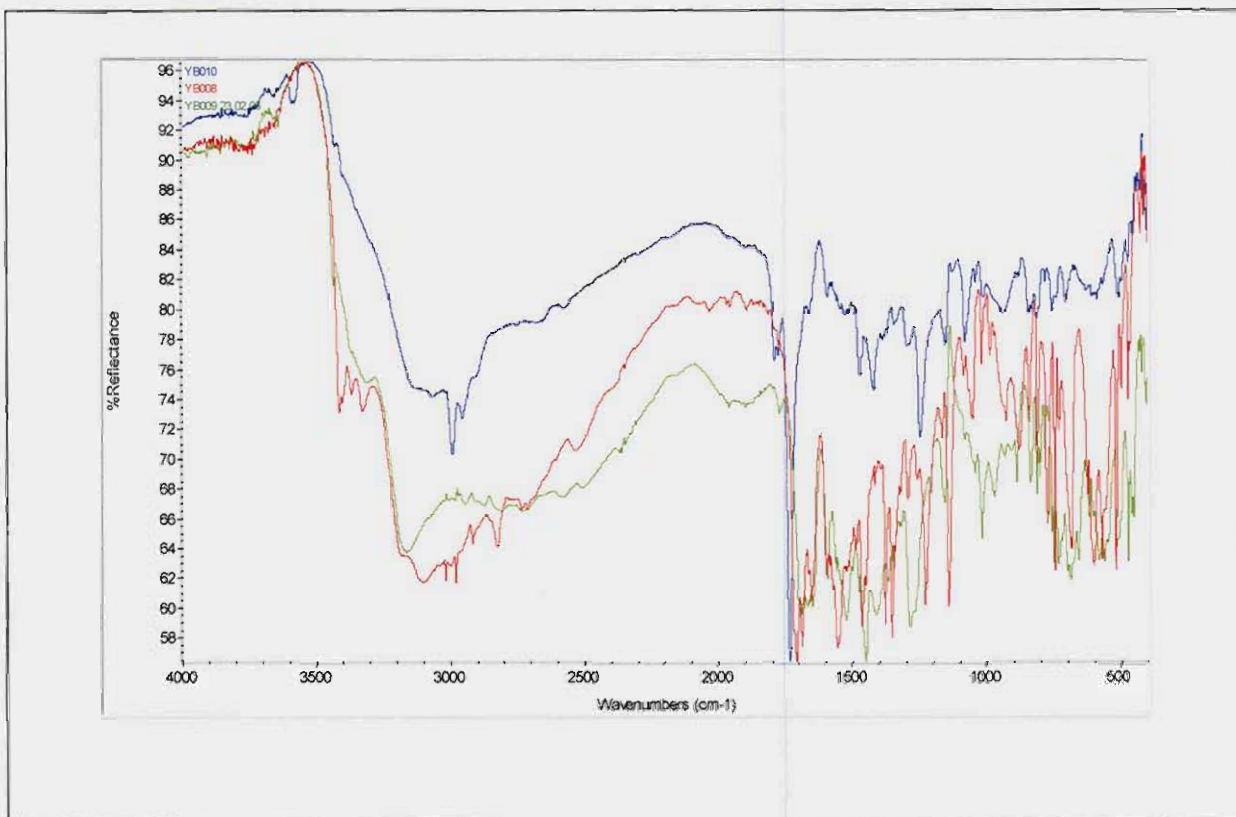


Figure 3.10 The IR spectra of triamterene crystals recrystallised from formic acid (YB008 = red), acetic acid (YB009 = green), and propionic acid (YB010 = blue).

3.8.2.1.6 Discussion of the data generated from acid solvents

The TGA weight loss measured was 26.27% for the crystals obtained from the formic acid recrystallisation, whilst the theoretical value for a formic acid solvate is 15.5%.

From the data generated, it appeared that these crystals that were formed during recrystallisation, were formic acid disolvates, since the Karl Fischer results showed insignificantly low water contents.

Unfortunately the crystals were a light yellow powder, which made it difficult to prepare for single x-ray crystallography, which could have ultimately identified the specific crystal type.

The experimental weight loss of the crystals recrystallised from acetic acid was 32.2%, whilst the theoretical weight loss for an acetic acid solvent is 19.2%. KF results showed only a weight loss of 2.1%, which proved that the crystals were also solvates.

Again, the crystal yielded were a yellow powder, which made it difficult to prepare single x-ray crystallography.

The experimental weight loss measured for crystals, prepared from propionic acid, was measured by means of TGA as 40.2%, whilst the theoretical weight loss for a propionic acid solvate is 22.6%. The KF result was 0.5%, which proved that the crystals were also disolvates. A white powder was obtained with propionic acid as recrystallisation medium which made it difficult to prepare single x-ray crystallography.

The general trend of the results was that triamterene formed a disolvate with each of the three acid solvents. Dahl *et al.* (1987) reported the XRPD, TGA and DSC results on DMF, DMF:water and alcoholic mixtures, and stated that triamterene was soluble in these solutions. Literature studies did not mention any recrystallisation studies regarding the acids used in this study, though.

The IR and the XRPD patterns differed significantly from each other, as can be expected, since the three forms were different pseudopolymorphic forms.

The melting points of the three solvates were comparable, but the desolvation peaks were different.

Recrystallisation was hampered by low solubility and hence a low crystal yield. This made it impossible to obtain enough crystals on which to perform solubility studies.

3.8.2.2 Alcohols

In this study, all the alcohols used, i.e. methanol, ethanol, n-propanol, iso-propanol and n-butanol, produced crystals with the same physico-chemical properties, as were reflected by the DSC, TGA, XRPD and IR results.

For the purpose of this discussion, ethanol was used to report the data obtained for this class of crystals. The physico-chemical properties of the crystals obtained from 2-butanol differed significantly from the other alcohol recrystallisation studies and will be discussed.

3.8.2.2.1 Thermo-microscopy (TM)

Tables 3.10(a) and (b) illustrate TM pictures of the crystals obtained from 2-butanol and ethanol over an elevated temperature range, respectively.

Table 3.10(a) TM results of crystals recrystallised from 2-butanol

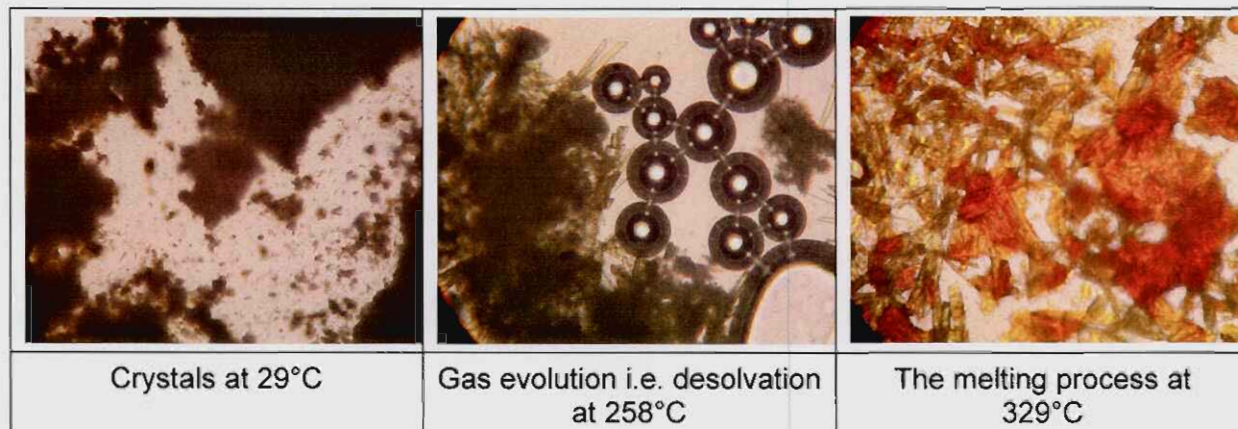


Table 3.10(b) TM results of crystals recrystallised from ethanol



3.8.2.2.2 X-ray powder diffractometry (XRPD)

The peak angles ($^{\circ}2\theta$) and relative intensities (I/I_0) of the main peaks in the XRPD patterns are listed in Table 3.11, whilst Figure 3.11 illustrates the XRPD patterns of triamterene crystals obtained from 2-butanol and ethanol recrystallisation.

Table 3.11 Main XRPD intensity ratios (I/I₀) and main peak angles (°2θ) of triamterene recrystallised from 2-butanol (YB006) and ethanol (YB004)

Peak angles (°2θ)	Relative intensities (I/I ₀)	Peak angles (°2θ)	Relative intensities (I/I ₀)
Crystals obtained from 2-butanol YB006		Crystals obtained from ethanol YB004	
4.3	100	7.8	0.8
4.8	34.5	9.4	100
5.4	37	11.4	6.6
8.6	14.6	13.0	2.6
8.9	35.3	14	0.9
9.9	35.7	14.7	6.1
10.5	25.7	14.9	6.9
10.7	23.7	15.4	2.1
11	15.4	16	1
13.2	7	16.4	3.5
14.1	7.9	16.8	6.3
16.6	17.5	17.9	7.9
17.4	32.9	18.8	3.8
18.5	12.3	19.6	3.3
19.3	9.6	20.9	9.8
21.6	11	21.3	15.9
22.0	11.8	21.5	15.2
23.9	18.9	21.7	10.8
26.1	52	22.9	2.4
26.5	43.2	23.3	1.2
28.8	14.1	24.2	2.3
33.1	6.5	25.1	3.9
34.4	8.9	26.3	47.2

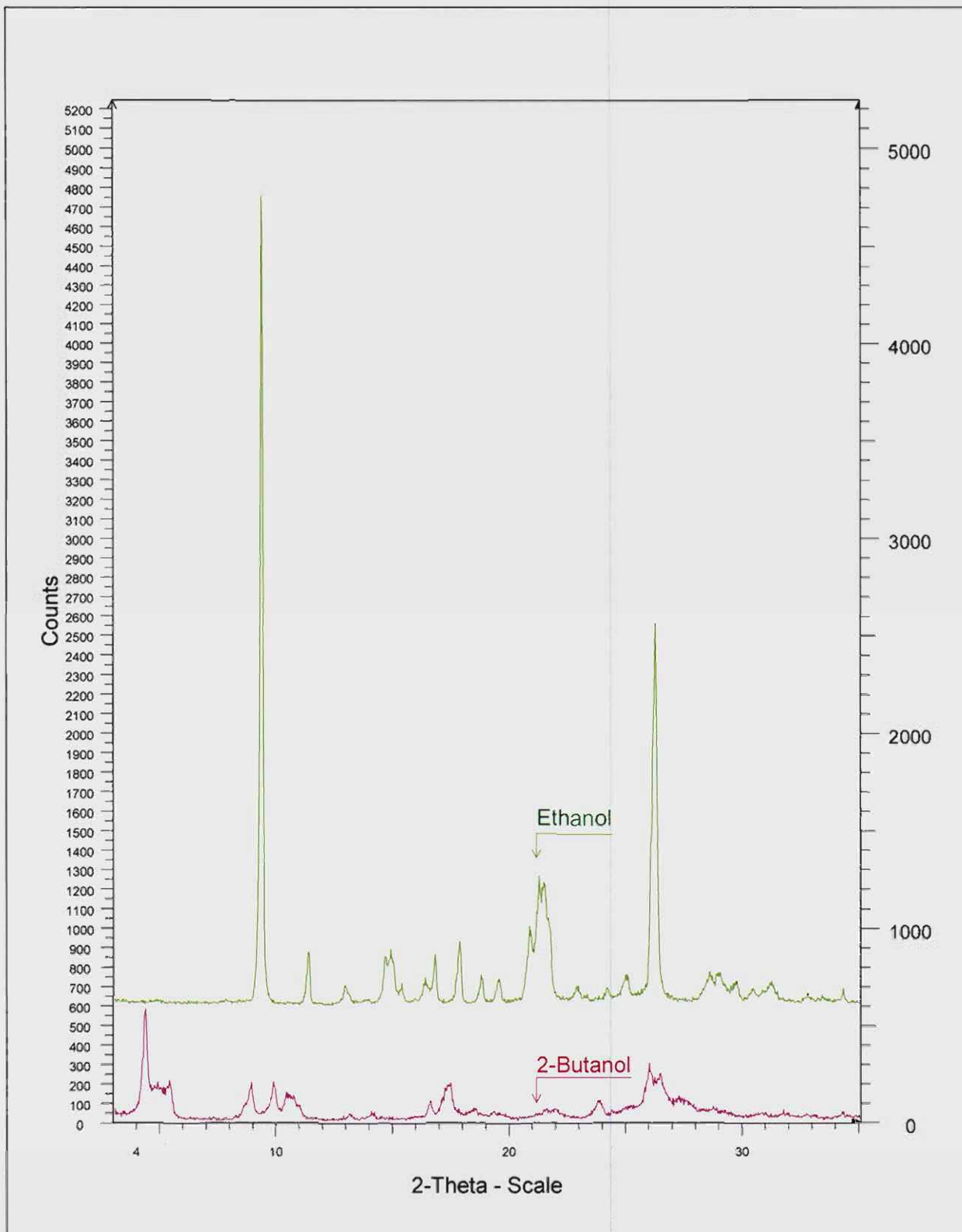


Figure 3.11 XRPD patterns of crystals recrystallised from 2-butanol (YB006 = pink) and ethanol (YB004 = green).

3.8.2.2.3 Differential scanning calorimetry (DSC)

Figure 3.12 illustrates the DSC thermograms of the crystals obtained from 2-butanol (YB006) and ethanol (YB004) solutions.

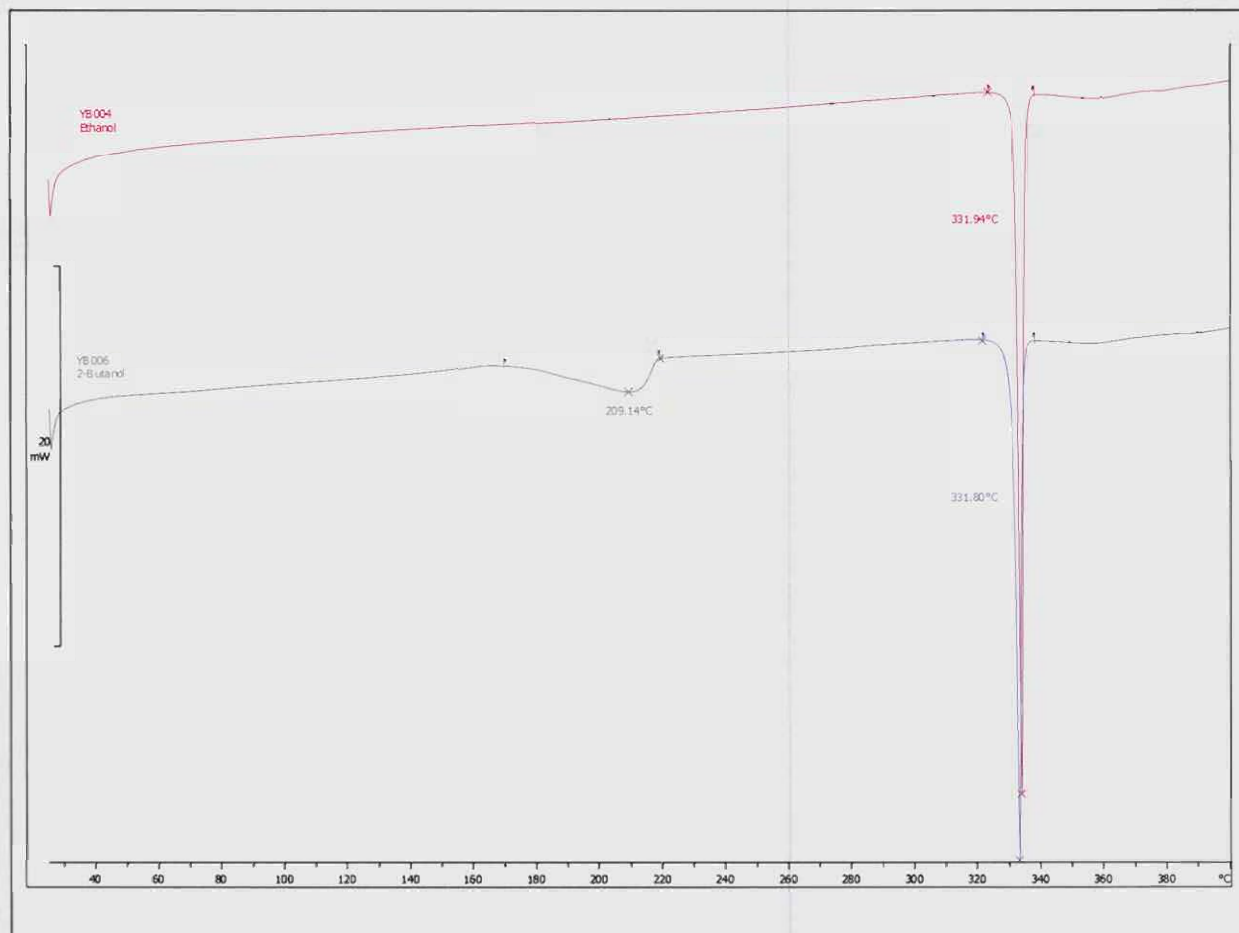


Figure 3.12 The DSC overlay of the crystals recrystallised from 2-butanol (YB006 = purple) and ethanol (YB004 = pink).

3.8.2.2.4 Thermogravimetric analysis (TGA)

The DSC thermogram of the crystals obtained from ethanol display no evidence of desolvation and/or dehydration, therefore no TGA analysis was performed. Figure 3.13 illustrates the TGA thermogram of the crystals obtained from 2-butanol.

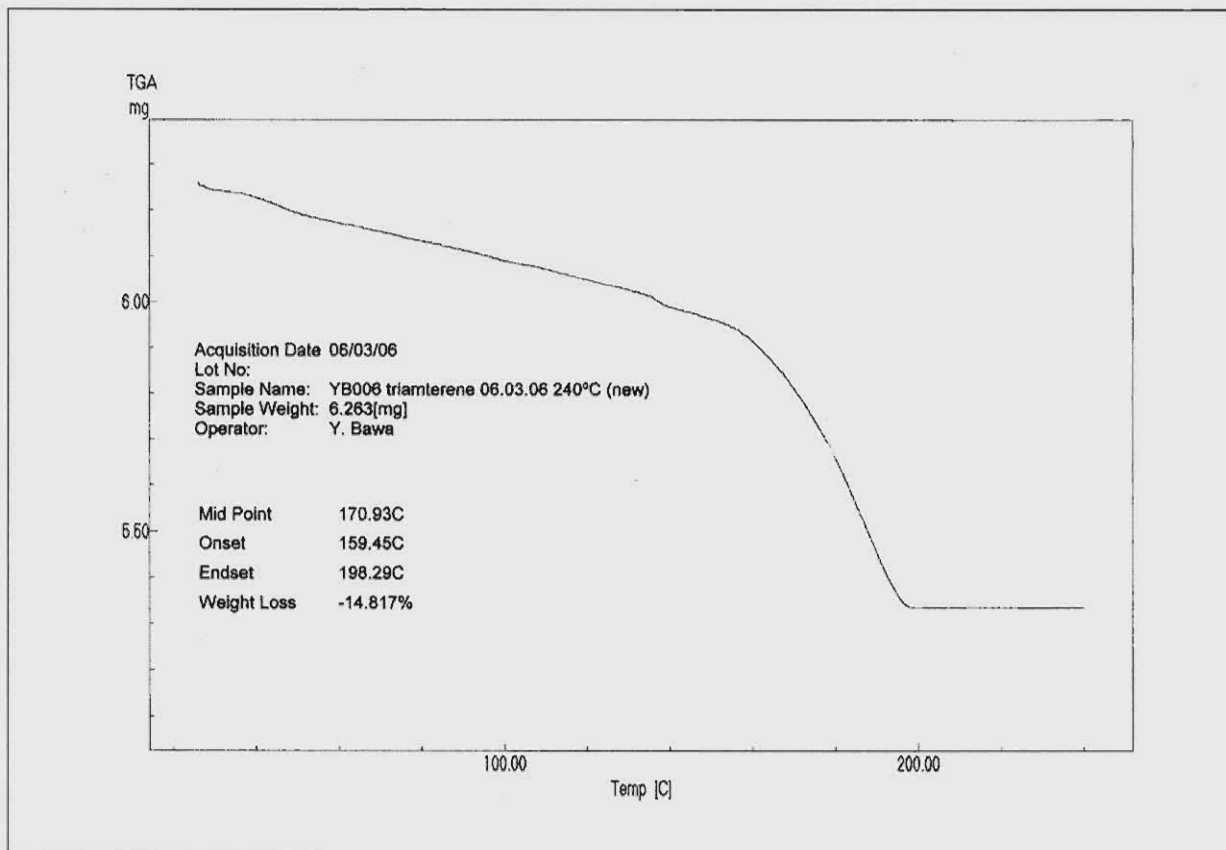


Figure 3.13 The TGA thermogram of crystals recrystallised for a 2-butanol solvate, with a 14.82% weight loss (theoretical weight loss for a 2-butanol solvate = 22.6%, and for a hydrate = 6.6%).

The Karl Fischer results of the recrystallisation product from 2-butanol was calculated as 4.1 %, which could be indicative of a hydrate.

3.8.2.2.5 IR spectroscopy

Table 3.12 lists the main absorption peaks with their corresponding wave numbers (cm^{-1}), and Figure 3.14 illustrates the IR spectra of triamterene crystals obtained from 2-butanol (YB006) and ethanol (YB004).

Table 3.12 Main absorption peaks of triamterene crystals recrystallised from 2-butanol (YB006) and ethanol (YB004)

Main absorptions	Wavenumbers (cm ⁻¹)	
	2-butanol	ethanol
1	3014.8	3627.6
2	2974.7	3014.8
3	2361.2	2974.6
4	1689.0	1683.6
5	1576.6	1412.2
6	1425.7	1370.8
7	1373.7	1139.0
8	1350.3	937.2
9	1258.6	867.6
10	1138.8	694.0
11	1077.9	487.1
12	1040.3	458.1
13	1017.4	422.5
14	944.1	414.6
15	868.0	-
16	834.2	-
17	808.3	-
18	739.3	-
19	697.5	-

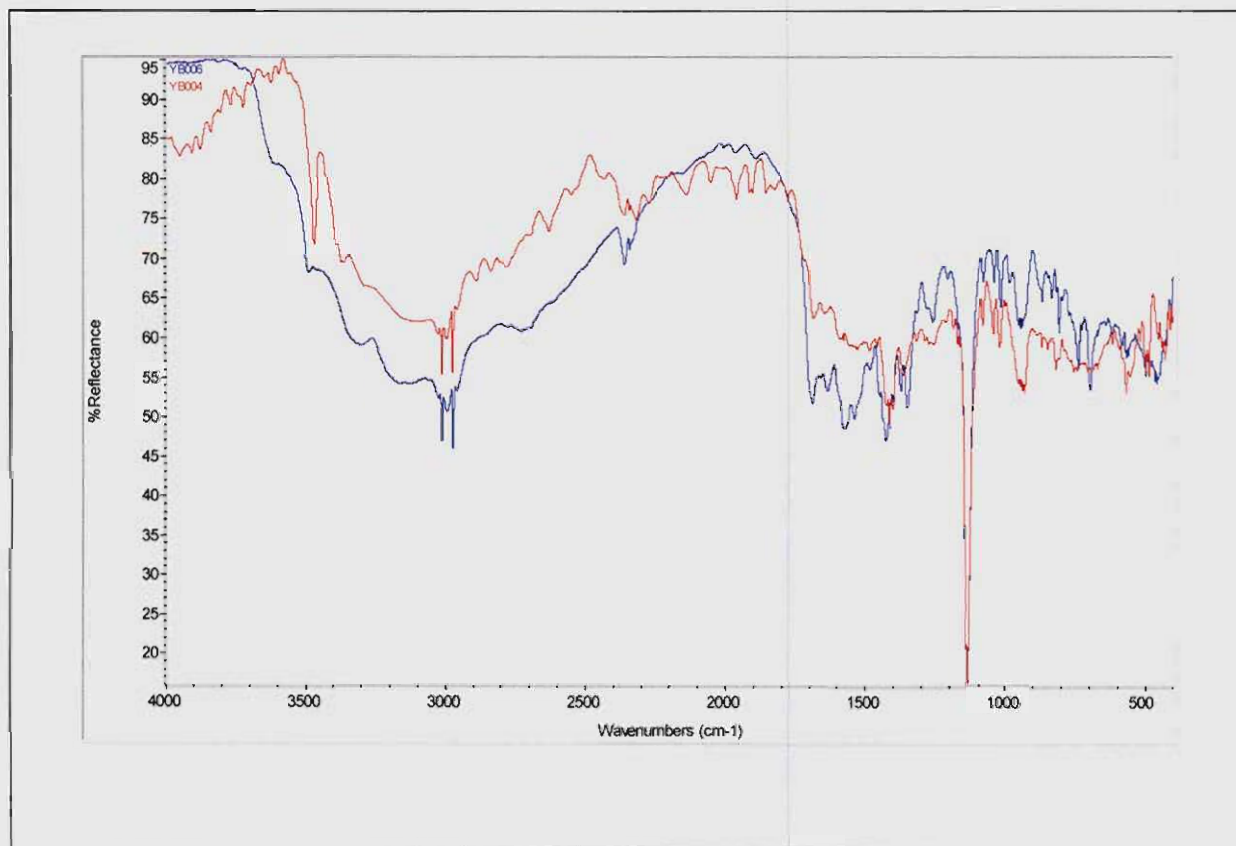


Figure 3.14 IR spectra of crystals recrystallised from 2-butanol (YB006 = blue) and ethanol (YB004 = red).

3.8.2.2.6 Discussion of the data generated from alcohol solvents

The physico-chemical data of the recrystallisation products from the group of alcohol solvents, i.e methanol, ethanol, n-propanol, iso-propanol and n-butanol, were identical and were comparable to those of the triamterene raw material being used.

The Karl Fischer and TGA analyses were inconclusive as to whether the recrystallisation product from 2-butanol was a hydrate, or a solvate, or a hydrated solvate. According to Dahl *et al.* (1989), the hydrated product has a lower melting point than the solvate, or the raw material, i.e. 314 - 318°C. However, the melting point of the 2-butanol crystals was 331°C. The DSC results showed that the melting peaks of the crystals were comparable, although a desolvation peak existed at 209.14°C, in the thermogram of the crystals obtained from the 2-butanol solution.

Again, recrystallisation was hampered by low solubility and hence a low crystal yield. This made it impossible to obtain enough crystals on which to perform solubility studies.

3.8.2.3 DMF (dimethylformamide) mixtures

3.8.2.3.1 Thermo-microscopy (TM)

Tables 3.13(a) and (b) illustrate the TM pictures of the crystals obtained from DMF (YB001) and DMF:water (YB011) crystals, over an elevated temperature range, respectively.

Table 3.13(a) TM results of crystals recrystallised from DMF (YB001)




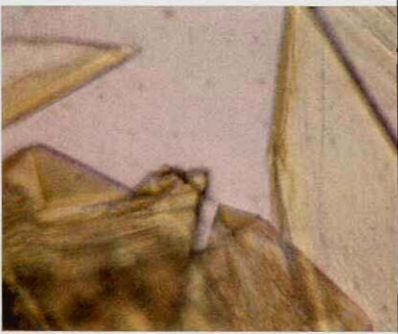
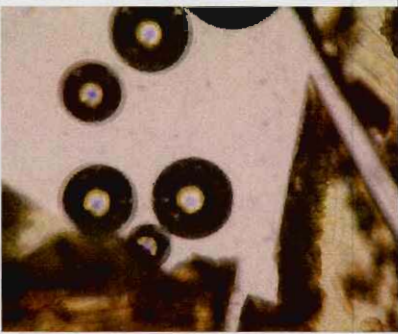
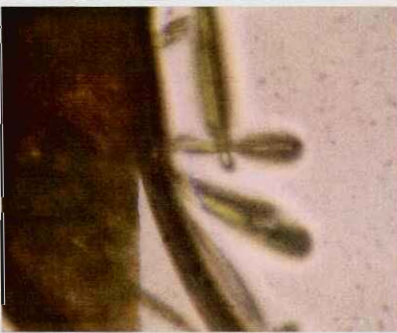
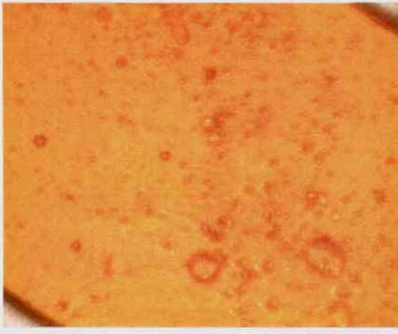
		
Crystals at 23°C	Gas evolution i.e. desolvation at 212°C	The melting process at 331°C

Table 3.13(b) TM results of crystals recrystallised from DMF:water (YB011)

		
Crystals at 28°C	Gas evolution i.e. desolvation at 215°C	Crystals form needle outgrowths at 323°C
		
The melting process at 335°C		

3.8.2.3.2 X-ray powder diffractometry (XRPD)

The peak angles ($^{\circ}2\theta$) and relative intensities (I/I_0) of the main peaks in the XRPD are listed in Table 3.14. Figure 3.15 illustrates the XRPD patterns of triamterene crystals obtained from DMF (YB001) and DMF:water (YB011) solutions.

Table 3.14 Main XRPD ratios (I/I_0) and main peak angles ($^{\circ}2\theta$) of triamterene recrystallised from DMF (YB001) and DMF:water (YB011)

Peak angles ($^{\circ}2\theta$)	Relative intensities (I/I_0)	Peak angles ($^{\circ}2\theta$)	Relative intensities (I/I_0)
Crystals obtained from DMF (YB001)		Crystals obtained from DMF:water mixture (YB011)	
4.7	0.7	7.2	1.2
9.6	10.9	10	19.1
10.3	44.2	10.2	21.4
12.6	2.2	12.6	3.1
13.6	4.5	13.5	4.3
14.5	19.1	14.5	68.6
15.8	2.5	15.8	6
17.0	1.1	16.9	1.3
18.5	8.8	18.5	11.2
19.2	100	19.2	100
19.5	26.1	19.5	22.7
20.5	53.4	20.5	53.8
21.2	3.7	21.2	3.2
22.4	1.9	22.4	3.5
23.3	4	23.2	5.9
24.2	9.1	24.1	10.6
25.3	2.2	25.2	3.5
26.3	18.7	26.3	21.2
27.3	4.1	27.2	5.4
27.7	3.6	27.7	4.3
29.2	30.7	29.1	19.4
29.7	3	29.5	3.6
30.1	3.9	30.1	6.1
31	7.7	30.9	10.6

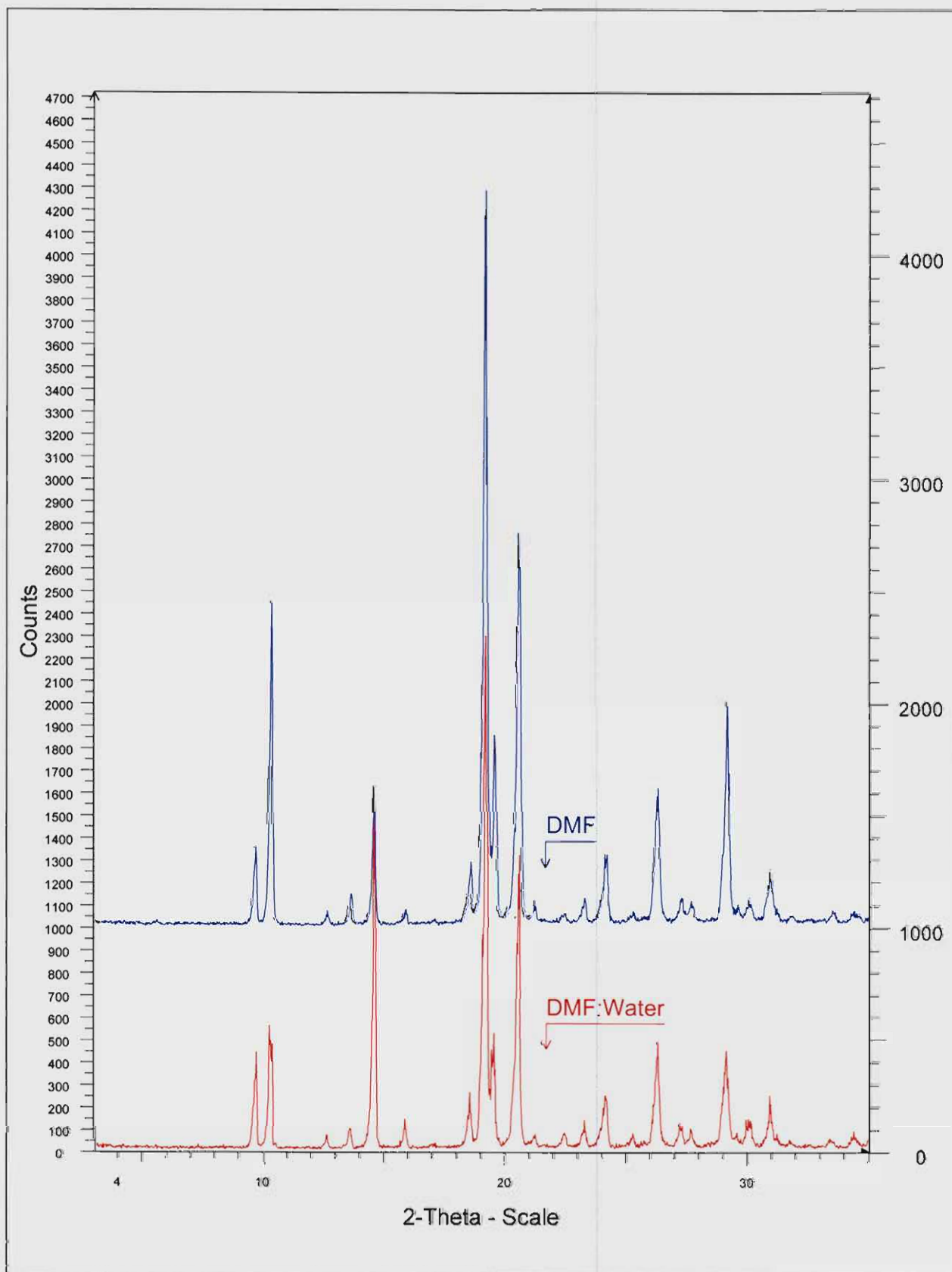


Figure 3.15 XRPD overlay of crystals recrystallised from DMF (YB001 = blue) and DMF:water (YB011 = red).

3.8.2.3.3 Differential scanning calorimetry (DSC)

Figure 3.16 illustrates the thermograms of the crystals obtained from DMF (YB001) and DMF:water (YB011) solutions.

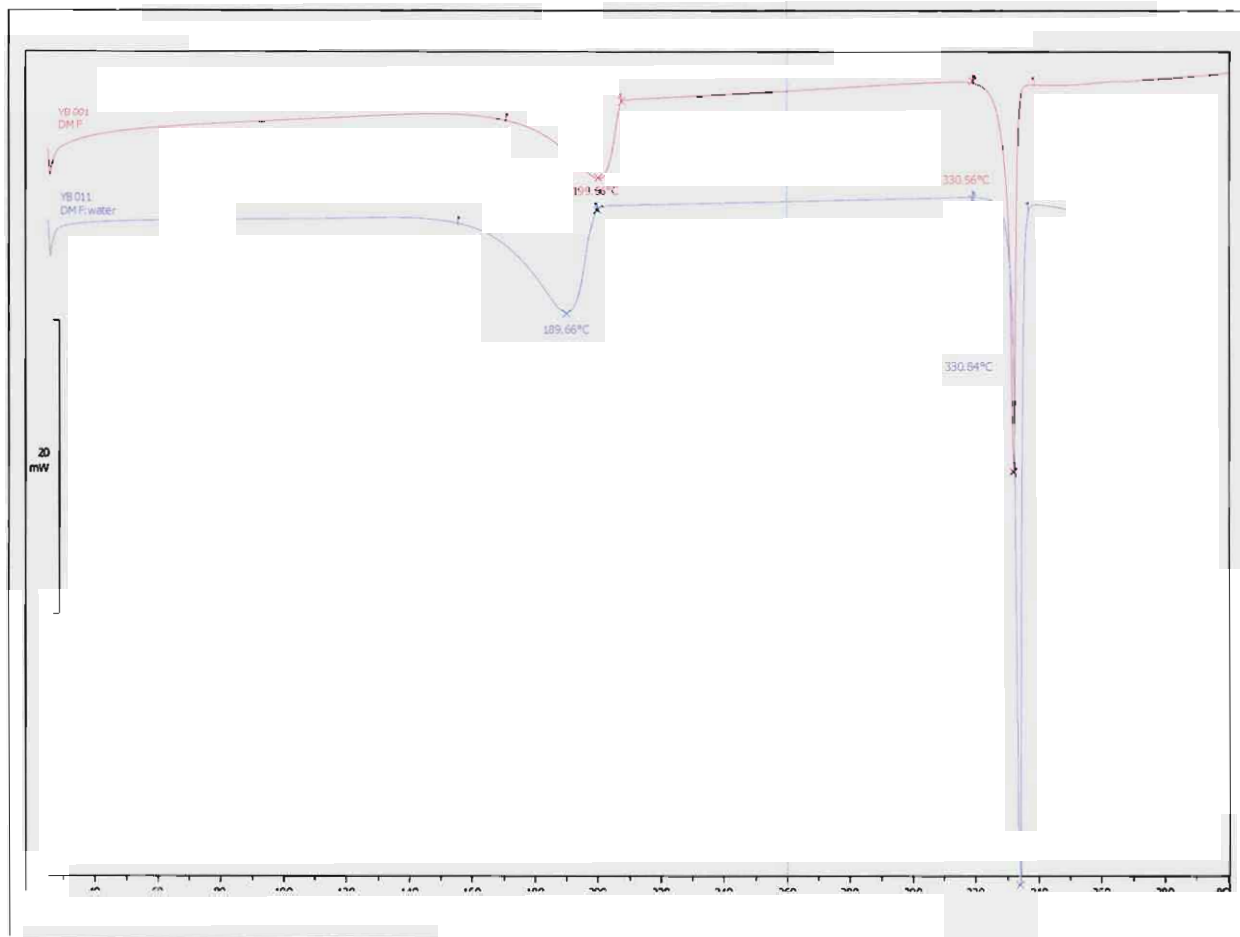


Figure 3.16 The DSC overlay of the crystals recrystallised from DMF (YB001 = pink) and DMF:water (YB011 = blue).

3.8.2.3.4 Thermogravimetric analysis (TGA)

Figures 3.17(a) and (b) illustrate the TGA thermograms of crystals obtained from DMF (YB001) and DMF:water (YB011), respectively. Karl Fischer results showed a weight loss of 1.3% for the crystals obtained from DMF.

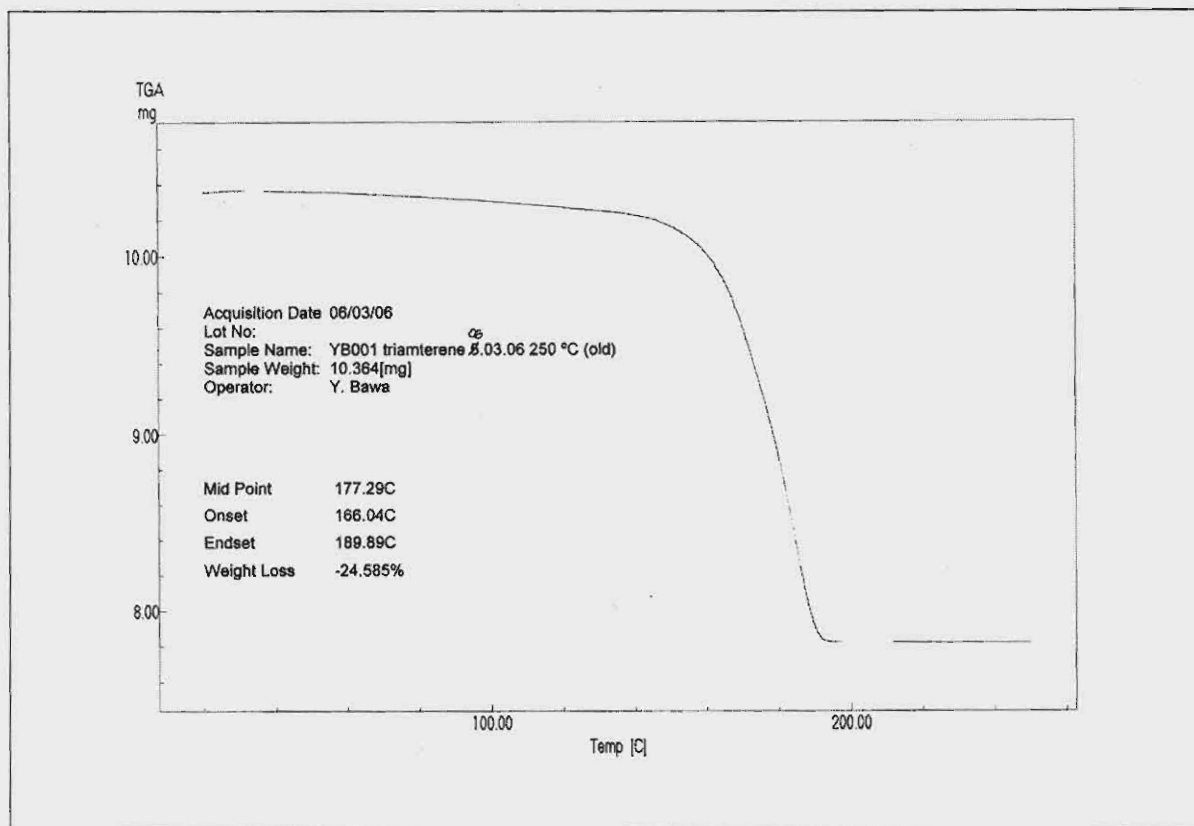


Figure 3.17(a) The TGA thermogram of crystals recrystallised from DMF (YB001). The theoretical weight loss for a DMF solvate is 22.4%.

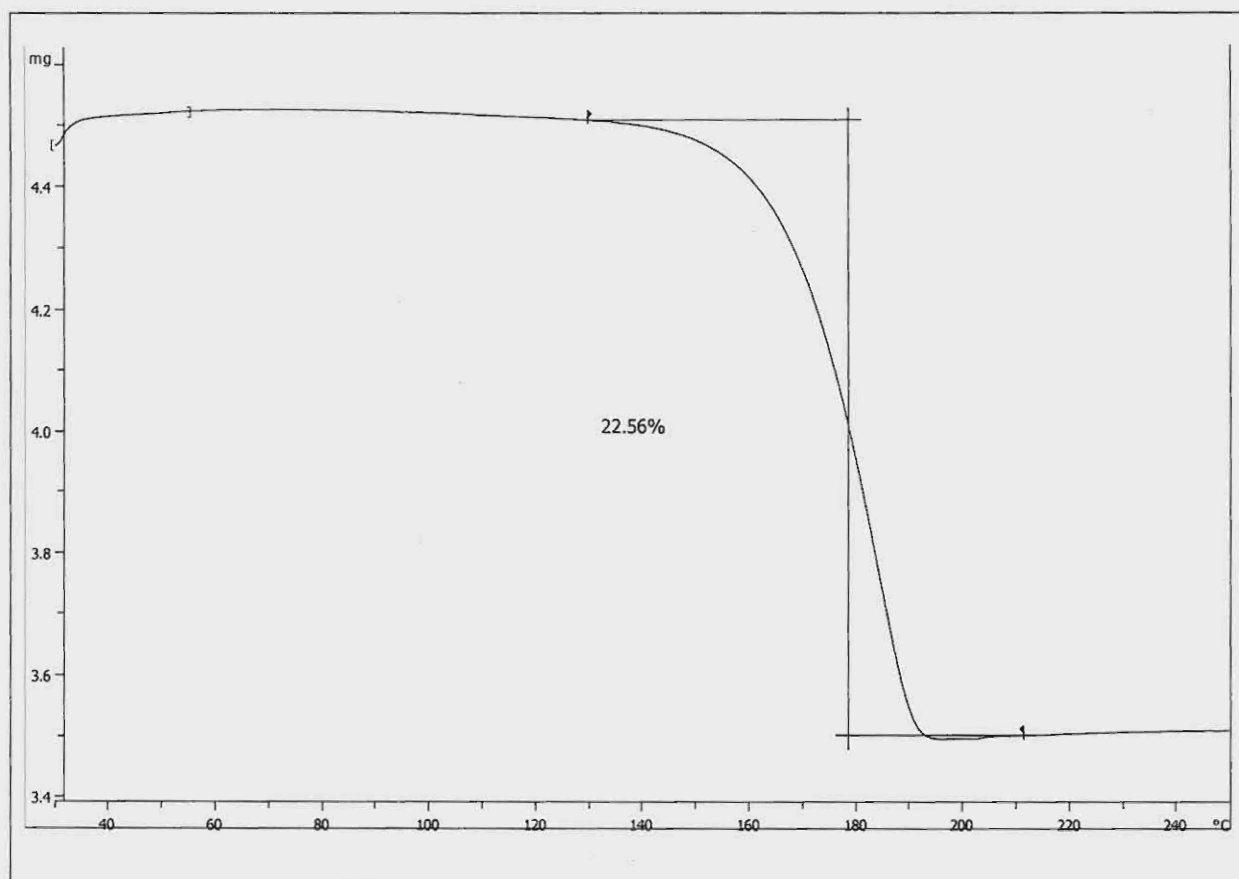


Figure 3.17(b) The TGA thermogram of crystals recrystallised from DMF:water (YB011). The theoretical weight loss for a DMF solvate is 22.4%.

3.8.2.3.5 Infrared spectroscopy (IR)

Table 3.15 lists the main absorption peaks with their corresponding wavenumbers (cm^{-1}) and Figure 3.18 illustrates the IR spectra of triamterene crystals, obtained from DMF (YB001) and DMF:water (YB011).

Table 3.15 Main absorption peaks of crystals recrystallised DMF (YB001) and DMF:water (YB011)

Main absorptions	Wavenumbers (cm ⁻¹)	
	YB001	YB011
1	3943.8	3828.2
2	3831.6	3787.1
3	3736.1	3725.6
4	3725.8	3563.7
5	3650.7	2686.1
6	3021.7	2369.1
7	2763.8	2048.4
8	2343.0	1957.7
9	1954.2	1890.1
10	1890.5	1766.6
11	1718.5	1671.3
12	1560.2	1503.4
13	1541.5	1101.5
14	1508.4	1015.3
15	1257.7	705.3
16	986.7	663.0
17	845.3	594.2
18	638.1	577.2
19	582.2	550.0
20	551.2	525.5
21	530.2	501.3
22	509.3	485.9
23	485.5	477.3
24	474.8	458.7
25	466.1	435.6
26	443.1	426.8
27	430.3	414.2
28	421.5	403.8
29	405.1	

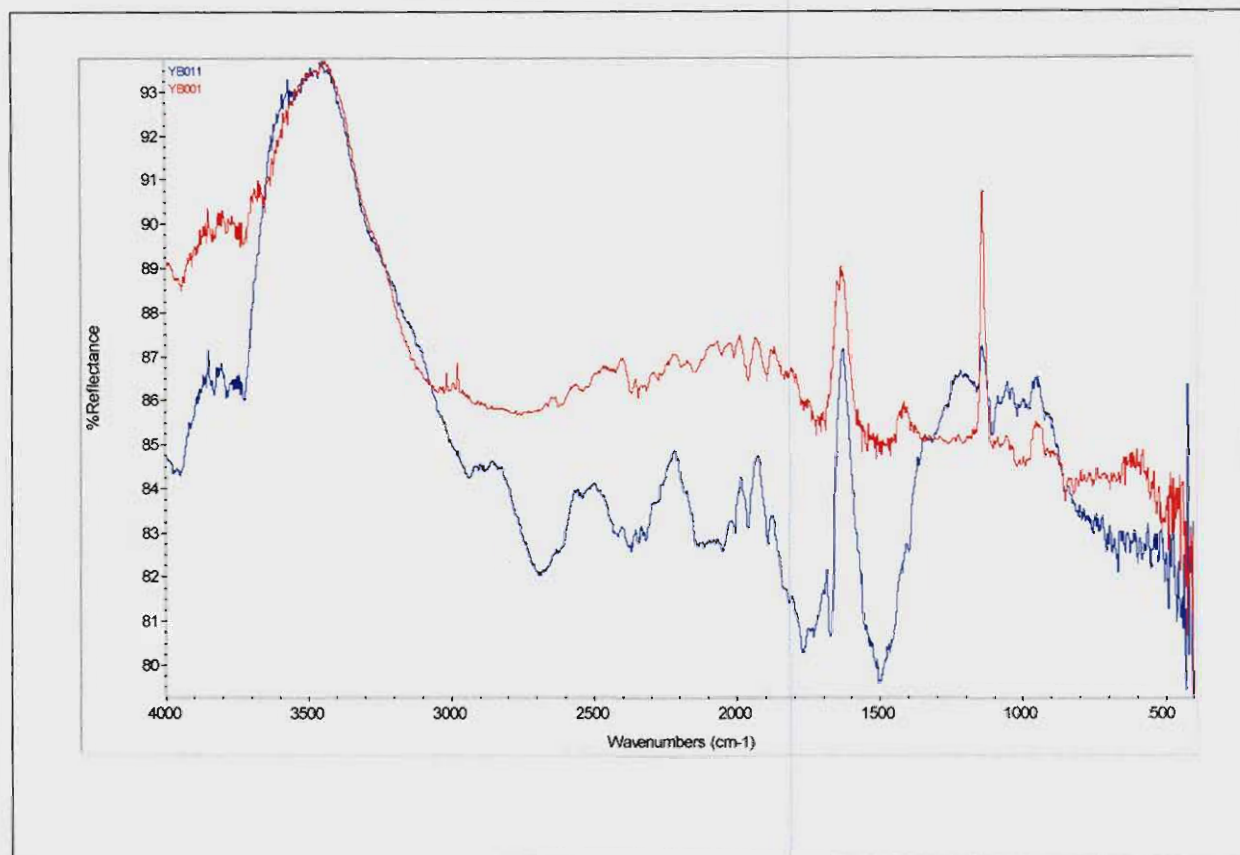


Figure 3.18 IR spectra of triamterene crystals recrystallised from DMF (YB001 = red) and DMF:water (YB011 = blue).

3.8.2.3.6 Discussion of the data generated from DMF mixtures as solvents

According to the results obtained by Dahl *et al.* (1987), the DSC thermogram had 2 desolvation peaks between temperatures of 100 - 200°C, for crystals obtained from DMF:water solutions, whilst the TGA results indicated a weight loss of 21.28%.

From their XRPD results they concluded that there were different degrees of solvation by organic molecules (DMF) and water. The IR spectra obtained by Dahl *et al.* (1987) showed that the crystals of triamterene recrystallised from DMF:water, or mixtures of DMF and / or water, were identical between 250 and 4000 cm^{-1} . They (Dahl *et al.*, 1987) made the conclusion that the DMF:water recrystallisation product consisted of one molecule DMF, one molecule triamterene and a partially occupied water molecule. These crystals also showed different behaviour than those obtained from alcoholic solutions in the absence of water.

In contrast to the findings by Dahl *et al.* (1987), the recrystallisation products from DMF and DMF:water were only solvates. The recrystallisation products for both solutions generated identical physico-chemical data. TM data was clearly indicative of a solvate. The DSC

analysis showed that the melting endotherms of both crystals were comparable and that their desolvation peaks were 199.66°C and 189.66°C, respectively. TGA showed a weight loss of 24.6% and 22.6%, respectively, whilst the theoretical weight loss for a DMF solvate is 22.4%.

Recrystallisation was hampered by low solubility and hence a low crystal yield. This made it impossible to obtain enough crystals on which to perform solubility studies.

3.8.3 Conclusion

To obtain sufficient sample (± 200 mg) for XRPD analysis, the amount of solvent required for recrystallisation was 2 - 3 litres. Because of the extremely low crystallisation yields, solubility studies could not be performed. The amount of sample required for a solubility study of 5 test tubes per solvent, was about 4 g of sample. Hence, the volume of solvent that would be needed, made recrystallisation impractical and impossible to conduct in the small scale recrystallisation facility at our disposal. This was unfortunate, since it was reported in the literature that active pharmaceutical ingredients (API's) with low solubilities, such as mebendazole, showed significant differences in solubilities between the different polymorphic forms (Liebenberg *et al.*, 1998; Swanepoel *et al.*, 2003).

From the data generated during this study it was concluded that:

- The recrystallisation products from the three acid solvents produced disolvates, i.e. novel pseudopolymorphic forms of triamterene;
- The 2-butanol recrystallisation products were either hydrates, solvates, or hydrated solvates; and
- DMF and DMF:water mixtures only yielded solvates.

CHAPTER 4

Roxithromycin

4.1 Introduction

Roxithromycin is a macrolide antibiotic that consists of an erythronolide ring (polyfunctionalised, 14-membered, lactone ring), and is considered as a medically important antibiotic (Gharbi-Benarous *et al.*, 1991). Roxithromycin is a derivative of the parent compound, macrolide antibacterial erythromycin, and has *in vitro* antibacterial activity, resembling that of the parent compound (Markham & Faulds, 1994).

Roxithromycin is more stable than erythromycin under acidic conditions and thus exhibits improved pharmacokinetic properties (Qi *et al.*, 2004).

Clinical efficacies of roxithromycin have been proven in the upper and lower respiratory infections, skin and soft tissue infections, urogenital infections and orodental infections, and it appears to be as effective as more established treatments, including erythromycin, amoxicillin / clavulanic acid and cefalor (Markham & Faulds, 1994). Roxithromycin has been clinically used for the treatment of respiratory infections, caused by Gram-positive and Gram-negative cocci, Gram-positive bacilli and some Gram-negative bacilli (Qi *et al.*, 2004).

It can therefore be concluded that roxithromycin is an attractive therapeutic alternative in its established indications, especially when the option of once-daily administration is considered (Markham & Faulds, 1994).

As was mentioned in chapter 1, before a drug can be absorbed into the body from the gastro-intestinal tract, it must normally be in solution. For a drug to go into solution it should be first wetted by the liquid phase and then dissolved (Forster *et al.*, 1991). Drugs with low water solubility need specific attention to allow the formulation to be improved. The dissolution rate and solubility in a solvent medium are two of the most important characteristics of an active pharmaceutical ingredient, because these quantities determine the bioavailability of the drug for its intended therapeutic use (Brittain & Grant, 1999).

Roxithromycin is very slightly soluble in water, slightly soluble in diluted hydrochloric acid, and freely soluble in acetone, alcohol and dichloromethane (BP, 2002). Du Plessis (2004) reported that some of the roxithromycin polymorphic forms gave problems during a powder dissolution study, due to poor wettability in the dissolution medium. Furthermore, prior to the

dissolution, during vortexing of the powder, a gel formed, which complicated the quantitative transfer of the samples into the dissolution vessels, hence resulting in poor dissolution results.

The aim of this investigation thus was to prepare different crystal forms of roxithromycin, and, instead of performing powder dissolution studies, to determine the solubility thereof, which would arguably be a better method of discriminating between the solubilities of the different forms.

4.2 Description

4.2.1 Nomenclature

Chemical name

(3R,4S,5S,6R,7R,9R,11S,12R,13R,14R)-6-[(2S,3R,4S,6R)]-4-dimethylanmethyl-oxan-2-yl]oxy-14-ethyl-7,12,13-trihydroxy-4-[(2S,4R,5S,6S)-5-hydroxy-4-6-dimethyl-oxan-2-yl]oxy-10-(2-methoxyethoxymethoxyimino)-3,5,7,9,11,1-oxacyclotetradican-2-one

(DrugBank, 2006:1).

Non-proprietary name

Roxithromycin.

Proprietary names

Rulide®, and Roithromycin-Hexal® (Johnnic communications, Feb. 2004).

ROX®, Rulid®, and Surlid® (DrugBank, 2006:1).

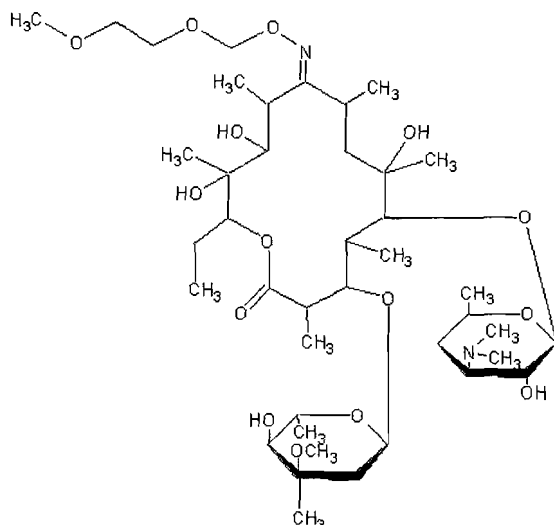
Biaxsig®, Roxar®, and Roximycin® (Wikipedia, 2007).

4.2.2 Formulae

Empirical formula

C₄₁H₇₆N₂O₁₅ (DrugBank, 2006:1).

Structural formula



(DrugBank, 2006:1).

4.3 Molecular weight

837.047 g/mol (DrugBank, 2006).

4.4 Pharmaceutics of roxithromycin

4.4.1 Pharmaceutics

Rulide®, supplied by Aventis, and Roxithromycin-Hexal®, supplied by Hexal, are the two roxithromycin formulations that are available in South Africa:

- each tablet contains 150 mg of roxithromycin;
- schedule 4 medication;
- available as tablets, and thus only for oral administration;
- available in packaging of 10; and
- store at room temperature and away from light (Johnnic communications, Feb. 2004).

4.4.2 Dosage and administration

It is recommended that Roxithromycin is taken daily; an oral dosage of 300 mg for adults, which may be administered as either 150 mg every 12 hours, or 300 mg once daily. The

recommended dose for infants and children is 5 - 8 mg/kg of body weight, administered in 2 divided doses, for a maximum of 10 days (Markham & Faulds, 1994).

4.5 Pharmacology of roxithromycin

4.5.1 Pharmacokinetic properties

There is a substantial difference between the pharmacokinetic profile of roxithromycin and that of its parent compound, erythromycin (Markham & Faulds, 1994).

4.5.1.1 Absorption

Roxithromycin is very rapidly absorbed and diffuses into most of the tissues and phagocytes, and thus roxithromycin is actively transported to the site of infection (DrugBank, 2006).

A mean plasma concentration of roxithromycin ranges between 6.6 mg/L and 7.9 mg/L within 2 hours after administration of a single, oral, 150 mg dose. When compared to erythromycin, there was a 3.3 difference in the concentration between the two antibiotics (Markham & Faulds, 1994).

Figure 4.1 shows the plasma concentration differences between roxithromycin 150 mg that was taken every 12 hours, and erythromycin 250 mg that was taken every 6 hours, in 12 volunteers (Markham & Faulds, 1994).

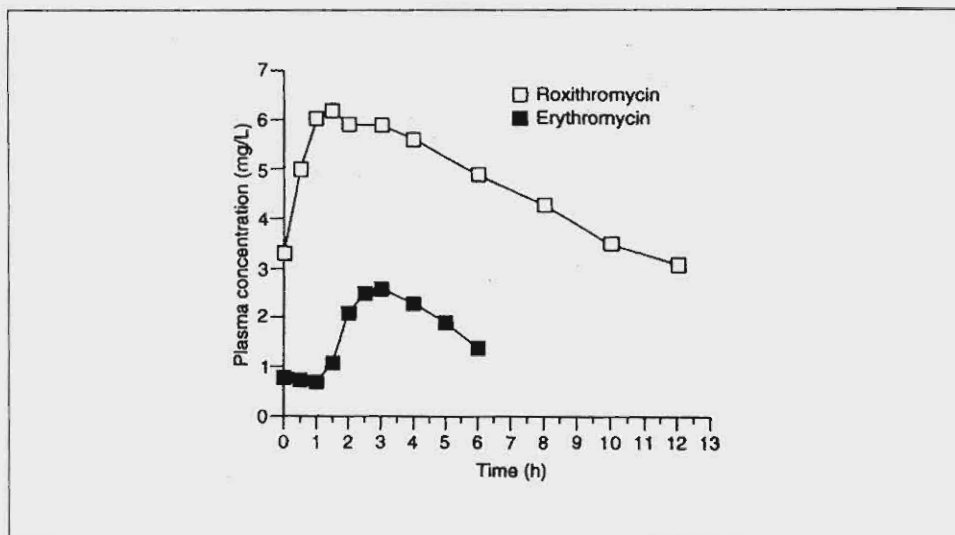


Figure 4.1 Plasma concentration against time curves for roxithromycin 150 mg and erythromycin 250 mg (Markham & Faulds, 1994).

According to Markham and Faulds (1994), administration of roxithromycin 15 minutes after a standard meal, may result in reduced bioavailability and it is therefore recommended to take the drug at least 15 minutes before a meal.

4.5.1.2 Metabolism and elimination

According to Jarukamjorn (1998), the *in vivo* anti-microbial potency of roxithromycin is greater than that of erythromycin. This difference may be caused by the slow rate of metabolism of roxithromycin, through mono- and didemethylation, or cleavage of the cladinose.

According to Markham and Faulds (1994), descladinose, N-didemethyl and N-mono-demethylated derivatives of roxithromycin have been identified in urine and faeces, whilst only erythromycin was found in the plasma. The parent drug was detected in the plasma only, whereas these biotransformation products of roxithromycin have been identified in the urine and faeces of man (Jarukamjorn, 1998).

Roxithromycin does not induce cytochrome P450 (CYP) 3 A 1/2 and CYP3A4, the enzymes that catalyse the N-demethylation of all macrolide antibiotics in the liver microsomes of rat and man, respectively, which is in contrast to the action of erythromycin (Jarukamjorn, 1998).

Roxithromycin is metabolised in small portions. Most of the unchanged roxithromycin is secreted unchanged into the bile and some in exhaled air. Less than 10% is excreted into the urine. The half-life is 12 hours (Wikipedia, 2007).

The plasma clearance appears to be dose- or plasma concentration-dependent (Markham & Faulds, 1994).

According to Markham and Faulds (1994), it was found that the mean elimination half-life of roxithromycin 150 mg, or 300 mg, was 8.4 - 15.5 hours. This was much longer than that of the patent drug erythromycin.

According to their studies, it was suggested that the pharmacokinetics of roxithromycin were nonlinear and may include a saturable process involving the release of plasma α 1-acid glycol-protein-bound roxithromycin, for distribution and elimination (Markham & Faulds, 1994).

4.5.1.3 Distribution

The concentrations of roxithromycin in tissue and body fluids are generally higher than the MIC₉₀ values for susceptible bacteria. In bronchial secretions the mean peak roxithromycin concentration was 4.71 mg/L, after 2 - 4 hours in 7 intensive care patients who received a 300 mg loading dose each, followed by six 12-hourly 150 mg doses. After 1 hour the corresponding mean peak serum level was 8.74 mg/L (Markham & Faulds, 1994).

The gastric mucosal tissue concentrations, after roxithromycin 150 mg was given twice daily for 2 days, resulted in concentrations of 13.14 mg/kg, 4 hours after the last dose. The corresponding plasma concentration was 11.85 mg/L (Markham & Faulds, 1994).

In gingival tissue and alveolar bone the peak roxithromycin concentrations were 6.55 mg/L and 5.09 mg/L, respectively, which occurred approximately 2 hours after a peak plasma concentration of 6.12 mg/L was reached (Markham & Faulds, 1994).

4.5.2 Working mechanism of roxithromycin

According to Markham and Faulds (1994), roxithromycin disrupts the bacterial protein synthesis by binding to the 50S bacterial sub-unit. Roxithromycin has a lesser affinity for the target site than erythromycin. A balance is maintained by the higher body tissue and fluid

concentrations, resultant from increased absorption and distribution of roxithromycin, relative to erythromycin.

In resistant bacteria the ribosomal sub-unit is altered, hence preventing binding. *In vitro* it had been observed that this resistance mechanism affected all 14-membered macrolides and almost complete cross-resistance between roxithromycin and erythromycin (Markham & Faulds, 1994).

According to the DrugBank (2006), roxithromycin prevents bacteria from growing, by interfering with their protein synthesis. By binding to the sub-unit 50S of bacterial ribosome, it inhibits the translocation of peptides.

4.5.3 Drug interactions

As roxithromycin has a lower affinity for cytochrome P450 than erythromycin, it has fewer interactions than erythromycin. An increase in concentration of theophylline had been detected when roxithromycin was administered with theophylline. There was an interaction between roxithromycin and warfarin and severe bleeding episodes occurred (Wikipedia, 2007). *In vitro* roxithromycin may have interacted with the antiarrhythmic drug, disopyramide (Markham & Faulds, 1994).

The pharmacokinetic profile of carbamazepine, or the efficacy of oral contraceptives is not affected by roxithromycin, and does not interact with ranitidine, or antacids containing aluminium, or magnesium hydroxide (Markham & Faulds, 1994).

4.5.4 Side effects

Amongst the most common side effects are those gastrointestinal, including (Wikipedia, 2007):

- Diarrhoea;
- Nausea;
- abdominal pain; and
- vomiting.

Amongst the less common side effects include central or peripheral nervous system events such as (Wikipedia, 2007):

- dizziness;

- headaches;
- vertigo;
- rarely seen rashes;
- abnormal liver function values; and
- alteration in senses of smell and taste.

4.6 Physico-chemical properties of roxithromycin raw material

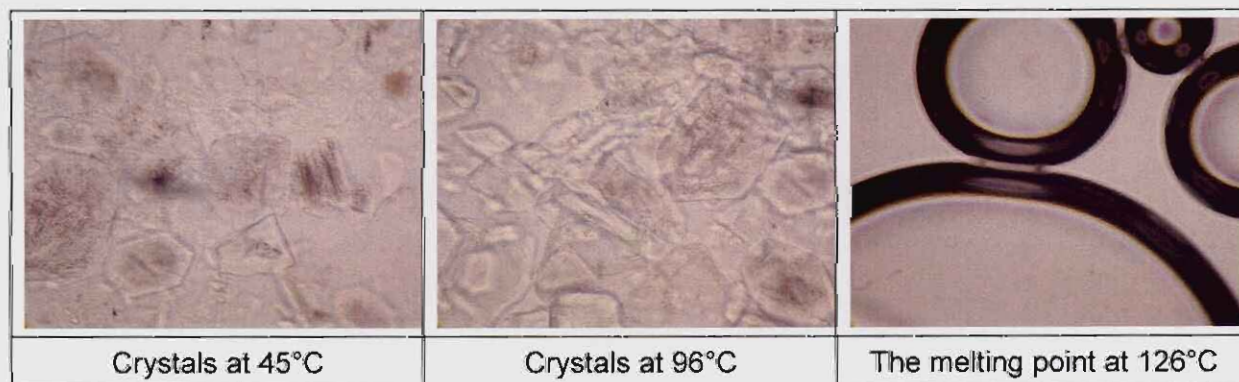
4.6.1 Results generated during this study

The physico-chemical properties of the roxithromycin polymorphic forms and those of the raw material were investigated, using the analytical methods as was described in chapter 2.

4.6.1.1 Thermo microscopy (TM)

A small sample of roxithromycin raw material (B/N: 62206005, Alembic) was immersed in a drop of silicone oil on an object plate, and covered with a cover plate. Table 4.1 shows the TM pictures recorded over the elevated temperature range of roxithromycin raw material (YBR00).

Table 4.1 TM results of crystals recrystallised from roxithromycin raw material (YBR00)



4.6.1.2 X-ray powder diffractometry (XRPD)

Roxithromycin raw material was carefully ground and prepared for XRPD analysis.

The procedure comprised the packing of approximately 200 mg of powdered samples into aluminium sample holders. The measurement conditions were: target, Cu; voltage, 40 kV;

current, 30 mA; divergence slit, 2 mm; antiscatter slit, 0.6 mm; detector slit, 0.2 mm; monochromator; scanning speed, 2°/min with step size, 0.025° and step time, 1.0 sec.

The peak angles ($^{\circ}2\theta$) and relative intensities (I/I₀) of the main peaks are listed in Table 4.2. The XRPD pattern of roxithromycin raw material is illustrated in Figure 4.2.

Table 4.2 Main XRPD intensity ratios (I/I₀) and main peak angles ($^{\circ}2\theta$) of roxithromycin raw material (YBR00)

Peak angles ($^{\circ}2\theta$)	Relative intensities (I/I ₀)
7.3	3.2
8.4	13.5
9.9	100
10.5	5.9
11.1	19.3
11.7	70.2
12.2	8.3
13.3	21.3
14.3	13
14.7	36.8
15.2	4.4
16.1	17.4
16.5	7.6
16.9	12.9
17.4	19
17.8	11.3
18.9	7.1
19.1	7.5
19.5	4.7
19.8	5.4
20.6	7.4
21.2	7.6
21.8	12.5
22.2	11.4
22.6	5.3
23.1	11.7

23.5	6
23.7	6.1
24.4	15.7
25.4	4.4
26.1	5.4
27.8	5.2
28.2	6.7
29.5	8.5

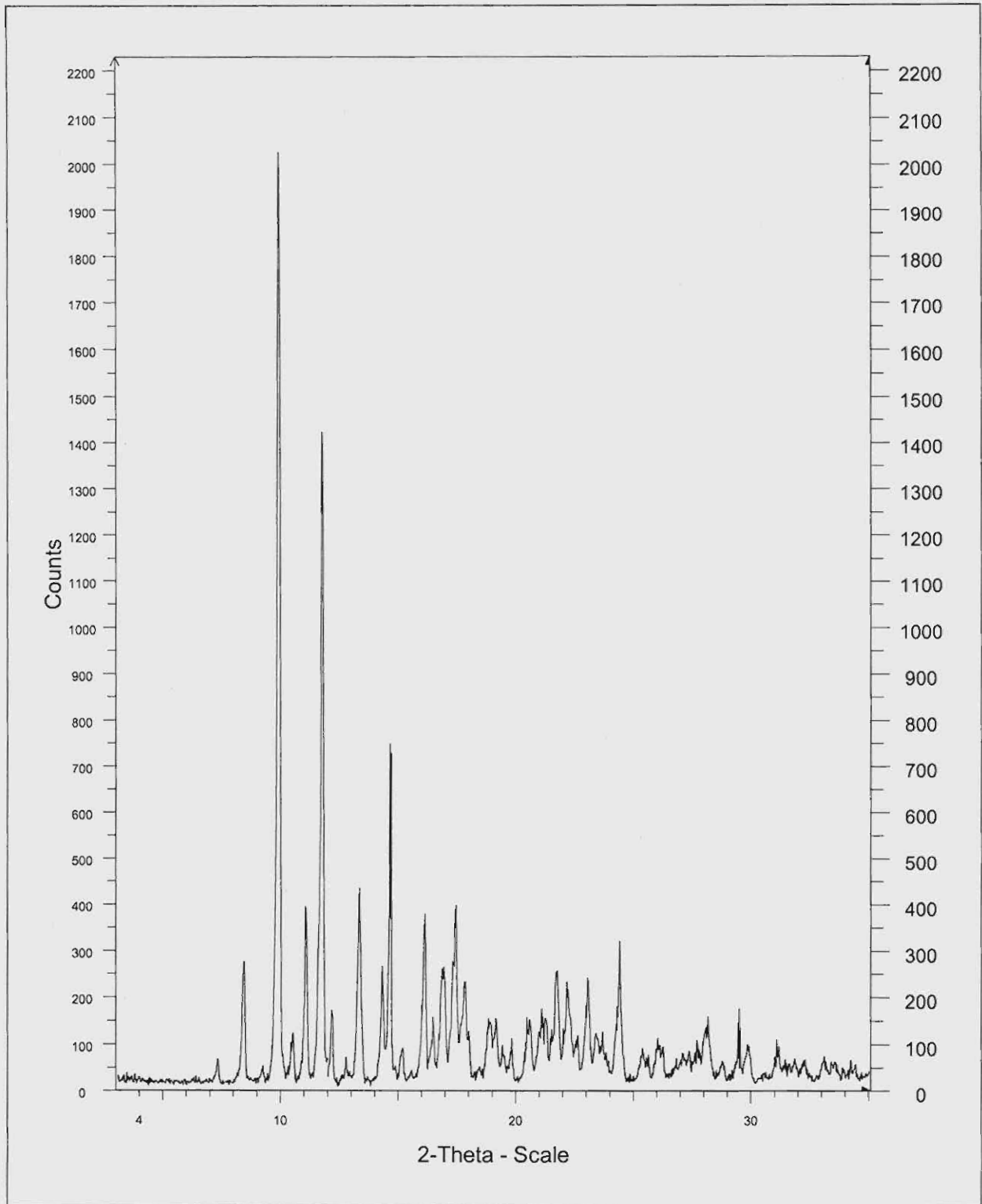


Figure 4.2 XRPD pattern of roxithromycin raw material (YBR00).

4.6.1.3 Differential scanning calorimetry (DSC)

A mass of approximately 2 – 4 mg of samples each was weighed and heated in closed aluminium crimp cells with pierced lids, at a heating rate of 10°C/min. The samples were heated under a nitrogen purge with a flow rate of 50 ml/min, to a maximum temperature of 200°C.

Figure 4.3 shows the DSC thermogram of the crystals recrystallised from roxithromycin raw material, with the melting point at peak maximum i.e. at 122°C.

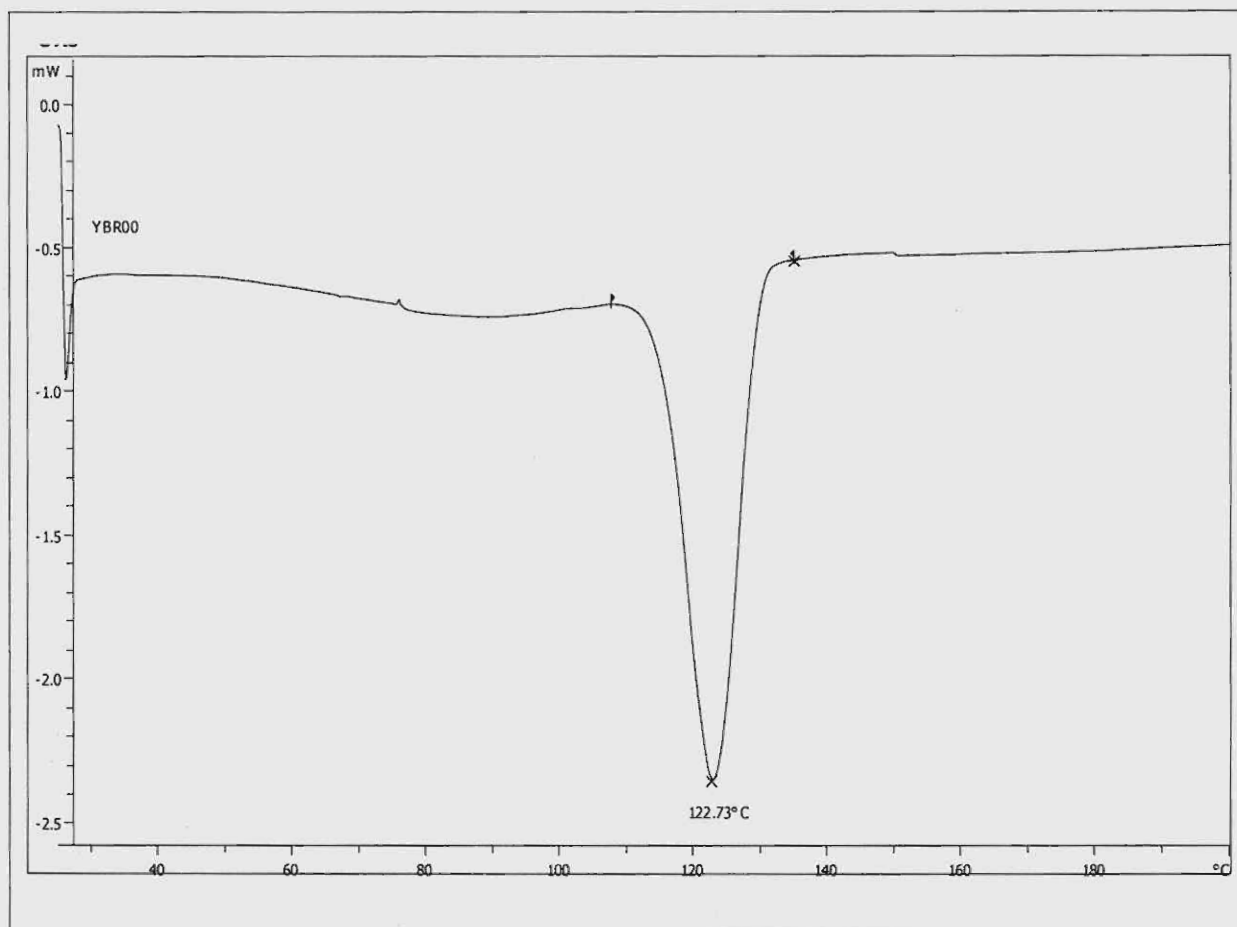


Figure 4.3 DSC thermogram of roxithromycin raw material (YBR00).

The DSC thermogram of the powder obtained for roxithromycin raw material displays no evidence of desolvation and/or dehydration, therefore no TGA analysis was performed.

4.6.1.4 Infrared spectroscopy (IR)

The raw material sample and KBr powder were ground and placed in the IR spectrophotometer, where the IR was generated by means of diffuse reflectance infrared Fourier transform spectroscopy (DRIFTS), over a range of 400 – 4000 cm^{-1} .

Table 4.3 lists the main absorption peaks with their corresponding wavenumbers (cm^{-1}) of roxithromycin raw material, whilst Figure 4.5 shows the IR spectrum of roxithromycin raw material.

Table 4.3 Main IR absorption peaks of roxithromycin raw material (YBR00)

Main absorptions	Wavenumbers (cm^{-1})
1	3678.1
2	3577.2
3	3524.0
4	3463.2
5	3269.0
6	2980.5
7	2828.4
8	1975.9
9	1725.9
10	1629.0
11	1466.4
12	1387.6
13	1368.8
14	1344.7
15	1289.3
16	1241.0
17	1170.6
18	1128.3
19	1112.6
20	1078.1
21	1050.4
22	1012.0
23	983.2
24	958.3

25	914.1
26	891.6
27	866.1
28	847.9
29	831.7
30	803.0
31	790.1
32	767.7
33	723.5
34	707.0
35	698.0
36	635.1
37	603.4

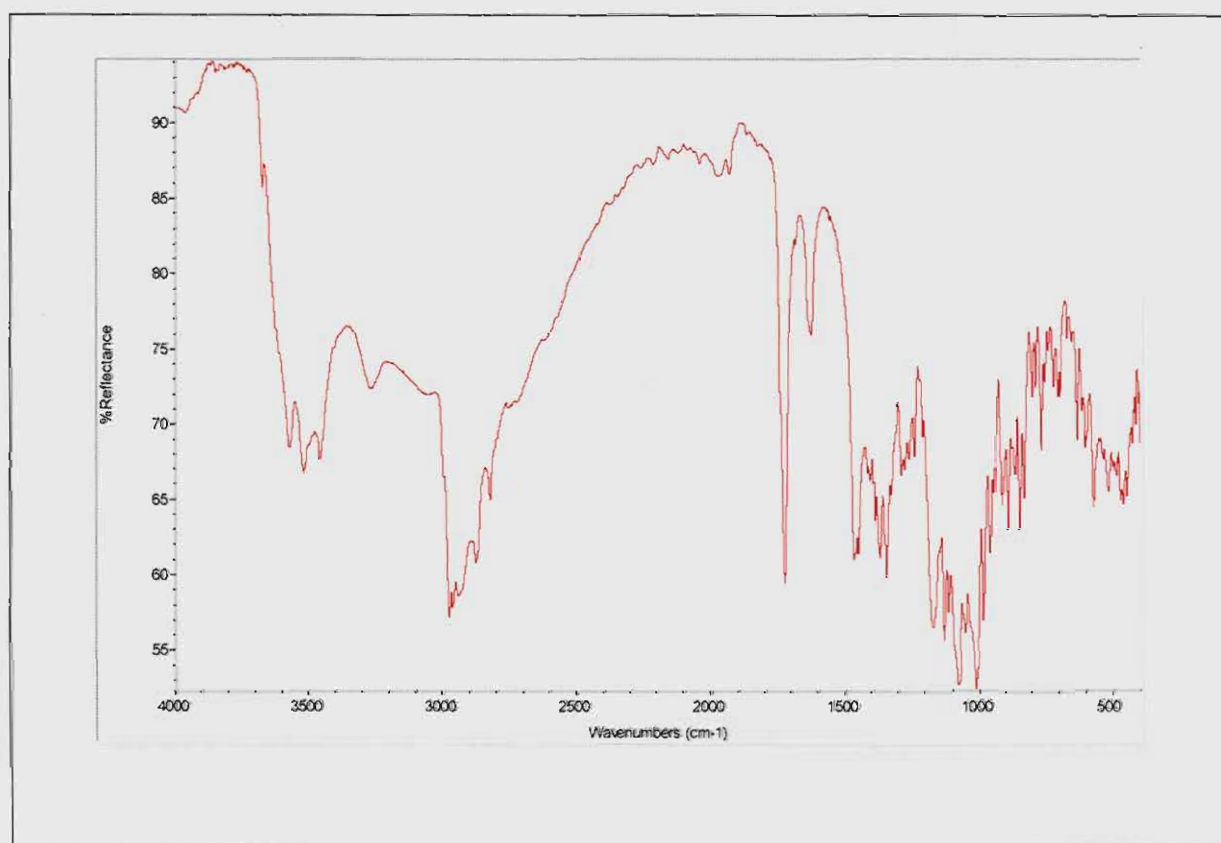


Figure 4.5 IR spectrum of roxithromycin raw material (YBR00).

4.6.1.5 Solubility

A 24-hour solubility test was performed, using three media, i.e. 0.1 N HCl, phosphate buffer, and milli-Q water. The samples for the solubility test in different media were obtained from the same batch of roxithromycin, having a median particle size of 191 μm . Approximately 0.2 g of each sample was weighed into 10 ml test tubes with screw caps; 5 labeled test tubes for each solvent. 5 ml of solvent was added to the samples. These samples were rotated at 54 rpm (Heidolph RZR-2000 rotator, Germany), in a thermostatically (Julabo EM/4 thermostat, Germany) controlled water bath, at $39 \pm 2^\circ\text{C}$.

After 24 hours the samples were removed from the bath and withdrawn, using a 10 ml syringes per sample, to which a 0.45 μm , low protein binding, durapore (PVDF) membrane was attached. 2 ml of each sample was diluted to 50 ml, using the 3 media. The concentrations of the diluted samples were determined spectrophotometrically at 206 nm. A Beckman DU-650i spectrophotometer (USA) was used.

Calculations

$$\text{theoretical concentration} = \frac{\text{experimental mass (mg)}}{\text{theoretical mass (mg)}} \times \text{dilution factor} \times 1000$$

$$\text{theoretical absorbance} = \frac{(y - \text{intercept} \times \text{theoretical concentration})}{x - \text{intercept}}$$

$$\text{experimental concentration (in buffer)} = \frac{(\text{theoretical concentration} \times \text{absorbance})}{\text{theoretical absorbance}}$$

Table 4.4 illustrates the differences in solubility in the different media: 0.1 N HCl, and phosphate buffer and water.

Table 4.4 Solubility test results of roxithromycin raw material (YBR00)

Test tube	Concentration ($\mu\text{g/ml}$)		
	0.1 N HCl	Phosphate buffer (pH 6)	H ₂ O
1	34.874	10.584	0.744
2	34.574	10.452	0.695
3	34.525	11.519	0.719
4	34.622	9.982	0.684
5	34.001	10.438	0.610
Average	34.6576	10.8515	0.7193

It is clear from these solubility test results that roxithromycin raw material was almost insoluble in water, and the best solubility results were obtained in the 0.1 N HCl medium.

4.7 Characterisation of roxithromycin crystal forms

4.7.1 Preparation of roxithromycin crystals

Du Plessis (2004) recrystallised roxithromycin from chloroform, ethyl acetate, dichloromethane and acetonitrile. The chosen forms were more amorphous than the raw material. These different crystal forms obtained and reported by Du Plessis (2004) were used as the basis of this study.

4.7.2 Method of preparation of roxithromycin crystals

Approximately 1 g of roxithromycin powder was added to a beaker each that was filled with a different solvent. The beaker was placed on a hot plate Heidolph MR 3001 (Heidolph, Germany) and a stirring magnet added. The solution was made supersaturated by gradually adding solvent into the beaker, until all the crystals dissolved. The beaker was then removed from the hot plate, the stirring magnet removed and the beaker opening covered with parafilm, which had been perforated. These samples were then placed in a cupboard and left undisturbed for a period of time, to allow for the slow evaporation of the solvents at room temperature. The solvents that were used are listed in Table 4.5.

Table 4.5 Solvents used for the recrystallisation of roxithromycin


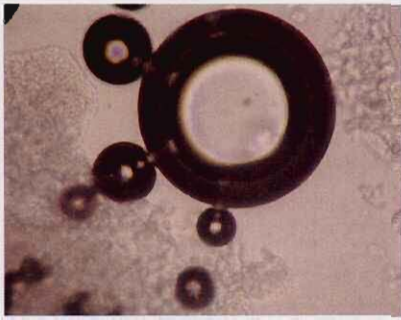
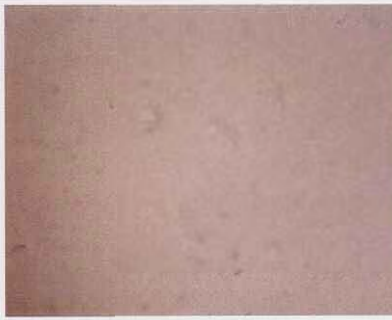
Solvent	Boiling point at NTP	Manufacturer
Ethyl acetate	77	Saarchem, South Africa
Acetonitrile	76	BDH Laboratory Suppliers, England.
Dichloromethane	39	Saarchem, South Africa
Chloroform	62	Saarchem, South Africa

4.7.3 Ethyl acetate

4.7.3.1 Thermo-microscopy (TM)

Table 4.6 illustrates the TM pictures taken over the elevated temperature range for the crystals recrystallised from ethyl acetate (YBR01).

Table 4.6 TM results of crystals recrystallised from ethyl acetate (YBR01)

		
Crystals at 25°C	Gas evolution, i.e. desolvation at 120°C	The melting point at 132°C

4.7.3.2 X-ray powder diffractometry (XRPD)

The peak angles (2θ) and relative intensities (I/I_0) of the main peaks are listed in Table 4.7. The XRPD pattern of roxithromycin crystals recrystallised from this solution is illustrated in Figure 4.6.

Table 4.7 Main XRPD intensity ratios (I/I₀) and main peak angles (°2θ) of roxithromycin crystals recrystallised from ethyl acetate (YBR01)

Peak angles (°2θ)	Relative intensities (I/I ₀)
4.7	12.4
6.8	47
7.5	23.5
8.0	30.8
8.3	26.8
9.4	20.1
9.9	100
10.4	12.6
11.1	36.6
11.7	59.6
12.8	20.6
13.3	20.6
13.6	14.2
14.3	18
14.6	21.6
16.1	27.8
16.4	13.9
16.8	25.9
17.4	22.9
17.8	19.1
18.8	18.7
19.6	18
20.6	13.5
21.2	21.4
21.7	20.4
22.2	15.9
23.0	14.9
24.4	12.4
26.1	9.2
34.3	6.5

Figure 4.6 XRPD pattern of roxithromycin crystals recrystallised from ethyl acetate (YBR01).

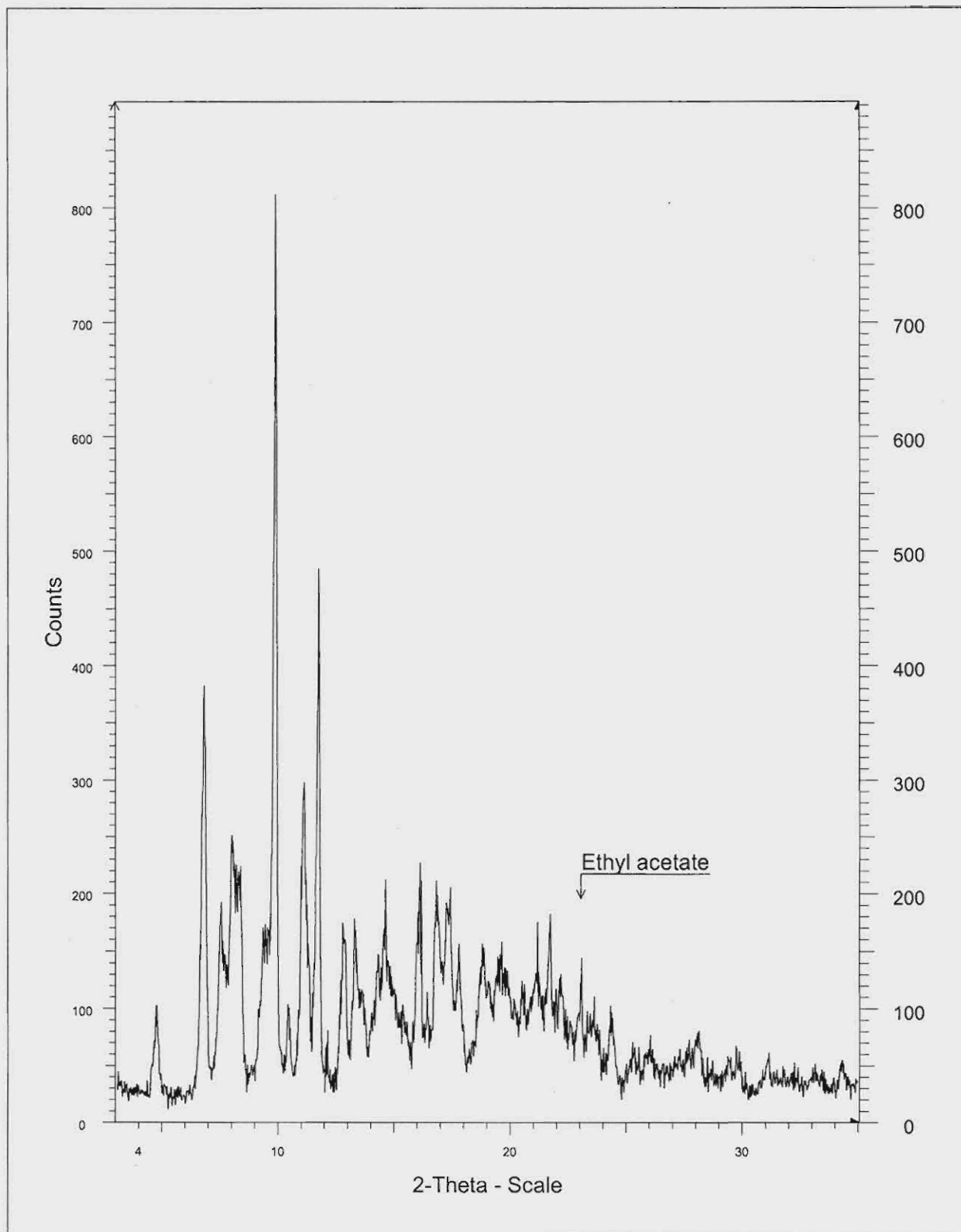


Figure 4.6 XRPD pattern of roxithromycin crystals obtained from ethyl acetate (YBR01).

4.7.3.3 Differential scanning calorimetry (DSC)

Figure 4.7 shows the DSC thermogram of the roxithromycin crystals recrystallised from ethyl acetate (YBR01). The peak at 96°C represents desolvation and the endotherm at 131°C the melting point.

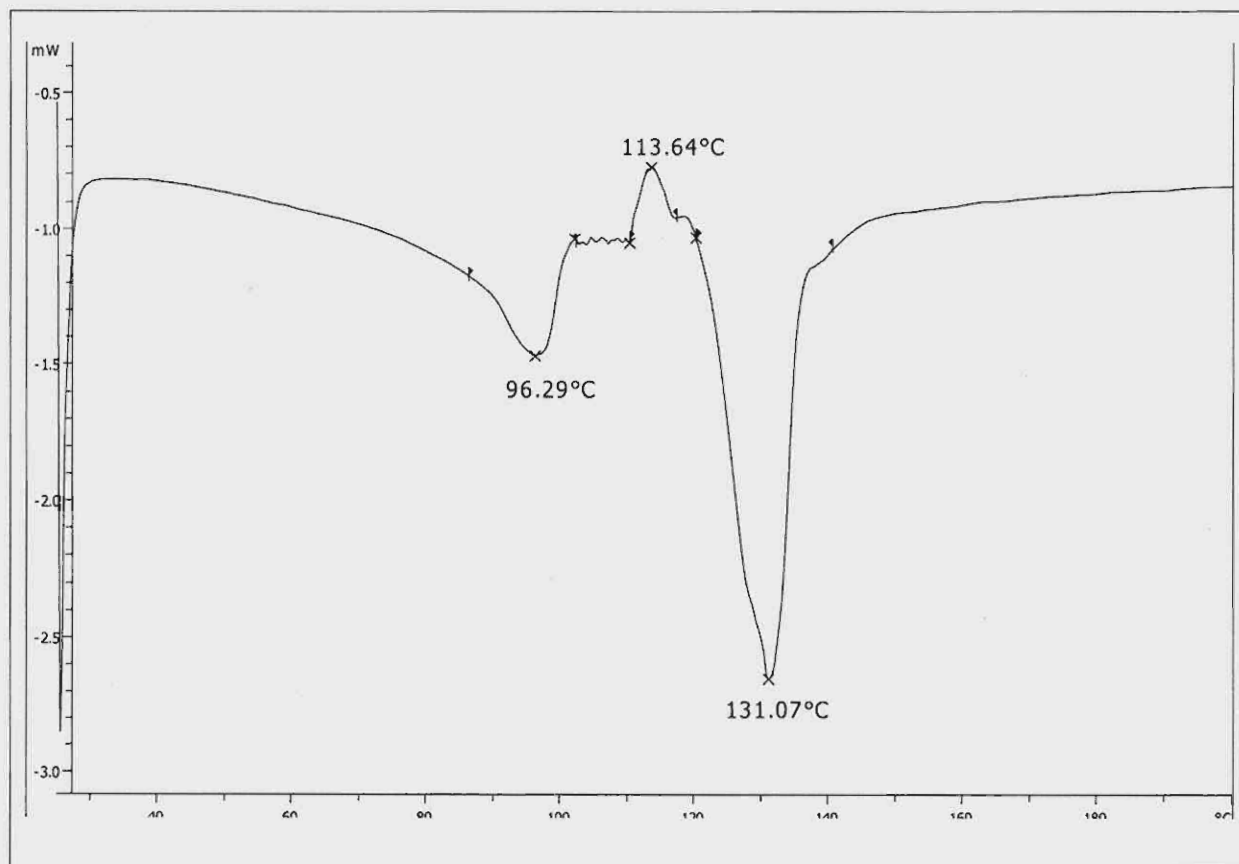


Figure 4.7 DSC thermogram of roxithromycin crystals recrystallised from ethyl acetate (YBR01).

4.7.3.4 Thermogravimetric analysis (TGA)

Figure 4.8 shows the TGA thermogram of the crystals recrystallised from ethyl acetate (YBR01). Karl Fischer determination gave a total moisture content of only 1.4%, which was considered as surface moisture.

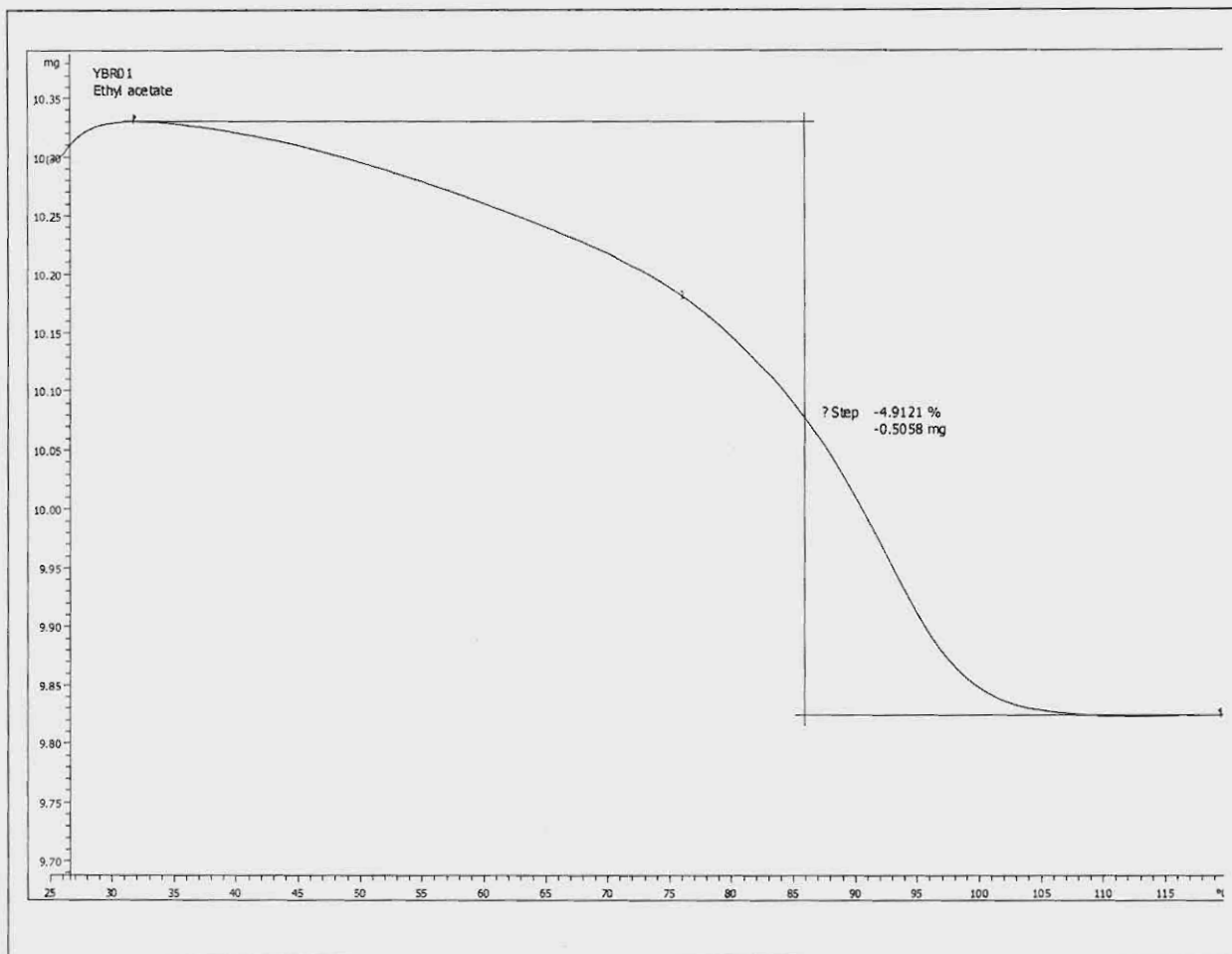


Figure 4.8 The TGA thermogram of crystals recrystallised from ethyl acetate (YBR01) with a 4.9 % weight loss (theoretical weight loss of an ethyl acetate solvate = 9.5%).

4.7.3.5 Infrared spectroscopy (IR)

Table 4.8 lists the main absorption peaks with their corresponding wavenumbers (cm^{-1}) of the crystals recrystallised from ethyl acetate, whilst Figure 4.9 shows the IR spectrum of these crystals.

Table 4.8 Main IR absorption peaks of roxithromycin crystals recrystallised from ethyl acetate (YBR01)

Main absorptions	Wavenumbers (cm^{-1})
1	3670.0
2	3619.8

3	3417.2
4	2970.0
5	2827.8
6	2781.7
7	2241.1
8	1957.3
9	1736.7
10	1634.0
11	1463.3
12	1376.1
13	1341.9
14	1242.3
15	1165.5
16	1052.8
17	1010.7
18	958.9
19	891.6
20	863.3
21	834.9
22	804.8
23	773.3
24	749.2
25	736.3
26	712.6
27	697.4

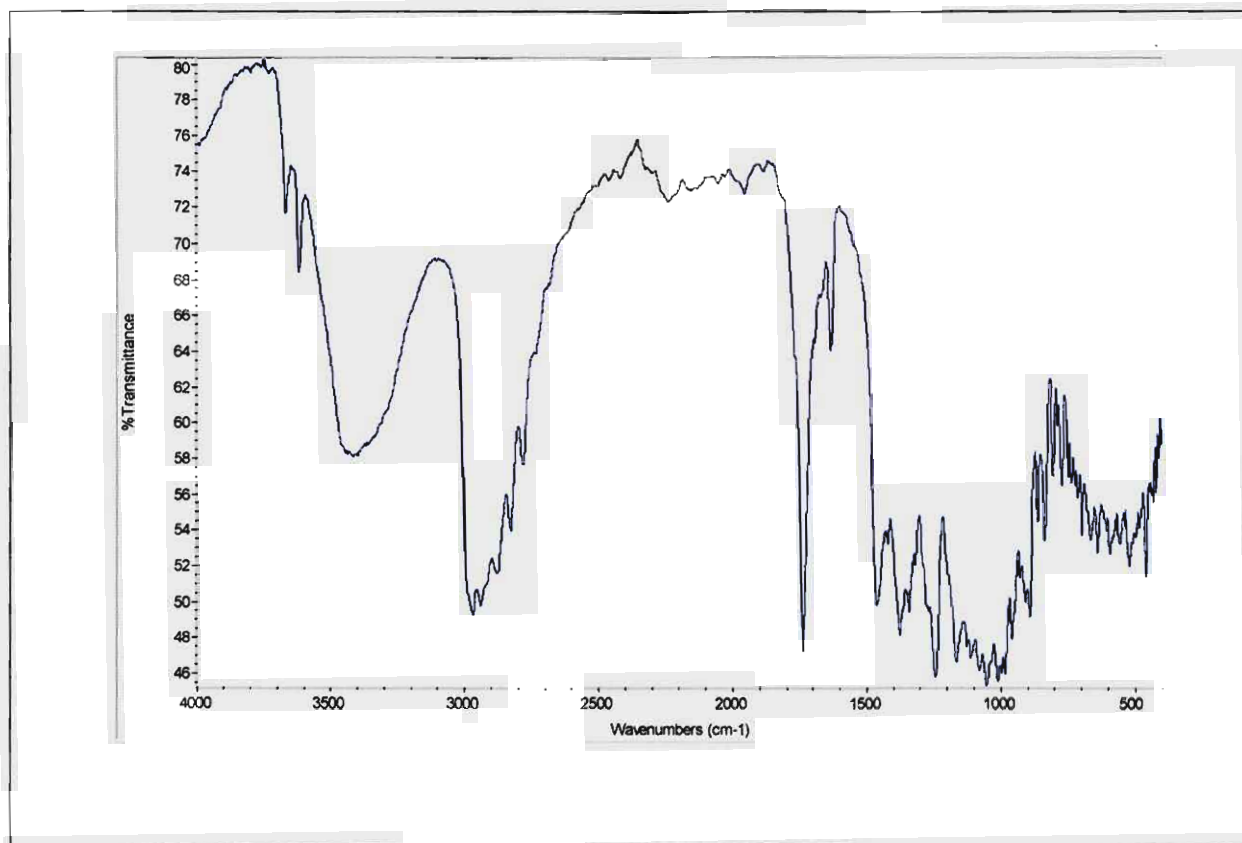


Figure 4.8 IR spectrum of crystals recrystallised from ethyl acetate (YBR01).

4.7.3.6 Solubility

Due to rapid desolvation of the prepared crystal forms, grinding and sieving of all the prepared forms, prior to performing the solubility tests, were omitted. The solubility test was performed over a 24-hour period, with the measurement being taken at the end of the period, which would have made any particle size difference irrelevant for the purpose of this test.

The media used were 0.1 N HCl, phosphate buffer, and water.

Table 4.9 is a summary of the solubility test results being generated for the ethyl acetate recrystallisation product.

Table 4.9 Solubility test results of roxithromycin crystals recrystallised from ethyl acetate (YBR01)

Test tube	Concentration ($\mu\text{g/ml}$)		
	0.1 N HCl	Phosphate buffer (pH 6)	H ₂ O
1	Experimental error	18.883	10.106
2	32.109	16.535	12.083
3	32.736	23.297	10.794
4	34.254	20.110	12.969
5	34.681	17.115	12.447
Average	33.445	19.5718	10.9945

The solubility of the crystals was in the following order: 0.1 N HCl > phosphate buffer (pH 6) > water.

4.7.3.7 Discussion of the data generated from ethyl acetate as solvent

Gas evolution was observed during the TM study. According to the DSC results, a desolvation peak was measured at 96°C. The TGA measured a 4.9% weight loss, whilst the theoretical weight loss of an ethyl acetate solvate = 9.5%. All these measurements and analytical results indicated that this crystal form probably was a hemi ethyl acetate solvate.

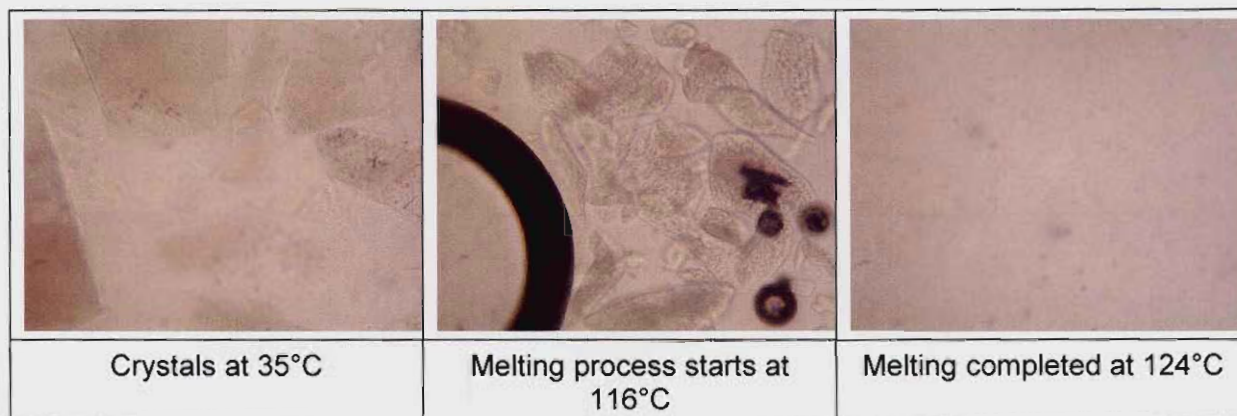
The crystals that were recrystallised from ethyl acetate (YBR01) were unexpectedly highly soluble in all the media. The solubility of these polymorphs in water was 10.9 $\mu\text{g/ml}$, compared to the 0.72 $\mu\text{g/ml}$ for the raw material in water. The concentration of dissolved crystals in 0.1 N HCl was, however, similar, i.e. 34.7 $\mu\text{g/ml}$ and 33.4 $\mu\text{g/ml}$, for the raw material and ethyl acetate, respectively.

4.7.4 Acetonitrile (ACN)

4.7.4.1 Thermo-microscopy (TM)

Table 4.10 shows the TM pictures taken over the elevated temperature range for ACN (YBR02).

Table 4.10 TM results of crystals recrystallised from ACN (YBR02)



4.7.4.2 X-ray powder diffractometry (XRPD)

The peak angles ($^{\circ}2\theta$) and relative intensities (I/I_0) of the main peaks are listed in Table 4.11. The XRPD pattern of roxithromycin crystals being recrystallised from this solution is illustrated in Figure 4.10.

Table 4.11 Main XRPD intensity ratios (I/I_0) and main peak angles ($^{\circ}2\theta$) of roxithromycin crystals recrystallised from ACN (YBR02)

Peak angles ($^{\circ}2\theta$)	Relative intensities (I/I_0)
4.2	1.4
8.3	14.5
8.9	1.7
9.7	100
10.2	8
10.9	13.9
11.6	41.3
13.2	18.4
14.2	14.9
14.6	6.5
15.9	12.0
16.8	17.3
17.2	20.3
17.5	8.5
17.9	5.4

18.7	5.4
19.0	4.3
19.2	4.1
19.8	4.1
20.4	6.5
21.0	9.4
21.6	11.6
21.9	10.2
22.8	10.9
23.3	4.8
24.3	5.6
27.0	4.4
28.0	6.8
29.5	4.8

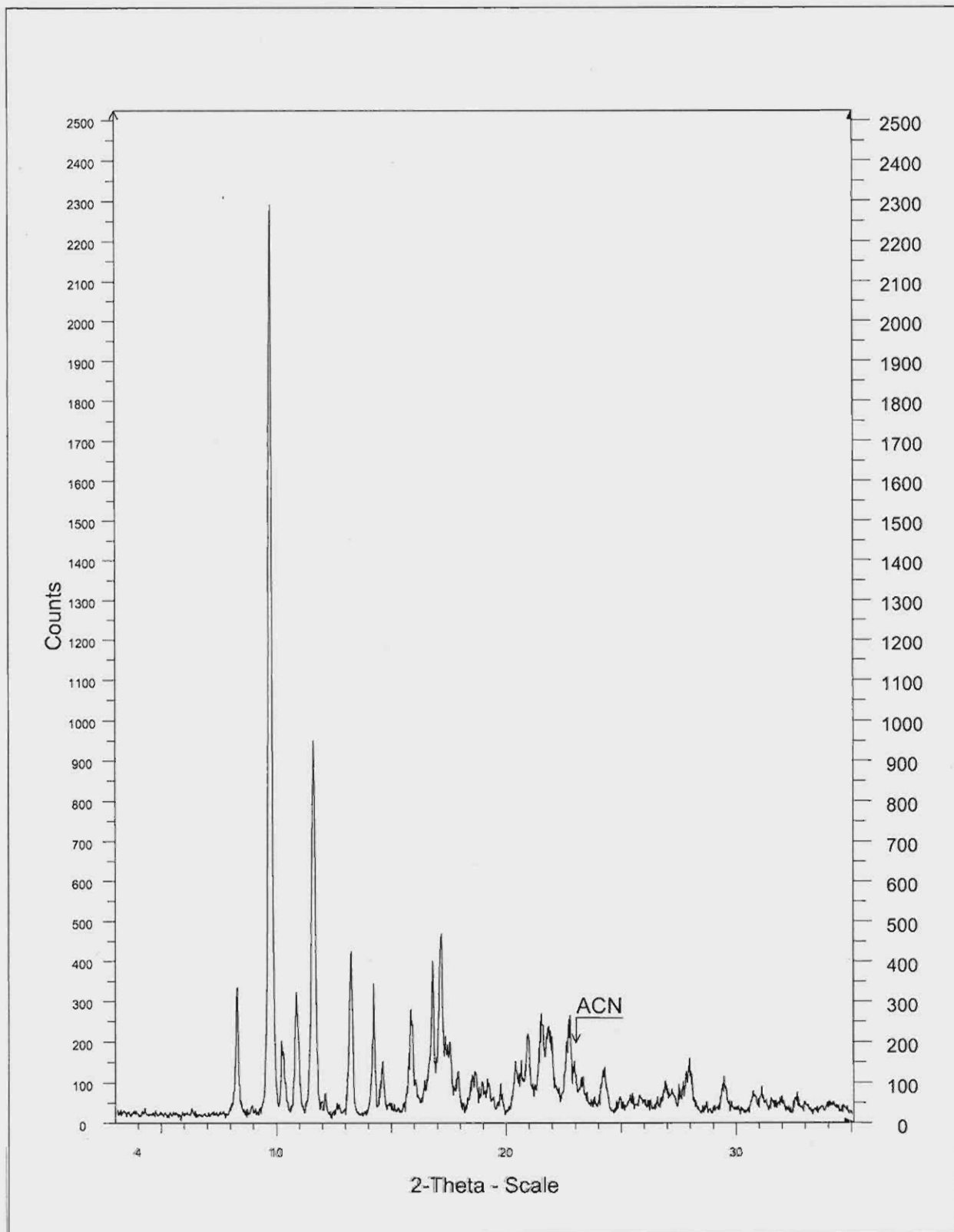


Figure 4.10 XRPD pattern of roxithromycin crystals recrystallised from ACN (YBR02).

4.7.4.3 Differential scanning calorimetry (DSC)

Figure 4.11 shows the DSC thermogram of the crystals being recrystallised from ACN (YBR02).

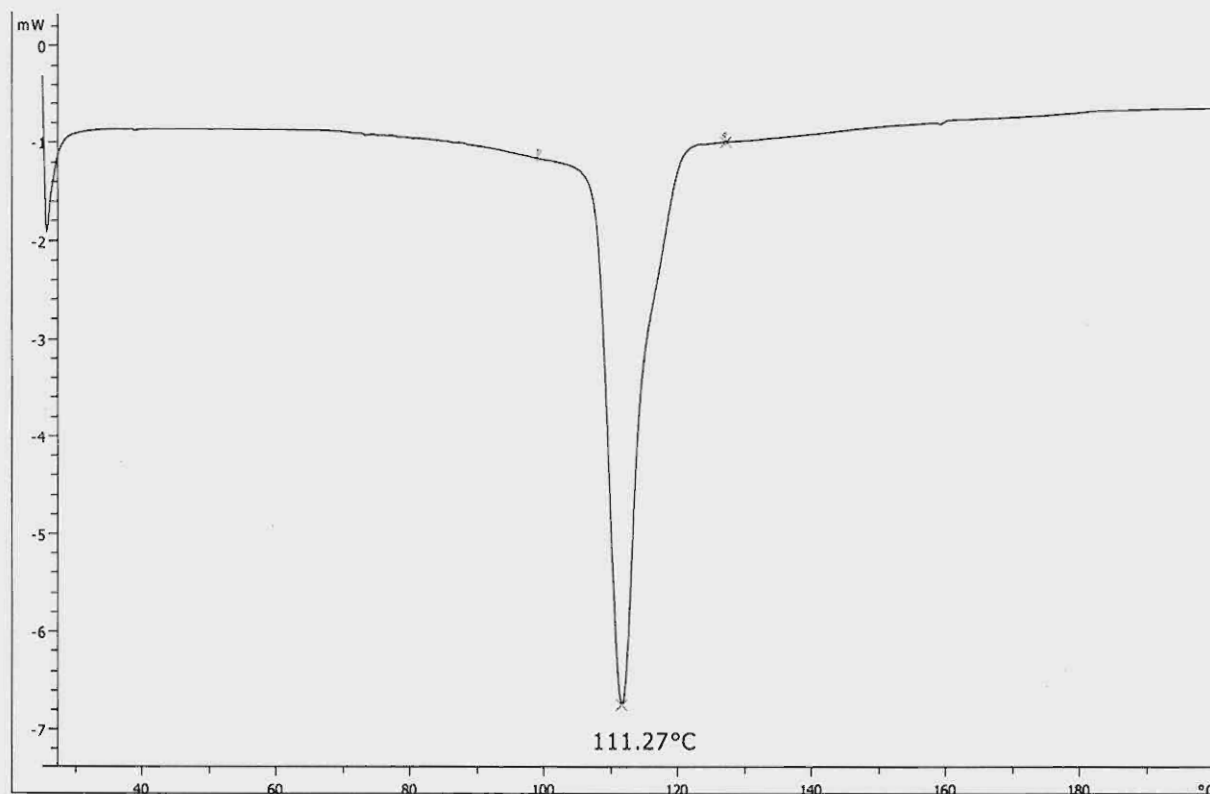


Figure 4.11 DSC thermogram of roxithromycin crystals recrystallised from ACN (YBR02).

4.7.4.4 Thermogravimetric analysis (TGA)

Figure 4.12 shows the TGA thermogram for crystals recrystallised from ACN (YBR02).

Karl Fischer total moisture content was measured as 0.2%, which was considered as surface moisture.

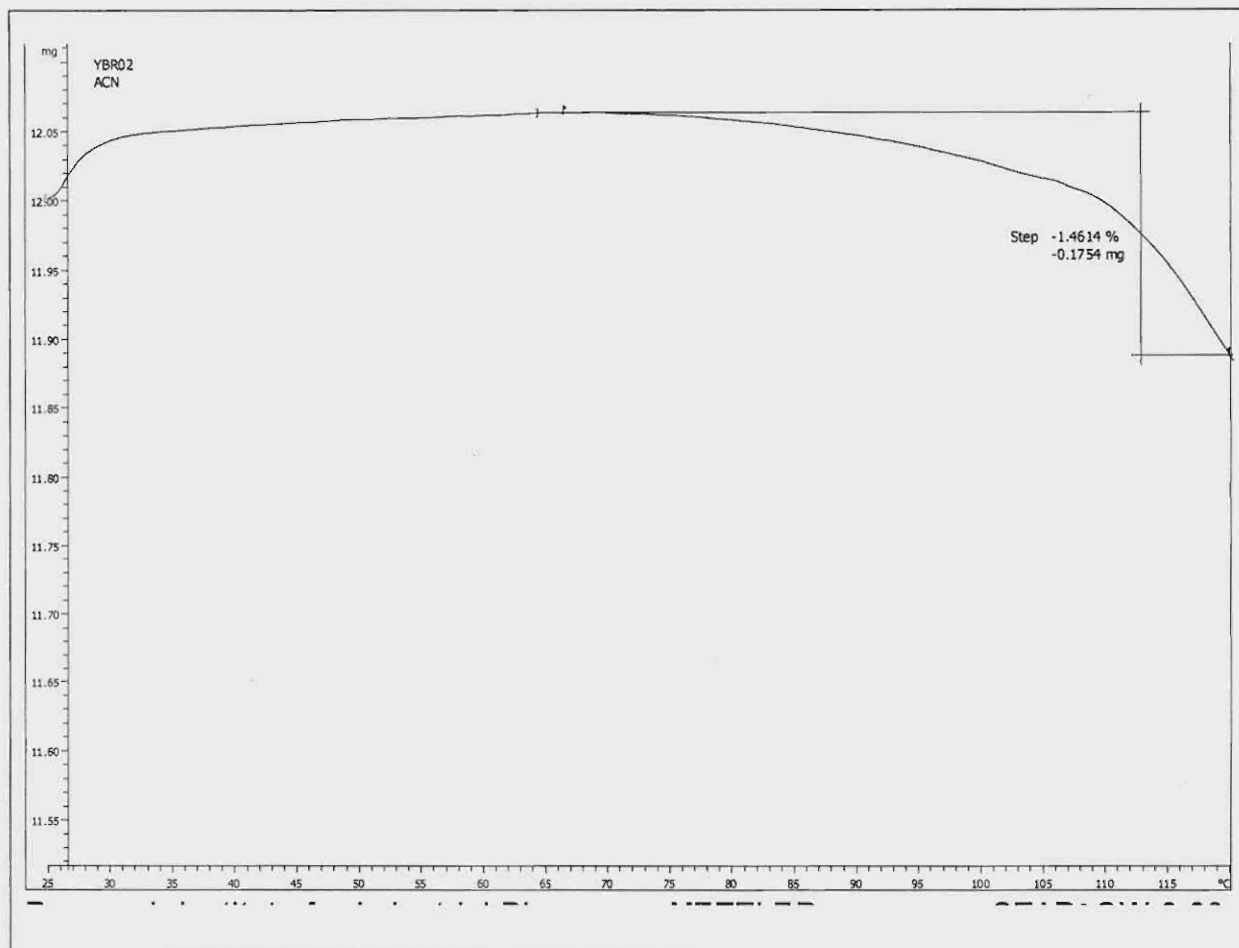


Figure 4.12 The TGA thermogram of crystals recrystallised from ACN (YBR02) with a 1.46% weight loss (theoretical weight loss of an ACN solvate = 4.7%).

4.7.4.5 Infrared spectroscopy (IR)

Table 4.12 lists the main absorption peaks with their corresponding wavenumbers (cm^{-1}) of the crystals recrystallised from ACN (YBR02), Figure 4.13 shows the IR spectrum of these crystals.

Table 4.12 Main IR absorption peaks of crystals recrystallised from ACN (YBR02)

Main absorptions	Wavenumbers (cm^{-1})
1	3532.9
2	3464.4
3	3014.7
4	2974.8

5	2290.9
6	2250.1
7	1736.1
8	1633.5
9	1458.2
10	1412.0
11	1369.4
12	1288.6
13	1239.7
14	1138.9
15	1092.7
16	1003.0
17	982.7
18	955.8
19	914.7
20	891.2
21	846.8
22	830.7
23	802.7
24	790.4
25	770.9
26	753.8
27	725.7
28	698.0

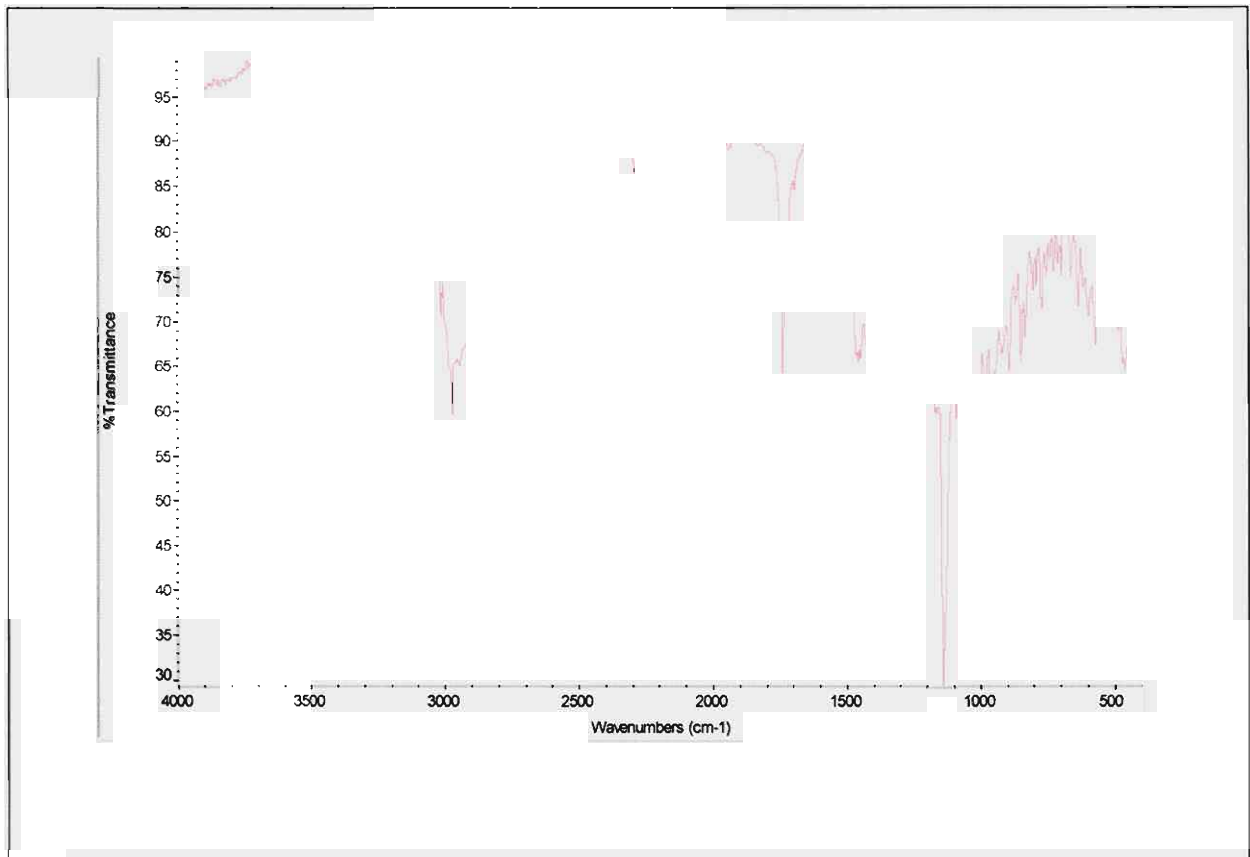


Figure 4.13 IR spectrum of crystals recrystallised from ACN (YBR02).

4.7.4.6 Solubility

Table 4.13 lists the solubility test results generated for the ACN recrystallisation product.

Table 4.13 Solubility test results of roxithromycin crystals recrystallised from ACN (YBR02)

Test tube	Concentration ($\mu\text{g/ml}$)		
	0.1 N HCl	Phosphate buffer (pH 6)	H ₂ O
1	28.952	8.153	0.350
2	30.433	0.000	0.390
3	28.843	7.931	0.396
4	27.789	7.870	0.506
5	17.622	8.606	0.494
Average	29.4093	8.1400	0.3789

The solubility of the crystals was in the following order: 0.1 N HCl > phosphate buffer (pH 6) > water.

4.7.4.7 Discussion of the data generated from acetonitrile as solvent

The DSC thermogram of the crystals being recrystallised from ACN matched the reported Form F_M, an unstable mid-melting point, which transformed into a high melting point form (Du Plessis, 2004). The melting point of 111°C was much lower than that of the raw material (122°C).

The TGA results showed a weight loss of 1.4% (theoretical weight loss of an ACN solvate = 4.7%), whilst the KF value was 0.2%, hence confirming that this form was a true polymorphic form of roxithromycin, and not a pseudopolymorphic form.



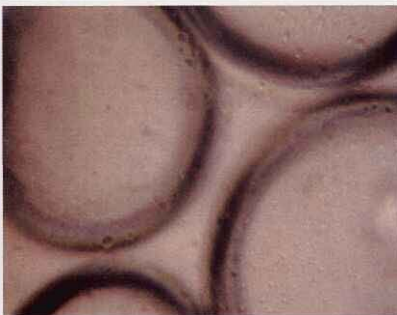
The solubility of the ACN (YBR02) crystals varied in solubility, from insoluble in water, to slightly soluble in the phosphate buffer (pH 6), to very soluble in 0.1 N HCl.

4.7.5 Dichloromethane

4.7.5.1 Thermo-microscopy (TM)

Table 4.14 shows the TM pictures taken over the elevated temperature range for dichloromethane (YBR03).

Table 4.14 TM results of crystals recrystallised from dichloromethane (YBR03)

		
Crystals at 30°C	Gas evolution, i.e. desolvation at 89°C	The melting point at 126°C

4.7.5.2 X-ray powder diffractometry (XRPD)

The peak angles ($^{\circ}2\theta$) and relative intensities (I/I_0) of the main peaks are listed in Table 4.15. The XRPD pattern of roxithromycin crystals being recrystallised from this solution is shown in Figure 4.14.

Table 4.15 Main XRPD intensity ratios (I/I_0) and main peak angles ($^{\circ}2\theta$) of roxithromycin crystals recrystallised from dichloromethane (YBR03)

Peak angles ($^{\circ}2\theta$)	Relative intensities (I/I_0)
5.3	55
6.8	69.9
8.1	10.1
8.5	100
8.8	19.7
10.5	8.1
11.3	60
11.8	6.3
12.9	11.9
13.6	16.3
13.9	30.2
15.1	15.8
15.6	15.4
16	40.7
16.6	21.9
17.1	11.1
17.4	10.5
18.1	17.2
19.1	9
19.3	10.9
19.9	13.9
20.2	11.5
20.6	9
21.1	11.4
21.8	13.8
22.9	10

24.0	9.5
25.1	5.3
26.6	5.6

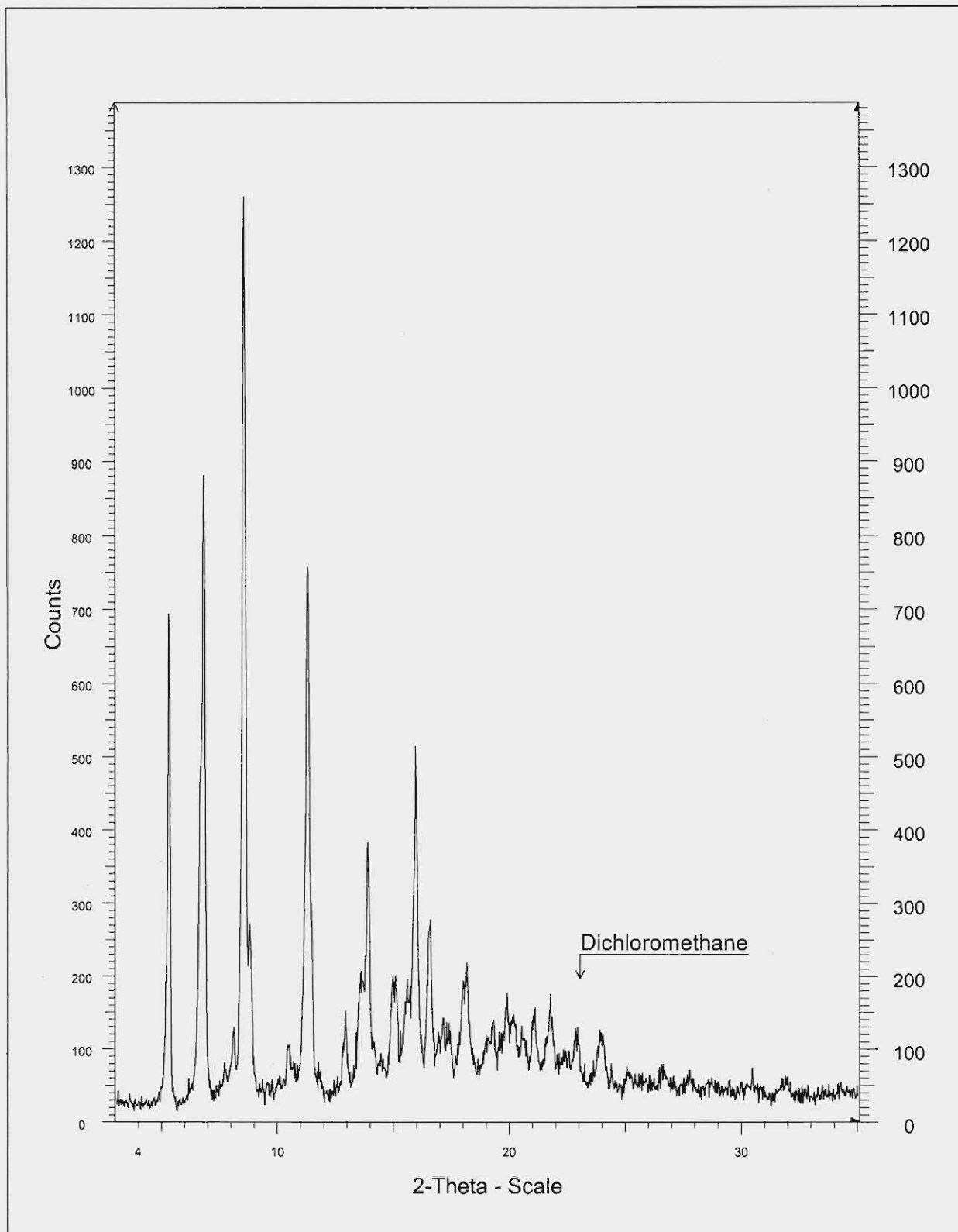


Figure 4.14 XRPD pattern of roxithromycin crystals recrystallised from dichloromethane (YBR03).

4.7.5.3 Differential scanning calorimetry (DSC)

Figure 4.15 shows the DSC thermogram of the crystals recrystallised from dichloromethane (YBR03).

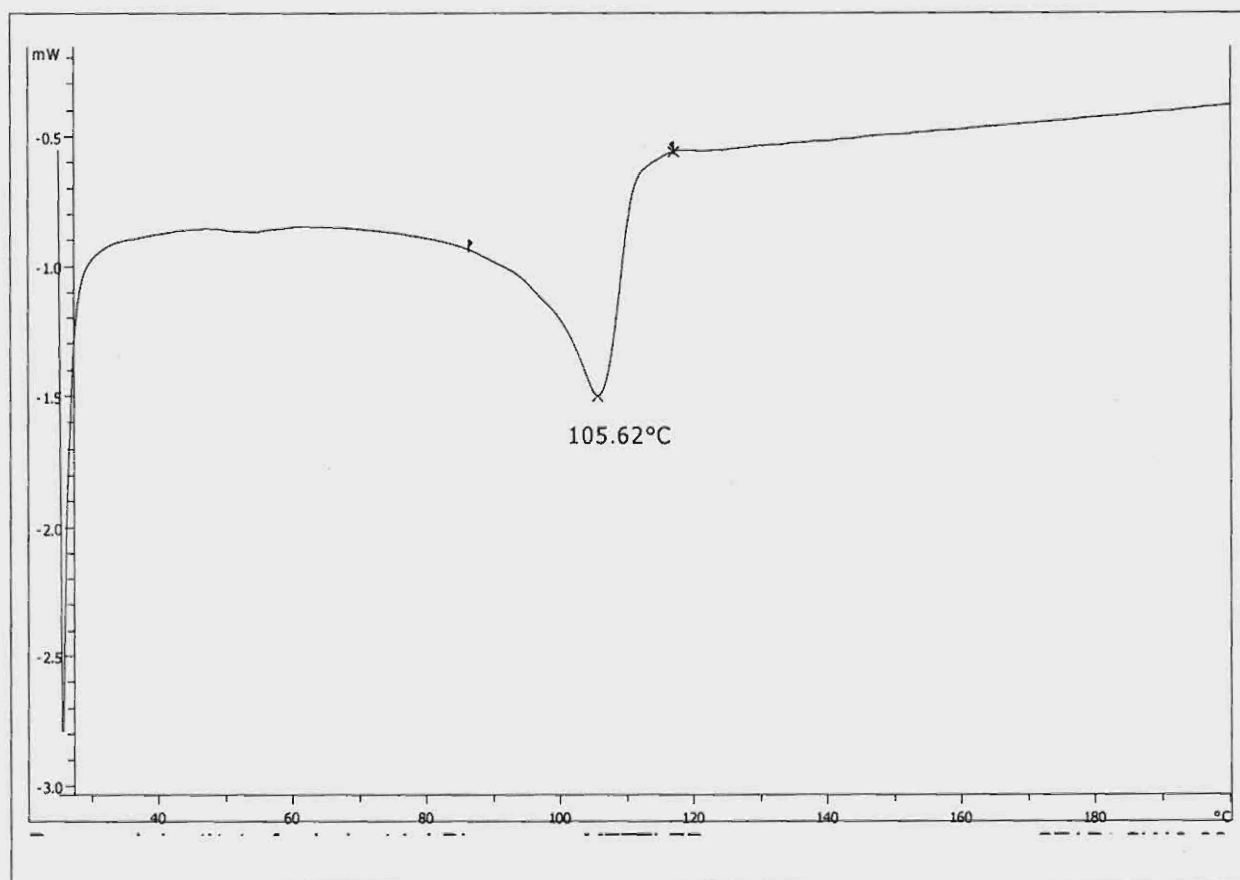


Figure 4.15 DSC thermogram of roxithromycin crystals recrystallised from dichloromethane (YBR03).

4.7.5.4 Thermogravimetric analysis (TGA)

Figure 4.16 shows the TGA thermogram of crystals recrystallised from dichloromethane (YBR03). Karl Fischer determination of the total moisture content of the crystals recrystallised from dichloromethane was 1.8%.

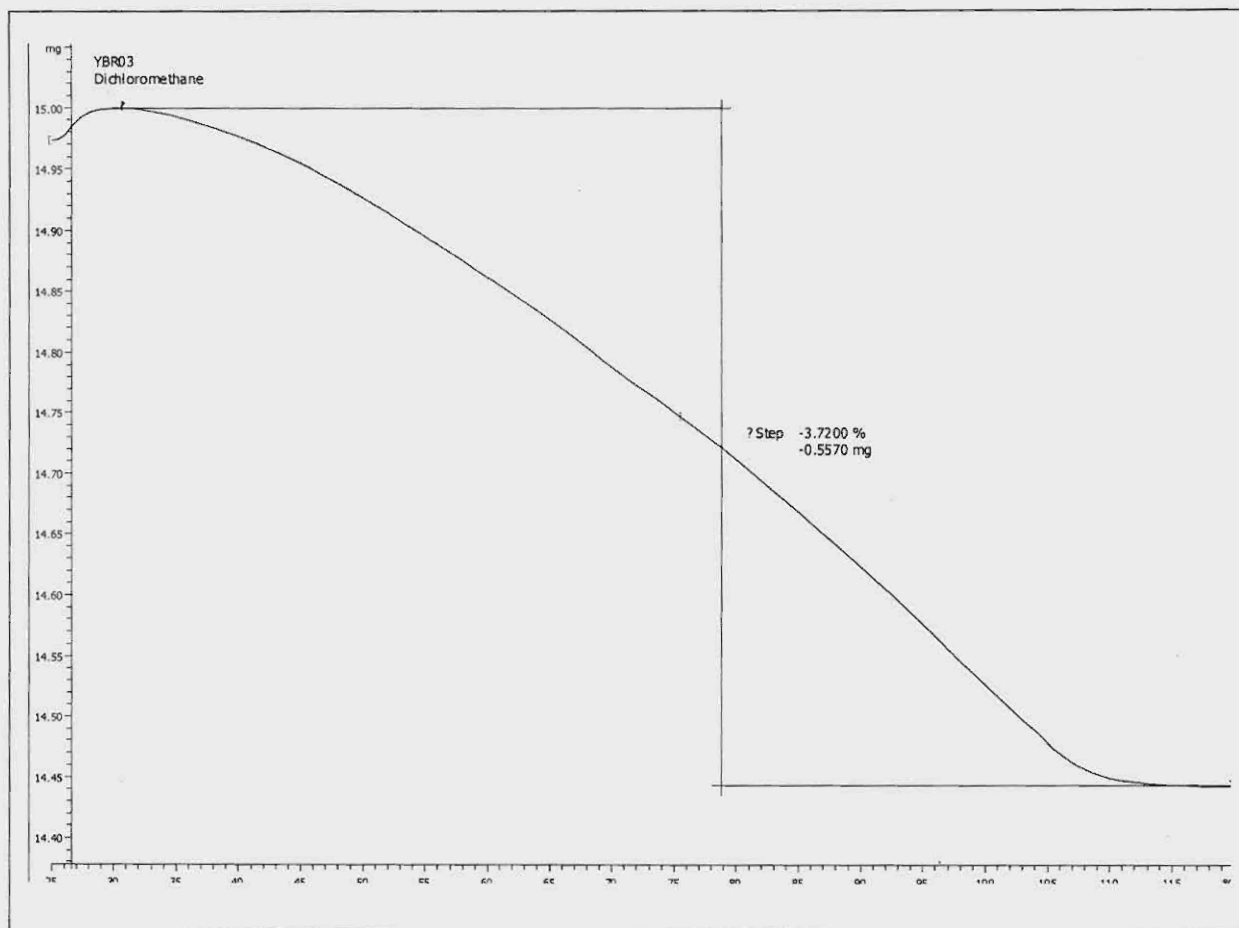


Figure 4.16 The TGA thermogram of crystals recrystallised from dichloromethane (YBR03) with a 3.7% weight loss (theoretical weight loss of a dichloromethane solvate = 9.2%).

4.7.5.5 Infrared spectrophotometry (IR)

Table 4.16 lists the main absorption peaks with their corresponding wavenumbers (cm^{-1}) of the crystals recrystallised from dichloromethane (YBR03), whilst Figure 4.17 shows the IR spectrum of these crystals.

Table 4.16 Main IR absorption peaks of crystals recrystallised from dichloromethane (YBR03)

Main absorptions	Wavenumbers (cm ⁻¹)
1	3669.7
2	3620.6
3	3406.0
4	3045.7
5	2969.3
6	2827.6
7	2784.1
8	2244.6
9	1957.1
10	1736.0
11	1692.1
12	1633.6
13	1460.3
14	1377.4
15	1342.7
16	1276.8
17	1166.1
18	1081.6
19	1012.7
20	958.5
21	892.7
22	863.2
23	835.3
24	804.6
25	772.8
26	734.7
27	698.0
28	662.4
29	638.2
30	592.3

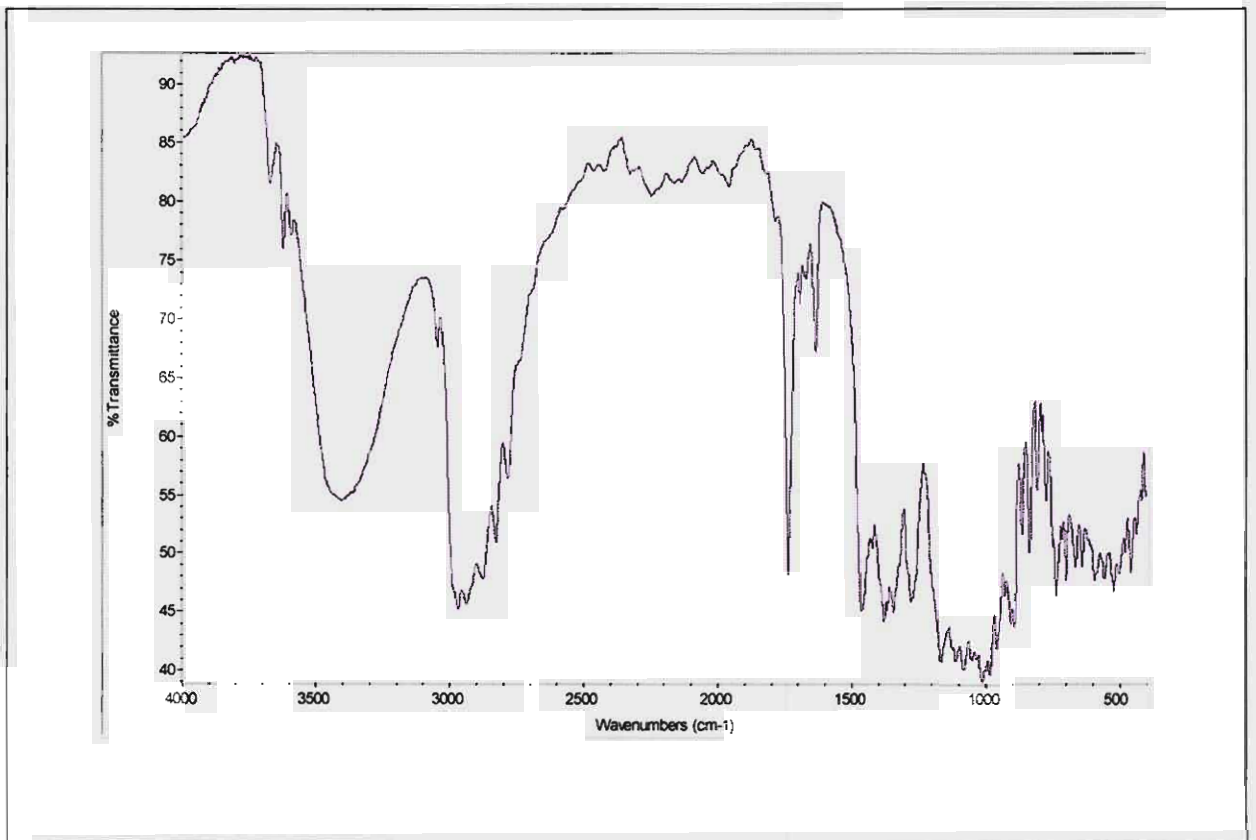


Figure 4.17 IR spectrum of roxithromycin crystals recrystallised from dichloromethane (YBR03).

4.7.5.6 Solubility

Table 4.17 is a summary of the solubility test results of roxithromycin crystals being recrystallised from dichloromethane.

Table 4.17 Solubility test results of roxithromycin crystals recrystallised from dichloromethane (YBR03)

Test tube	Concentration ($\mu\text{g/ml}$)		
	0.1 N HCl	Phosphate buffer (pH 6)	H ₂ O
1	Experimental error	11.306	2.145
2	Experimental error	Experimental error	1.806
3	13.219	19.020	1.888
4	34.758	8.727	2.159
5	31.600	16.997	1.838
Average	26.5256	14.0125	1.9461

The solubility of the crystals was in the following order: 0.1 N HCl > phosphate buffer (pH 6) > water.

4.7.5.7 Discussion of the data generated from dichloromethane as solvent

TM analysis showed gas evolution at a temperature of 89°C, whereas it was not detected with the DSC measurement. This thermo event was, however, a broad endotherm, starting at approximately 80°C and ending at 118°C. It may possibly have included both the desolvation and the melting processes. Du Plessis (2004) also reported this lower melting point form being recrystallised from dichloromethane, but did not identify it as a solvate.

The TGA thermogram of crystals recrystallised from dichloromethane (YBR03) showed a 3.7% weight loss (theoretical weight loss of a dichloromethane solvate = 9.2%). Karl Fischer determination of the moisture content of the crystals recrystallised from dichloromethane was 1.8%.


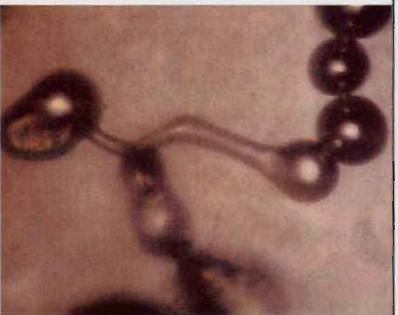

These crystals were highly soluble in 0.1 N HCl, reasonably soluble in phosphate buffer (pH 6), and insoluble in water.

4.7.6 Chloroform

4.7.6.1 Thermo-microscopy (TM)

Table 4.18 shows the TM pictures recorded over the elevated temperature range for chloroform (YBR04).

Table 4.18 TM results of crystals recrystallised from chloroform (YBR04)

		
Crystals at 30°C	Gas evolution, i.e. desolvation at 92°C	The melting point at 117°C

4.7.6.2 X-ray powder diffractometry (XRPD)

The XRPD pattern of roxithromycin crystals being recrystallised from this solution is showed in Figure 4.18, illustrating a halo-shaped diffractogram, characteristic of amorphous forms (Guillory, 1999).

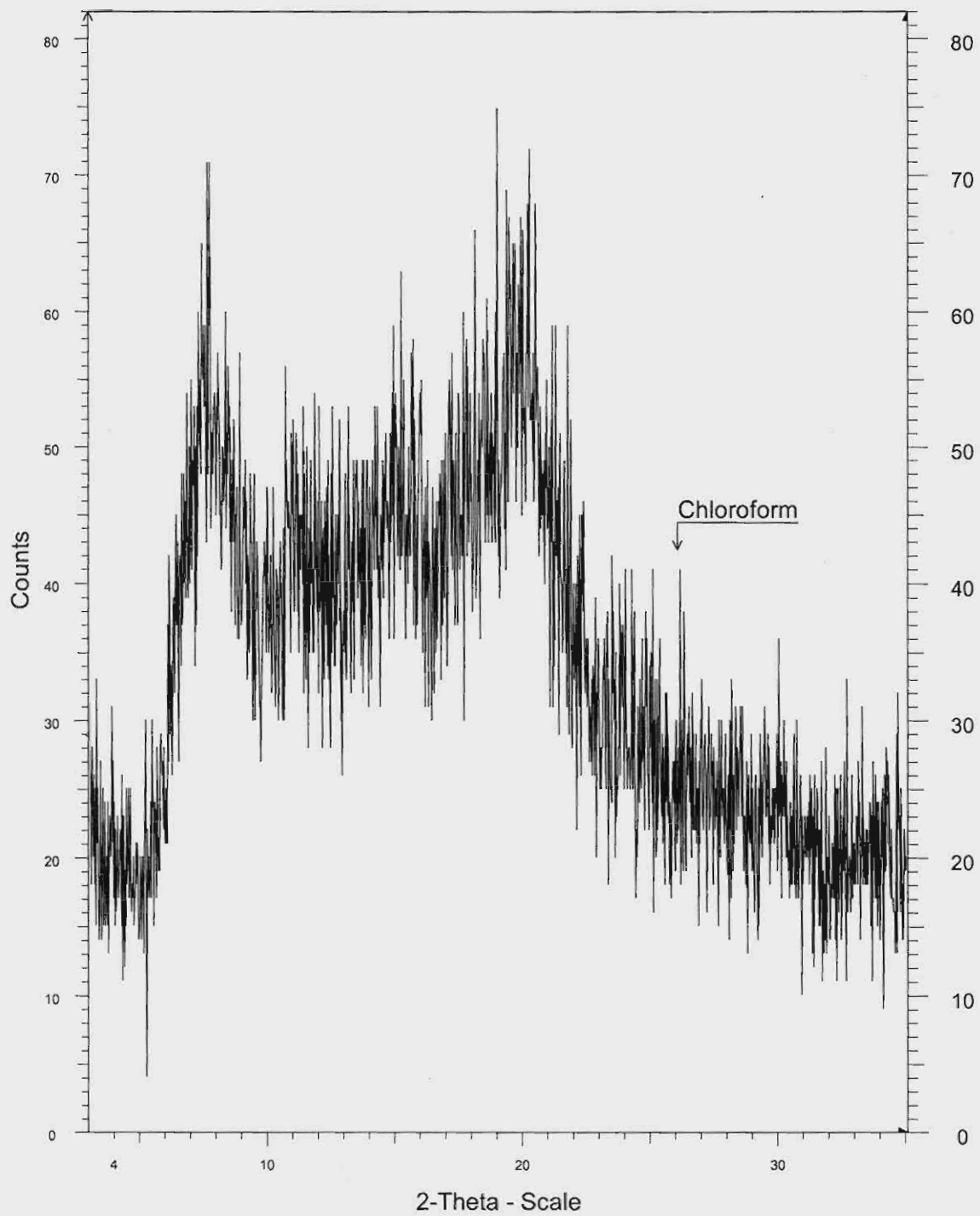


Figure 4.18 XRPD pattern of crystals recrystallised from chloroform (YBR04).

4.7.6.3 Differential scanning calorimetry (DSC)

Figure 4.19 shows the DSC thermogram of the crystals recrystallised from chloroform (YBR04).

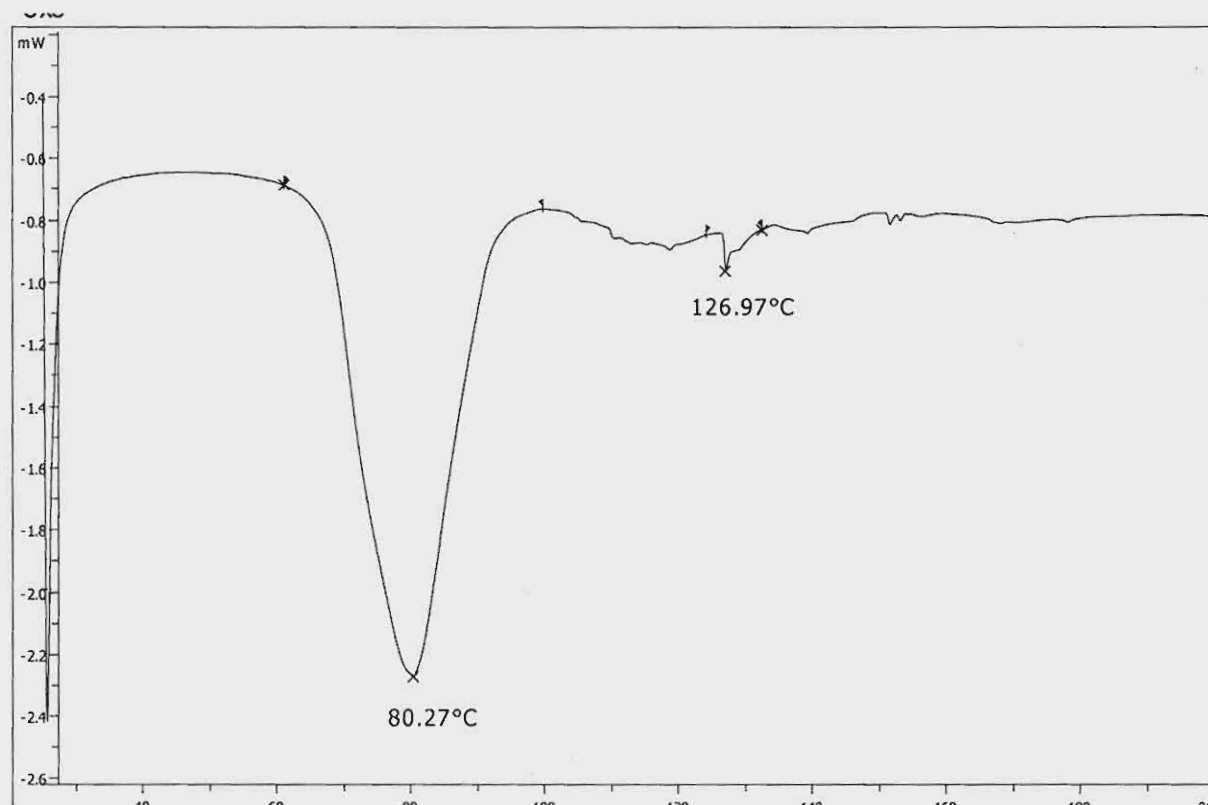


Figure 4.19 DSC thermogram of roxithromycin crystals recrystallised from chloroform (YBR04).

4.7.6.4 Thermogravimetric analysis (TGA)

Figure 4.20 shows the TGA thermogram of chloroform (YBR04). Karl Fischer determination of the moisture content of the crystals recrystallised from chloroform was 0.6%.

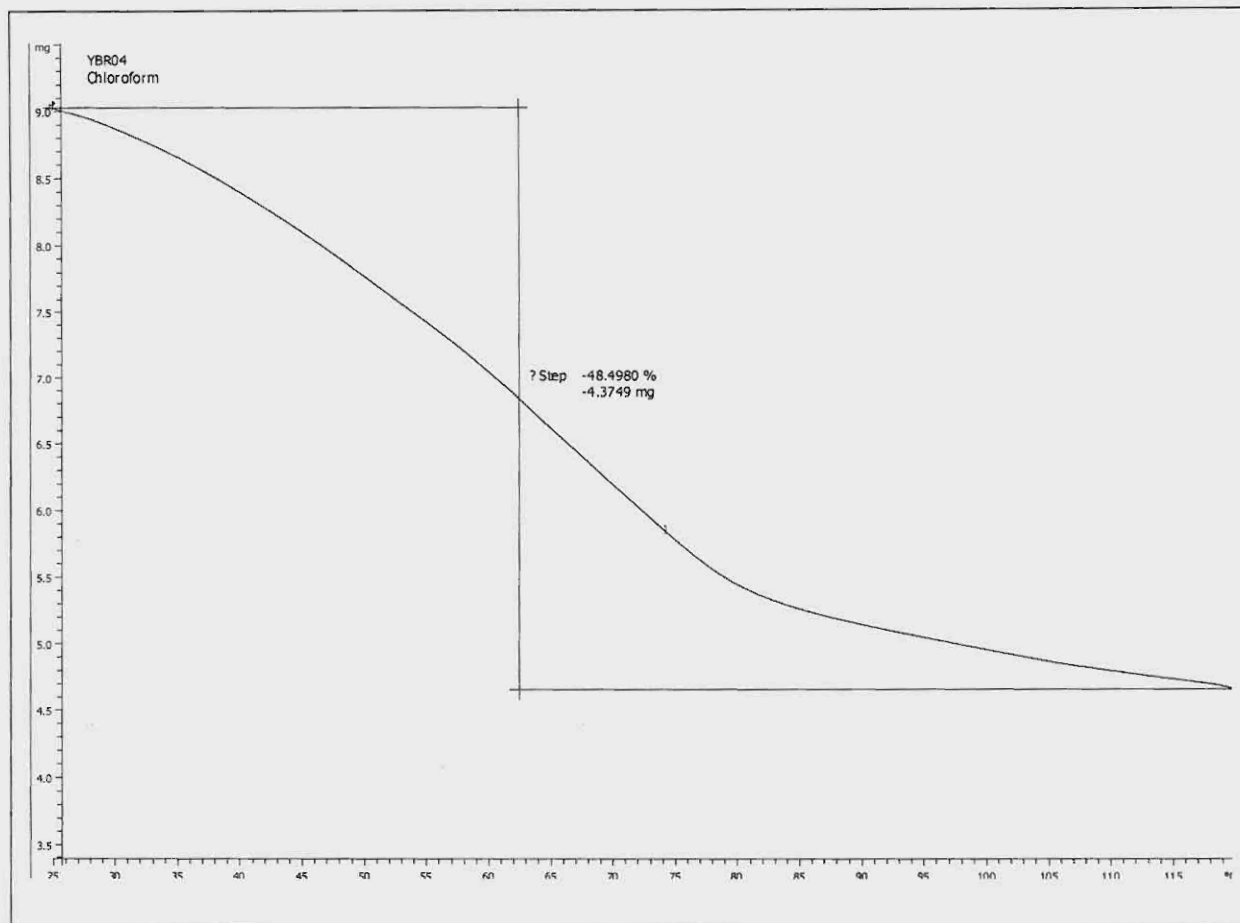


Figure 4.20 The TGA thermogram of crystals recrystallised from chloroform (YBR04) with a 48% weight loss (theoretical weight loss of a chloroform solvate = 12.5%).

4.7.6.5 Infrared spectroscopy (IR)

Table 4.19 lists the main absorption peaks with their corresponding wavenumbers (cm^{-1}) of the crystals recrystallised from chloroform (YBR04), whilst Figure 4.21 illustrates the IR spectrum of these crystals.

Table 4.19 Main IR absorption peaks of crystals recrystallised from chloroform (YBR04)

Main absorptions	Wavenumbers (cm^{-1})
1	3853.3
2	3750.8
3	3735.2
4	3675.7
5	3648.5

6	3391.5
7	2974.4
8	2830.9
9	2125.2
10	1735.5
11	1635.1
12	1457.5
13	1376.0
14	1279.2
15	1168.7
16	1139.1
17	1079.5
18	1011.5
19	958.0
20	892.9
21	863.6
22	833.5
23	805.1
24	770.5
25	698.3
26	663.3
27	635.6

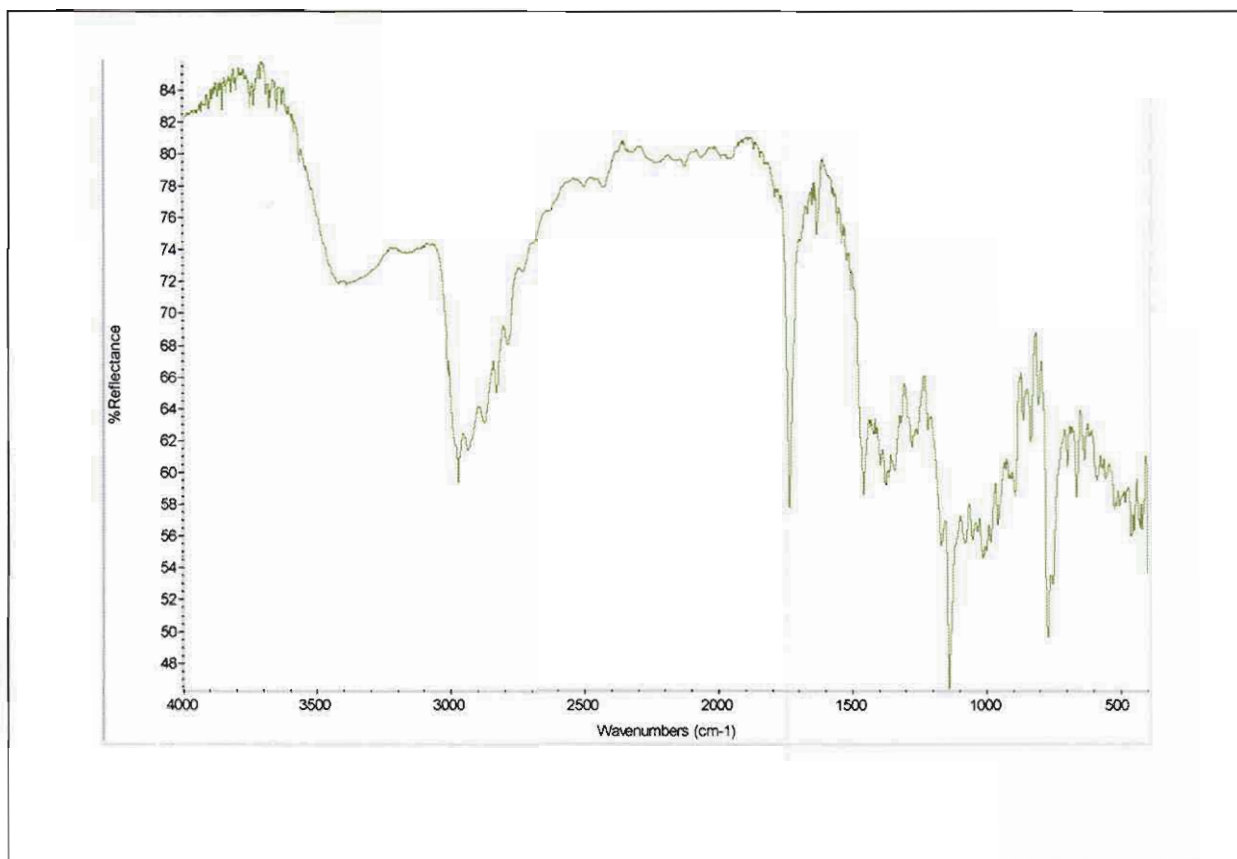


Figure 4.21 IR spectrum of roxithromycin crystals recrystallised from chloroform (YBR04).

4.7.6.6 Solubility

Table 4.20 illustrates the solubility differences of roxithromycin crystals recrystallised from chloroform (YBR04).

Table 4.20 Solubility test results of roxithromycin crystals recrystallised from chloroform (YBR04)

Test tube	Concentration ($\mu\text{g/ml}$)		
	0.1 N HCl	Phosphate buffer (pH 6)	H ₂ O
1	39.284	2.580	2.274
2	38.714	2.694	1.915
3	40.376	2.402	2.002
4	39.434	3.069	2.289
5	39.583	2.820	1.949
Average	39.4581	2.5587	2.0638

The solubility of the crystals was in the following order: 0.1 N HCl > phosphate buffer (pH 6) > water.

4.7.6.7 Discussion of the data generated from chloroform as solvent

A large endothermic desolvation peak was observed at 80°C in the DSC thermogram.

The TGA thermogram of chloroform (YBR04) measured a weight loss of 48% (theoretical weight loss of a chloroform solvate = 12.5%). Due to the amorphous nature of the sample, this high value of 48% could not be regarded as accurate and the possibility of surface solution could not be excluded.

The solubility of these crystals in 0.1 N HCl was high, but less soluble in phosphate buffer (pH 6) and in water.

4.7.7 Conclusion

The different recrystallisation products that were obtained from the different solvents could be classified as:

- Ethyl acetate: A hemi ethyl acetate solvate (should be confirmed with single X-ray crystallography).
- ACN: A meta-stable lower melting point form.
- Dichloromethane: A hemi dichloromethane solvate (should be confirmed with single X-ray crystallography).
- Chloroform: An amorphous solvate.

The following graphs (figures 4.22 – 4.24) depict the solubility results.

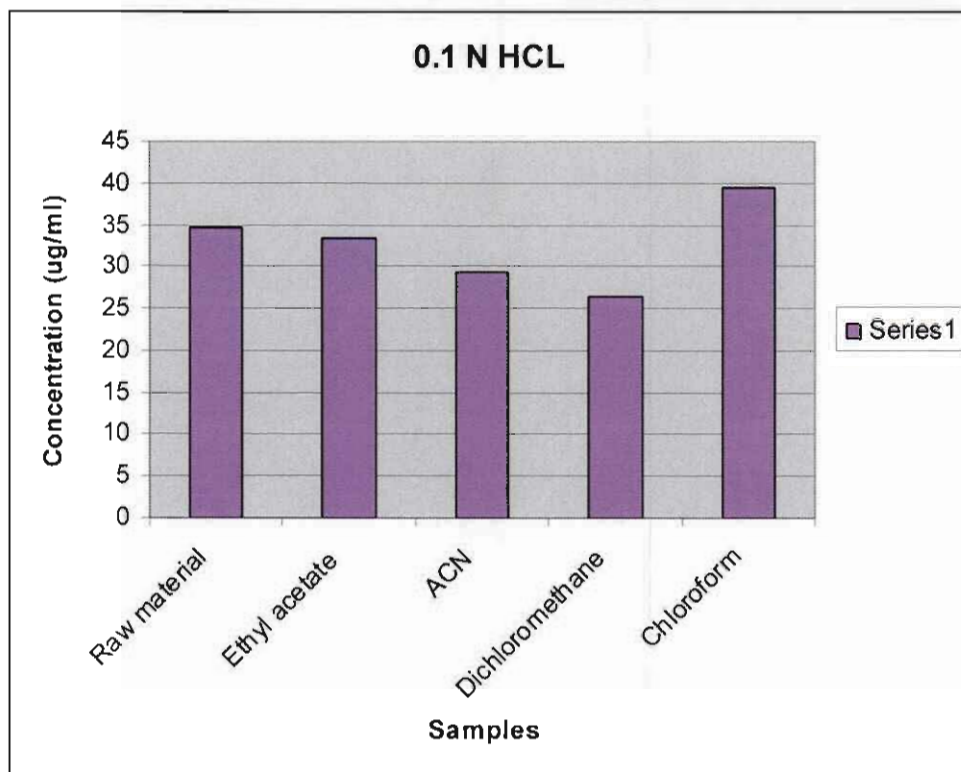


Figure 4.22 A comparison of the solubility of the crystal forms and the roxithromycin raw material in 0.1 N HCl.

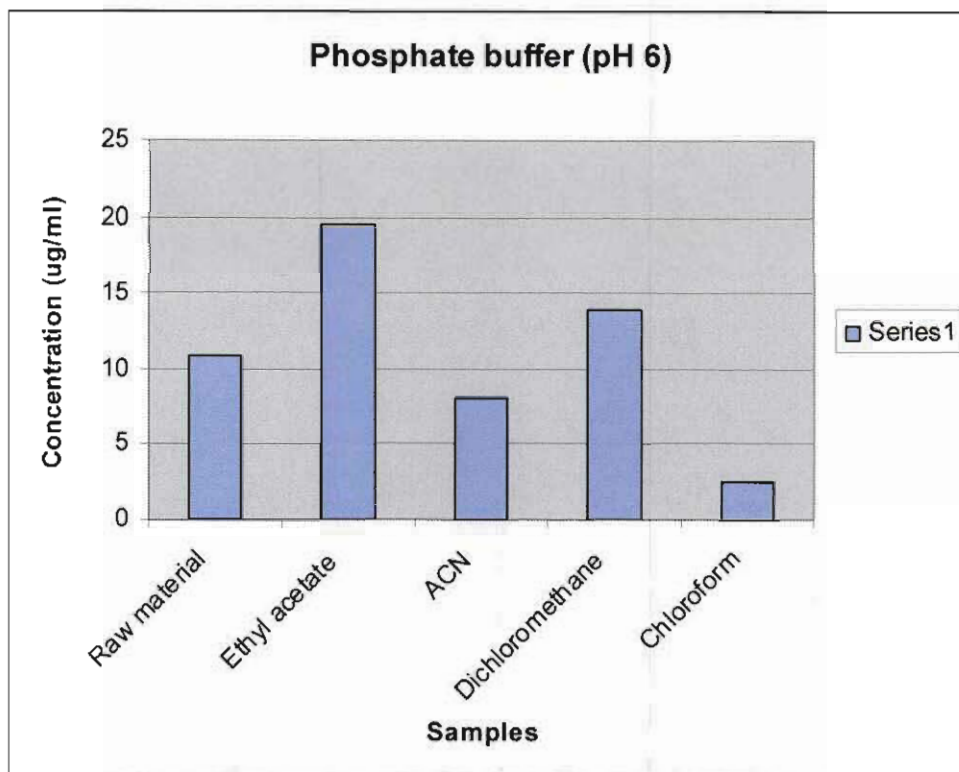


Figure 4.23 A comparison of the solubility of the crystal forms and the roxithromycin raw material in phosphate buffer (pH 6).

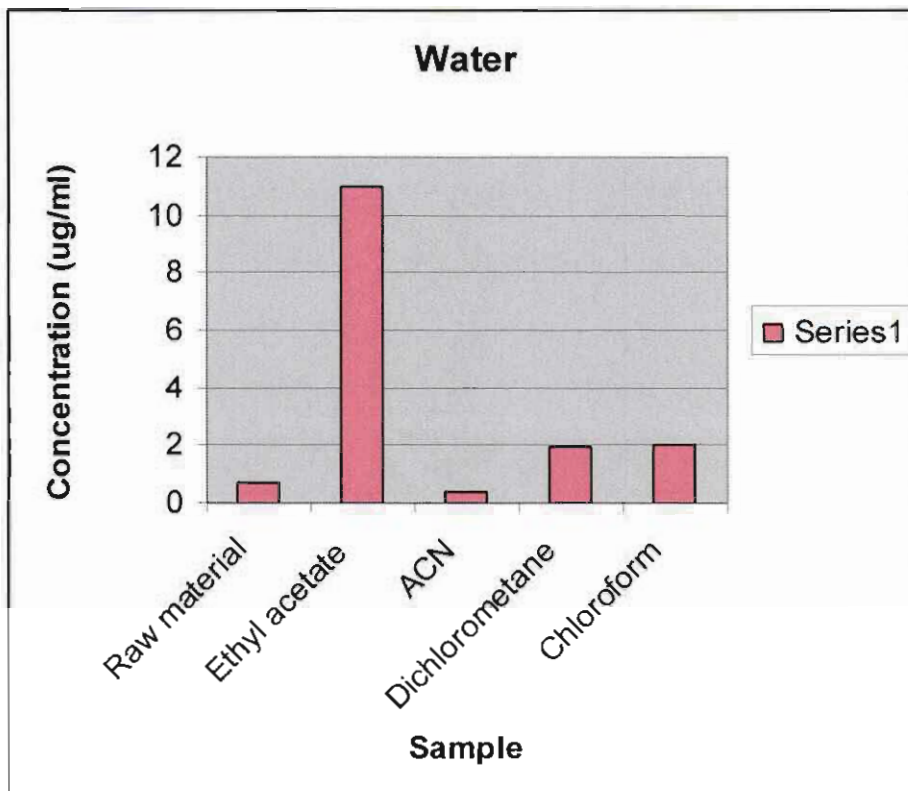


Figure 4.24 A comparison of the solubility of the crystal forms and the roxithromycin raw material in water.

The solubility of the four recrystallised forms and the raw material being tested during this study, was in the following order: 0.1 N HCl > phosphate buffer (pH 6) > water.

The test results showed that the crystals being recrystallised from ethyl acetate were more soluble in all the media, i.e. in 0.1 N HCl, phosphate buffer and water, compared to that of the roxithromycin raw material.

Crystals that were recrystallised from acetonitrile (ACN) were, however, only soluble in 0.1 N HCl, partially soluble in phosphate buffer, and insoluble in water.

Contrary, the crystals being recrystallised from dichloromethane and chloroform, were soluble in 0.1 N HCl and in the phosphate buffer, but very weakly soluble in water.

According to the solubility test results, it seemed that the recrystallisation product from ethyl acetate had the best solubility profile, especially in water, which differed significantly from the solubility of the other recrystallised forms, as well as from that of the raw material.

Table 4.21 is a summary of the solubility in the different media, of the roxithromycin crystals that were recrystallised from the various solvents.

Table 4.21 Summary of the solubility of roxithromycin recrystallisation products

Sample	Solubility / Dissolve media		
	0.1 N HCl (µg/ml)	Phosphate buffer (pH 6) (µg/ml)	Water (µg/ml)
Raw material	34.6576	10.8515	0.7193
Ethyl acetate	33.445	19.5718	10.9945
ACN	29.4093	8.14	0.3789
Dichloromethane	26.5256	14.0125	1.9461
Chloroform	39.4581	2.5587	2.0638

In conclusion, four different crystal forms of roxithromycin were prepared, characterised and tested, along with the raw material. The ethyl acetate hemi-solvate proved to be the only form with a significantly better solubility profile in all three media tested, than that of the raw material.

These results have created new questions regarding the morphology and differences in crystal forms of roxithromycin. It should be a challenge to prepare quality crystals, suitable for single X-ray crystallography, in order to clarify the actual crystal forms of this complex antibiotic, since all the recrystallisation products tended to be more amorphous, having low peak intensity counts (XRPD).

Furthermore, the fact that roxithromycin has no free hydroxyl groups, explains the poor wettability and the hydrophobicity, hence its poor solubility in water. The outcomes of this study, however, raised the question as to why the solubility of the prepared ethyl acetate crystal form differed so much from the other prepared forms, especially with regards to its higher solubility in water. This finding, especially, has therefore created the need for further investigation and it is anticipated that such further studies would solve the solubility problems of roxithromycin in aqueous media.

CHAPTER 5

Summary and Conclusion

The importance of knowing the polymorphic behaviour of a drug is vital for manufacturing purposes. Changes in the crystal form at any stage of the production process can alter the bioavailability of the drug. Pseudopolymorphic forms, i.e. solvates (stoichiometric and non-stoichiometric), desolvates and hydrates, all with different physico-chemical properties, can be detrimental to production processes. The characterisation thereof is thus of utmost importance. An amorphous state is a non-crystalline solid, and in many literature studies it is described as a precursor to the crystalline state. No precise definition has to date been established that differentiates between crystalline and amorphous solids.

Characterisation of these different crystal forms is important when considering the development of solid dosage forms. Various methods of analysis include microscopy, crystallography, thermal analysis, molecular motion, solubility, and Karl Fischer titrations. These methods were combined in this study for the identification and characterisation of triamterene and roxithromycin crystals.

Triamterene is a potassium sparing drug when used on its own and it is also used in combination with high ceiling diuretics, such as furosemide, or hydrochlorothiazide.

According to various studies, several physico-chemical techniques showed that triamterene exists in different crystal forms. Furthermore, the crystalline products from different solvents with distinct differences in melting points do not necessarily imply polymorphic crystal forms. Triamterene is insoluble in water and in most of the organic solutions, but it is more soluble in acids, such as formic acid.

Triamterene was recrystallised from various organic solvents (acids, alcohols, and DMF and DMF:water mixtures). From the data generated during this study it was concluded that:

- The recrystallisation products from the three acid solvents produced disolvates, i.e. novel pseudopolymorphic forms of triamterene;
- The 2-butanol recrystallisation products were either hydrates, solvates, or hydrated solvates; and
- DMF and DMF:water mixtures only yielded solvates.

Recrystallisation was hampered by low solubility and hence a low crystal yield. This made it impossible to obtain enough crystals on which to perform solubility studies. This was unfortunate, since it was reported in the literature that active pharmaceutical ingredients (API's) with low solubilities, such as mebendazole, showed significant differences in solubilities between the different polymorphic forms (Liebenberg *et al.*, 1998; Swanepoel *et al.*, 2003).

Roxithromycin is a relatively new, macrolide antibiotic and an ether oxime derivative of erythromycin A. Roxithromycin is very slightly soluble in water, slightly soluble in diluted hydrochloric acid, and freely soluble in acetone, alcohol and dichloromethane. Du Plessis (2004) reported that some of the roxithromycin polymorphic forms gave problems during a powder dissolution study, due to poor wettability in the dissolution medium. Furthermore, prior to the dissolution, during vortexing of the powder, a gel formed, which complicated the quantitative transfer of the samples into the dissolution vessels, hence resulting in poor dissolution results.

The aim of this investigation thus was to prepare different crystal forms of roxithromycin, and, instead of performing powder dissolution studies, to determine the solubility thereof, which would arguably be a better method of discriminating between the solubilities of the different forms.

Roxithromycin was recrystallised from chloroform, ethyl acetate, dichloromethane and acetonitrile. These chosen forms were more amorphous than the raw material.

The recrystallisation product of ethyl acetate was a hemi solvate. This form was unexpectedly highly soluble in all of the three media, and it was especially soluble in water, compared to the raw material.

The DSC thermogram of the crystals being recrystallised from ACN matched the reported Form F_M, an unstable mid-melting point, which transformed into a high melting point form (Du Plessis, 2004). The melting point of 111°C was much lower than that of the raw material (122°C). The TGA results showed a weight loss of 1.4% (theoretical weight loss of an ACN solvate = 4.7%), whilst the KF value was 0.2%, hence confirming that this form was a true polymorphic form of roxithromycin, and not a pseudopolymorphic form. The solubility of the ACN (YBR02) crystals varied in solubility, from insoluble in water, to slightly soluble in the phosphate buffer (pH 6), to very soluble in 0.1 N HCl.

The TGA thermogram of crystals recrystallised from dichloromethane (YBR03) showed a 3.7% weight loss (theoretical weight loss of a dichloromethane solvate = 9.2%). Karl Fischer

determination of the moisture content of the crystals recrystallised from dichloromethane was 1.8%. TM analysis showed gas evolution at a temperature of 89°C, whereas it was not detected with the DSC measurement. This thermo event was, however, a broad endotherm, starting at approximately 80°C and ending at 118°C. It may possibly have included both the desolvation and the melting processes. Du Plessis (2004) also reported this lower melting point form being recrystallised from dichloromethane, but did not identify it as a solvate. These crystals were highly soluble in 0.1 N HCl, reasonably soluble in phosphate buffer (pH 6), and insoluble in water.

The crystals obtained from chloroform were amorphous. A large endothermic desolvation peak was observed at 80°C in the DSC thermogram. The TGA thermogram of chloroform (YBR04) measured a weight loss of 48% (theoretical weight loss for a chloroform solvate = 12.5%). Due to the amorphous nature of the sample, this high measured value of 48% could not be regarded as accurate and the possibility of surface solution could not be excluded. The solubility of these crystals in 0.1 N HCl was high, but less soluble in phosphate buffer (pH 6) and in water.

In conclusion, four different crystal forms of roxithromycin were prepared, characterised and tested, along with the raw material. The ethyl acetate hemi-solvate proved to be the only form with a significantly better solubility profile in all three media tested, than that of the raw material.

These results have created new questions regarding the morphology and differences in crystal forms of roxithromycin. It should be a challenge to prepare quality crystals, suitable for single X-ray crystallography, in order to clarify the actual crystal forms of this complex antibiotic, since all the recrystallisation products tended to be more amorphous, having low peak intensity counts (XRPD).

Furthermore, the fact that roxithromycin has no free hydroxyl groups, explains the poor wettability and the hydrophobicity, hence its poor solubility in water. The outcomes of this study, however, raised the question as to why the solubility of the prepared ethyl acetate crystal form differed so much from the other prepared forms, especially with regards to its higher solubility in water. This finding, especially, has therefore created the need for further investigation and it is anticipated that such further studies would solve the solubility problems of roxithromycin in aqueous media.

BIBLIOGRAPHY

BERNSTEIN, J. 2002. Polymorphism in molecular crystals. Oxford : Clarendon Press. 410 p.

BRITISH PHARMACOPOEIA. 2002. London : HMSO. 2709 p.

BRITTAİN, H.G. 1995. Physical characterization of pharmaceutical solids. New York : Marcel Dekker, Inc. 427 p.

BRITTAİN, H.G & GRANT, D.J.W. 1999. Effects of polymorphism and solid-state solvation on solubility and dissolution rate. (*In* Brittain. H.G. *ed.* Polymorphism in Pharmaceutical Solids. New York : Marcel Dekker Inc. p. 427).

BYRN, S.R. 1982. Solid-state chemistry of drugs. New York : Academic Press. 29-50 p.

BYRN, S.R., PFEIFFER, R.R., & STOWELL, J.G. 1999. Solid-state chemistry of drugs. 2nd ed. West Lafayette : SSCI Inc. 574 p.

CRAIG, D.Q.M. 2006. Characterization of polymorphic systems using thermal analysis. (*In* Hilfiker, R., *ed.* Polymorphism in pharmaceutical industry. Weinheim : Wiley-VCH. p. 43-80).

DELICIOUSLIVING. 2007. Triamterene. [Web:] <http://www.deliciouslivingmag.com/healthnotes/healthnotes.cfm?org=nh&lang=EN> [Date of access: 23 March 2007].

DRUGBANK. 2006. Roxithromycin. [Web:] <http://redpoll.pharmacy.ualberta.ca/drugbank/cgi.../getCard.cgi?CARD=APRD01305.tx> [Date of access: 23 March 2007].

DU PLESSIS, C. 2004. Characterisation of polymorphic, pseudopolymorphic and amorphous forms of roxithromycin. Potchefstroom : NWU. (Dissertation – M.Sc) 73-158 p.

FORSTER, S., BUCKTON, G. & BEEZER, A.E. 1991. The importance of chain length on the wettability and solubility of organic homologs. *International journal of Pharmaceutics*, 72: 29-34.

GHARBI-BENAROUS, J., DELAFORGE, M., JANKOWSKI, C.K. & GIRAULT, J.P. 1991. A comparative NMR study between the macrolide antibiotic roxithromycin and erythromycin A with different biological properties. *Journal of medicine and chemistry*, 34:1117–1125.

GIBBON, C.J., ed. 2003. South African medicines formulary. 6th ed. Pinelands : South African Medical Association, Health and Medical Publishing Group. 569 p.

GRIESSER, U.J. 2006. The importance of solvates. (*In* Hilfiker, R., ed. Polymorphism in pharmaceutical industry. Weinheim : Wiley-VCH. p. 211-234).

GULLORY, J.K. 1999. Generation of polymorphs, hydrates, solvates, and amorphous solids. (*In* Brittain, H.G., ed. Polymorphism in pharmaceutical solids. New York : Marcel Dekker. p. 183-226).

HILFIKER, R., BLATTER, F & VON RAUMER, M. 2006. Relevance of solid-state properties for pharmaceutical products. (*In* Hilfiker, R., ed. Polymorphism in pharmaceutical industry. Weinheim : Wiley-VCH. p. 1-20).

IVES, H.E. 2001. Diuretic agent. (*In* Katzung, B.G., 8th ed. Basic and clinical pharmacology. New York : McGraw-Hill. p. 245-264).

JARUKAMJORN, K., THALHAMMER, T., GOLLACDNER, B., PITTENAUER, E. & JAGER, W. 1998. Metabolism of roxithromycin in the isolated perfused rat liver. *Journal of pharmacy and pharmacology*, 50:515-519.

KAPOOR, V.K. 1994. Triamterene. (*In* Brittain, H., ed. Analytical profiles of drug substances and excipients. India : Chandigarh. 23:571-605).

LIEBENBERG, W., DEKKER, T.G., LÖTTER, A.P. & DE VILLIERS, M.M. 1998. Identification of the mebendazole polymorphic form present in raw materials and tablets available in South Africa. *Drug development and industrial pharmacy*, 24(5):485-488.

LOHANI, S. & GRANT, D.J.W. 2006. Thermodynamics of polymorphs. (*In* Hilfiker, R., ed. Polymorphism in pharmaceutical industry. Weinheim : Wiley-VCH. p. 21-42).

MARKHAM, A. & FAULDS, D. 1994. Roxithromycin: an update of its antimicrobial activity, pharmacokinetic properties and therapeutic use. *Drugs*, 48:297-326.

MEDICINENET. 2006. Triamterene and hydrochlorothiazide. [Web:]
http://www.medicinenet.com/triamterene_and_hydrochlorothiazide/article.htm [Date of access: 10 Feb. 2006].

- MEDICINENET.** 2006. Triamterene oral. [Web:] <http://www.medicinenet.com/triamterene-oral/page2.htm> [Date of access: 10 Feb. 2006].
- O'NEIL, M.J., ed.** 2001. The Merck index: an encyclopaedia of chemicals, drugs and biologicals. 13th ed. Whitehouse Station, N.J. : Merck. 986 p.
- PETIT, S. & COQUEREL, G.** 2006. The amorphous state. (*In* Hilfiker, R., ed. Polymorphism in pharmaceutical industry. Weinheim : Wiley-VCH. p. 259-286).
- QI, M., WANG, P., CONG, R. & YANG, J.** 2004. Simultaneous determination of roxithromycin and ambroxol hydrochloride in a new tablet formulation by liquid chromatography. *Journal of pharmaceutical and biomedical analysis*, 35:1287-1291.
- StJOHNHEALTH.** 2006. Triamterene. [Web:] <http://www.stjohnhealth.file//E:\swArticle.htm> [Date of access: 10 Feb. 2006].
- StJOHNHEALTH.** 2006. Triamteren capsules. [Web:] <http://www.stjohn.org/HealthInfoLib/swArticle.aspz?26.626> [Date of access: 10 Feb. 2006].
- JOHNNIC COMMUNICATION.** 2004. MIMS: monthly index for medical specialities. 44(2):228,230,231,262, Feb. Johannesburg : Johnnic Communications. 349 p.
- SWANEPOEL, E., LIEBENBERG, W., DEVARAKONDA, B. & DE VILLIERS, M.M.** 2003. Developing a discriminating dissolution test for three mebendazole polymorphs based on solubility differences. *Pharmazie*, 58(2):117-121.
- VIPPAGUNTA, S.R., BRITTAIN, H.G. & GRANT, D.J.W.** 2001. Crystalline solids. *Advanced drug delivery reviews*, 41:3-26. [Web:] <http://www.dragonpharm.com.cn/pro3/10.gif> [Date of access: 15 Feb 2006].
- WIKIPEDIA.** 2007. Roxithromycin. [Web:] <http://en.wikipedia.org/wiki/Roxithromycin> [Date of access: 23 Mar. 2007].

ACKNOWLEDGEMENTS

I would like to thank God for giving me this opportunity and providing me with the determination and endurance to successfully complete this study.

I would like to take this opportunity to express my sincerest gratitude to several people who assisted and supported me during this study. Without whom this study would not have been possible.

- Prof. W. Liebenberg for her continued guidance, advice, encouragement, motivation, and friendship for the duration of this study.
- Marius Brits for his assistance, encouragement and friendship.
- Julia Handford for her assistance as proof reader.
- The National Research Foundation for financial support that made this study possible.
- To all my friends and colleagues at the Research Institute for Industrial Pharmacy for their support, friendship, motivation, and encouragement, in particular Raadhiya, Carin, and Schalk. You guys are the best.
- My dad, Akbar, and my mum, Reymoonisha, for all the love, support, encouragement, patience and motivation. Most importantly for always believing in me. To my brother, Joosub, and sister-in-law, Yasmin, for the love and support. To Aysha and Adel for all the encouragement, motivation and friendship.

ANNEXURE 1:

**Poster presented at 4th International Conference on
Pharmaceutical and Pharmacological Sciences**

21-23 September 2006



Triamterene crystals obtained from DMF and DMF/water

Yasmin Bawa¹, Elsa van Tonder¹, Wilna Liebenberg¹

¹Research Institute for Industrial Pharmacy, School for Pharmacy, North-West University, Potchefstroom Campus, Potchefstroom, 2520, South Africa.

PURPOSE

To investigate the different crystal forms and habits of triamterene in different DMF and DMF/water mixtures, and the thermal behaviour thereof.

BACKGROUND

Triamterene is a potassium-sparing diuretic. It reduces Na absorption in the collecting tubules and ducts, interfering with Na entry through the sodium selective ion channels in the apical membrane of the collecting tubule. Since K secretion is coupled with Na entry in this segment, these agents are also effective K sparing diuretics.⁽¹⁾ It is used as treatment for oedematous states and hypertension.⁽²⁾

METHODS

The DMF and DMF/water solvated form crystals were prepared by recrystallisation. These two forms and the raw material were analysed using XRPD, TGA, IR, DSC, TM photos.

RESULTS

The crystals from the DMF solution are small bright, orange and shiny, the DMF/water crystals are long shiny and yellow. (Figure 1)

The XRPD, DSC, TGA and IR results show that the triamterene crystals obtained from DMF and DMF/water are different from the raw material.

The melting point of the crystals obtained from DMF and DMF/water were identical: 330°C (raw material melting point = 331.9°C), but the desolvation peaks are different: 199°C and 189°C respectively. Figure 2 illustrates the DSC thermograms.

According to the XRPD there are major differences observed at 9 – 12 °2θ between the raw material and the DMF and DMF/water crystals (Figure 3).

The theoretical weight loss for a DMF solvate is 23.5% and DMF/water hydrated solvate is 27.5%, respectively. The TGA results however indicate that both crystal forms obtained from DMF and DMF/water are DMF solvates only, with a weight loss of approximately 23%, as illustrated in Figure 4.

The thermo-microscope shows us that the desolvation process starts at 135°C. Needle growth was observed at a temperature ranged between 261°C - 294°C, for the crystals obtained from DMF and DMF/water (Figure 5).



Fig 1. Photos of triamterene DMF and DMF/water crystals.



Fig 2. DSC thermograms for the raw material (black), DMF (red), and DMF/water (blue) crystals.

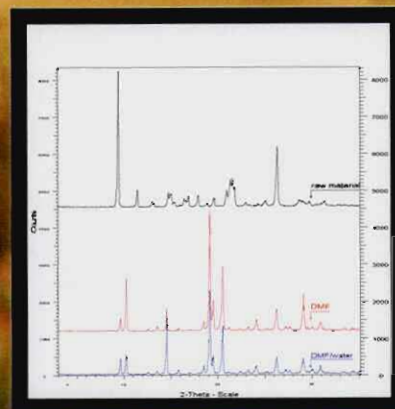


Fig 3. XRPD patterns of raw material (black), DMF crystal form (red) and DMF/water crystal form (blue).



Fig 4. TGA spectra of triamterene raw material (black), DMF (red), and DMF/water (blue) crystals.

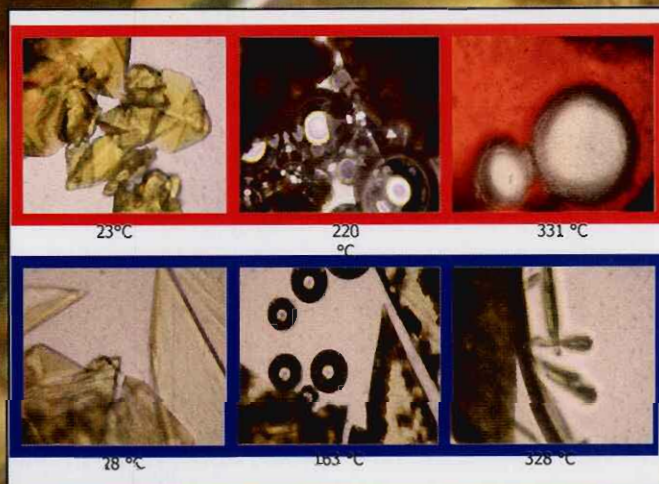


Fig 5. TM photos of the desolvation of triamterene DMF (red) and DMF/water crystals (blue).

CONCLUSION

It can be concluded that the DMF and various mixtures of DMF/water produce a solvate only. This is contrary to previous reports. According to Dahl et al. (1989), it was reported that DMF and DMF/water mixtures produce hydrated solvates.⁽³⁾

REFERENCES

- (1) Katzung B.G. 2001. Basic & Clinical Pharmacology, international ed. p 256-257.
- (2) Gibson, C. J. 2003. South African Medicines Formulary, 16th ed. p 280.
- (3) Dahl, O., et al., 1989. Journal of pharmaceutical sciences, 78:598-605.